Preface

This thesis was conducted at the Norwegian University of Science and Technology (NTNU), Department of Neuroscience, Trønderbrain Research Group, in the period of August 2013 to May 2014. The thesis was part of the international Master of Science programme in Neuroscience.

Foremost, I would like to express my sincere gratitude to my main supervisor Professor Linda White, PhD, for giving me the opportunity to do this project and for sharing her immense knowledge in a comprehensible way. I have truly valued her helpful guidance, constructive feedback, commitment and continuous support. Furthermore, I would like to thank my co-supervisor, Senior Consultant Sigrid Botne Sando, dr. med., who has collected all samples and data used in the present study. Her dedication and outstanding work in the field of dementia is of great inspiration and enormous value. All laboratory work was performed in co-operation with PhD student Camilla Lauridsen, MSc, and Senior Technician Ina Møller. I owe special thanks to Camilla, with whom I have worked closely with during the project and whose knowledge has helped me in several ways. She has willingly shared her previous experiences, and also provided insight to the present work. I deeply appreciate her useful advice, words of encouragement and thoughtfulness. I am also thankful to Ina for her excellent assistance in practical laboratory aspects, and for always being so kind and supportive. I would also like to thank PhD student Guro Berge, MSc, for her continuous support, positive spirit and great enthusiasm. I want to express my gratitude to the entire research group as a whole for providing a professional and social environment, which I have truly enjoyed being a part of. I am also grateful to Professor Grethe Albrektsen for taking time to thoroughly answer my questions regarding statistical issues. Last but not least, my sincere thanks go to my beloved family and friends, and my dear Espen.

Trondheim, May 2014

Ingrid Tøndel Medbøen

Abstract

Background: The cerebrospinal fluid (CSF) biomarkers amyloid-beta 42 (Aβ42), total tau (T-tau) and phosphorylated tau (P-tau) are considered to reflect core pathological features of Alzheimer's disease (AD), and have consistently been reported to have high diagnostic accuracy for discriminating patients with AD from healthy elderly controls. Yet there are limitations to their use, and little is known about alternative proteins in CSF, as well as in blood. The failure of Aβ immunotherapy has forced AD research to examine additional factors, particularly in the early stages of disease. The *APOE* ε4 allele is the major genetic risk factor for sporadic AD, and data suggest that ApoE may alter Aβ clearance and/or metabolism during the disease process. Another apolipoprotein associated with Aβ metabolism is clusterin (ApoJ), suggested to prevent aggregation and also be involved in clearance of Aβ. Moreover, angiotensin-converting enzyme (ACE) is a protease known to mediate cleavage of Aβ *in vitro*, and there is some indication that the *ACE* gene may be a risk factor for AD, depending on the insertion/deletion (I/D) genotype. Neurofilament-light (NF-L), like tau, is a neuronal cytoskeletal protein. In this pilot study, levels of ApoE, clusterin, ACE and NF-L in CSF and/or blood have been investigated in patients with early AD and healthy elderly individuals, and comparisons made with *ACE* and *APOE* ε4-allele genotype.

Aims: To assess whether levels of these proteins altered significantly in early AD compared to levels in elderly control individuals healthy for their age, whether additional information could be obtained from comparisons with *ACE* and *APOE* polymorphisms, and to assess their potential diagnostic value as early-stage biomarkers for AD compared to Aβ and tau protein.

Methods: Commercial ELISA kits were used to analyze and compare the levels of Aβ42, Aβ40, T-tau, P-tau, ApoE, clusterin, ACE and NF-L in CSF and/or plasma or serum samples from 20 patients with early AD and 20 age-matched individuals healthy for their age. Real-time polymerase chain reaction was performed on genomic DNA purified from samples of whole-blood from all participants to determine the *ACE* I/D polymorphism. Comparison was also made regarding *APOE* ε4-allele status.

Results: Despite the low number of samples, a high diagnostic accuracy in the discrimination between patients with early AD and elderly control individuals was obtained with concentrations of Aβ42 and tau in CSF. No significant differences were found between patients with early AD and controls regarding levels of ApoE in serum, clusterin in CSF or plasma, or ACE in CSF or serum. There was no pathological relationship regarding *ACE* genotype and allele distribution. The *APOE* ε4-allele was associated with lower levels of serum ApoE, irrespective of diagnosis. CSF NF-L levels were significantly higher in patients compared to controls.

Conclusion: No disease-specific alterations were found in relation to ApoE, clusterin or ACE. Although NF-L in CSF showed a fairly good potential to distinguish the patients with early AD from elderly individuals healthy for their age, the diagnostic accuracy was below that of Aβ and tau protein, and it did not seem to provide improved discrimination as a biomarker. Thus, none of these proteins are likely candidates as biomarkers for early AD.

Abbreviations

Aβ = amyloid-beta

ACE = angiotensin-converting enzyme

ACE = angiotensin-converting enzyme gene

AD = Alzheimer's disease

aMCI = amnestic mild cognitive impairment

ApoE = apolipoprotein E

APOE = apolipoprotein E gene

ApoJ = apolipoprotein J

APP = amyloid precursor protein

AUC = area under the curve

BACE1 = β-site APP cleaving enzyme-1

CSF = cerebrospinal fluid

EDTA = ethylene-diaminetetraacetic acid

ELISA = enzyme-linked immunosorbent assay

FDG = [^{18}F]-fluorodeoxyglucose

HRP = horseradish peroxidase

IWG = International Working Group

MCI = mild cognitive impairment

MMSE = mini mental state examination

MRI = magnetic resonance imaging

naMCI = non-amnestic mild cognitive impairment

NF-L = neurofilament-light

NIA-AA = National Institute on Aging and the Alzheimer Association

PCR = polymerase chain reaction

PET = positron emission tomography

PiB = [^{11}C]-Pittsburgh compound B

PS = presenilin

P-tau = phosphorylated tau

P-tau$_{181}$ = tau phosphorylated at threonine 181

P-tau$_{231}$ = tau phosphorylated at threonine 231

ROC = receiver operating characteristic

T-tau = total tau

Table of contents

1 Theoretical background

1.1 Alzheimer's disease is a progressive neurodegenerative disorder

Alzheimer's disease (AD) is a devastating brain disorder and the most common form of dementia, impacting on daily living through loss of cognitive ability. Being a neurodegenerative disease, AD is characterized by a series of abnormalities in the brain that selectively affects and irreversibly damages neurons in specific regions, causing extensive neuronal dysfunction and cell death. As neurons and the connections between them are progressively lost, drastic personality changes occur. Structures critical for declarative memory are often the first affected. Hence, impairment in the ability to form recent memories is usually an early clinical symptom of AD (Greene et al., 1996). Gradually, memory is lost along with other cognitive abilities such as language, proper judgement, decision-making, orientation and attention, leading to psychological and behavioural alterations that may include confusion, anxiety, depression, hallucinations, apathy and irritability (Purandare et al., 2000). In the final stages patients are generally incapacitated with severe to total loss of verbal skills, leading to complete dependence for basic functions of daily life, and premature death. The progression from mild forgetfulness to fatal, widespread brain impairment takes place slowly over several years.

In addition to neuronal and synaptic loss in the brain, AD is pathologically characterized by extensive amounts of extracellular deposits of dense, insoluble material commonly called amyloid plaques, and insoluble twisted protein strands that build up inside neurons called neurofibrillary tangles. Neuronal and synaptic loss, amyloid plaques and neurofibrillary tangles are considered the classical neuropathological hallmarks of AD, and were first described in 1907 by Alois Alzheimer (Alzheimer 1907, Translation 1987).

AD is classified according to age of onset, referred to as early- and late-onset AD. The division is at 65 years of age. Late-onset AD makes up more than 95% of cases (Lill and Bertram, 2011). Among the less common early-onset cases, there are rare familial forms of AD, caused by autosomal dominant mutations. Late-onset cases are mainly sporadic, and their cause remains unknown (Bertram et al., 2010). Other than the fact that familial AD is clearly hereditary and manifests at an earlier age, it is largely clinically indistinguishable from sporadic late-onset AD (Lopera et al., 1997).

The greatest known risk factor for AD is increasing age. AD is not part of normal aging, but the incidence of the disease significantly increases with increasing age (Launer et al., 1999). The prevalence of AD is approximately 11% in individuals aged 65 and older, and 32% in individuals above

the age of 85 (Thies and Bleiler, 2013). As the global population continues to age, the number of individuals at risk will also increase. In 2010, more than 35 million people were estimated to suffer from dementia worldwide. The frequency is expected to double by 2030 and triple by 2050 because of population growth and the anticipated increase in life expectancy (Prince et al., 2013).

Accounting for approximately 70% of dementia cases (Reitz and Mayeux, 2014), AD represents a major public health problem. At present, there are no available treatments that delay disease onset or prevent, reverse or stop the progression of AD. Medications available today only temporarily relieve symptoms in some patients. However, research and evaluation of potential therapeutic targets are ongoing (Citron, 2010). If interventions could delay disease onset and progression, even by a few years, this would greatly reduce the global burden of AD (Brookmeyer et al., 2007). The social and economic impact of AD worldwide is already enormous, and will grow even greater in the years to come if the disease is left untreated.

1.2 Risk factors for AD have been identified

Besides aging, a large number of factors have been associated with increased risk of AD.

1.2.1 Environmental risk factors and the concept of brain reserve

Consistently reported are cardiovascular risk factors, including hypertension, coronary heart disease, atherosclerosis, high cholesterol, stroke, diabetes, smoking and obesity, summarized in a recent review by Mayeux and Stern (2012). Furthermore, several epidemiological studies have shown that traumatic brain injury could be a potential risk factor for AD (Jellinger, 2004). Decreased reserve capacity of the brain is another proposed risk factor. The concept of brain reserve accounts for the differences in susceptibility to the effects of pathology, whereby some people can tolerate higher levels of brain injury than others without displaying clinical symptoms (Stern, 2009). Epidemiological studies suggest that individuals with intellectually enriched lifestyles that increase their brain reserve capacity have a reduced risk of expressing AD pathology clinically. For example, higher education has consistently been shown to have protective influence on the risk of developing clinical AD, also in Norway (Sando et al., 2008a).

1.2.2 The *APOE* ε4 allele is the major genetic risk factor for sporadic AD

The rare familial form of AD has a clear genetic background, affecting individuals that bear autosomal dominant mutations of specific genes. Although environmental factors might increase the risk of the more common sporadic AD, this form of the disease also has a significant genetic background. A large twin study estimated the extent of heritability for sporadic AD to be nearly 80% (Gatz et al., 2006). The most important genetic risk factor discovered in sporadic late-onset AD is possession of the ε4 allele of the apolipoprotein E (ApoE) gene (*APOE*) (Corder et al., 1993, Strittmatter et al., 1993). ApoE

has multiple functions including involvement in transport, redistribution and metabolism of cholesterol and other lipids, also after tissue injury, and will be discussed in more detail in section 1.10.1. *APOE* shows a genetic polymorphism where ε4 is one of three common alleles; ε2, ε3 and ε4 (Utermann et al., 1977), giving rise to six different genotypes, and three different isoforms of the protein (ApoE2, ApoE3 and ApoE4). Although the three common isoforms only differ by one or two of the total 299 amino acids, they significantly differ in structure and function (Mahley et al., 2006). The frequencies of the three *APOE* alleles vary in different populations. On a global scale, the ε3 variant of *APOE* is the most frequent, constituting 60-90% of the allelic variation, whereas the range is 0-20% for ε2 and 10-20% for ε4 alleles, with some exceptions (Singh et al., 2006, Corbo and Scacchi, 1999). However, the ε4 allele frequency is dramatically increased in patients with AD (Farrer et al., 1997). *APOE* ε4 acts in a dose-dependent manner, regarding both risk and age of onset; homozygous subjects have a higher risk and earlier onset of AD than heterozygous subjects. Carrying *APOE* ε4 seems to lower age of onset both in sporadic AD (Sando et al., 2008b, Corder et al., 1993) and familial AD (Pastor et al., 2003). Even though having the *APOE* ε4 allele increase the risk for AD, it is neither sufficient nor necessary to develop AD, even when present in the homozygous form, ε4/ε4 (Myers et al., 1996). In contrast to the *APOE* ε4 allele, carrying the *APOE* ε2 allele appears to be protective towards the development of AD, by lowering the risk and delaying the age at onset (Lovati et al., 2010). How the different ApoE isoforms contribute to AD pathogenesis is not clear, but will be discussed further in section 1.4.2.2.

1.3 The diagnosis of AD relies on specific criteria

To enable clinicians and researchers to maintain consistency in the diagnosis of AD, a uniform set of criteria was established in 1984 by the NINCDS-ADRDA[1] workgroup (McKhann et al., 1984). According to these criteria, a diagnosis of AD made during life can only be probabilistic, and is made purely on clinical grounds, without verification of neuropathological or biomarker evidence of the disease. For a *probable* AD diagnosis to be made, onset of dementia has to be established by clinical examination and neuropsychological testing, and other causes of dementia have to be excluded. Individuals meeting criteria with other ilnesses that may contribute to dementia are diagnosed with *possible* AD. A *definite* diagnosis of AD, however, requires postmortem conformation of the clinical diagnosis via the histological quantification of brain amyloid plaques and neurofibrillary tangles (McKhann et al., 1984). As will be discussed in section 1.8, proposals for new criteria have now been presented.

[1] National Institute of Neurological and Communicative Disorders and Stroke and the Alzheimer disease and Related Disorders Association

1.4 Pathophysiological changes in the AD brain

The most conspicuous changes in the AD brain are the three lesions described by Alzheimer more than 100 years ago, known as the classical hallmarks of AD; neuronal and synaptic loss, amyloid plaques and neurofibrillary tangles. Almost 80 years went by from Alzheimer's first description of plaques and tangles until their molecular composition was revealed (Glenner and Wong, 1984, Masters et al., 1985, Grundke-Iqbal et al., 1986), and their biochemical basis has now been well characterized. As discussed in section 1.6.1, the pathological changes in the AD brain begin years before the substantial neurodegeneration that accompanies dementia (Price and Morris, 1999).

1.4.1 Neuropathological hallmarks of AD

1.4.1.1 Amyloid plaques

The extracellular amyloid deposits appear in a variety of morphological forms, including *diffuse* plaques and plaques containing elements of degenerating neurons, termed *neuritic* plaques (Figure 1.1), summarized in a review by Selkoe and Schenk (2003). Neuritic plaques contain a core of amyloid fibrils surrounded by dystrophic neurites (swollen axons and dendrites), together with reactive astrocytes and activated microglial cells. The less dense, diffuse plaques invariably accompany neuritic plaques, and are not associated with dystrophic neurites, activated microglia or reactive astrocytes. These plaques are a common finding in the brain of cognitively intact elderly people (Katzman et al., 1988, Delaere et al., 1990, Dickson et al., 1992), leading to the suggestion that the diffuse plaques may be the precursors to pathogenic dense plaques (Selkoe and Schenk, 2003). Amyloid plaques also occur in the walls of cerebral blood vessels in the AD brain in the form of cerebral amyloid angiopathy (Rensink et al., 2003), illustrated in Figure 1.1.

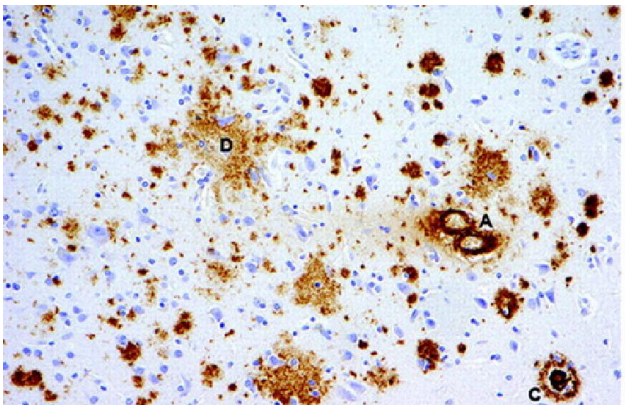

Figure 1.1 *Immunohistochemistry image of a diffuse plaque (D), a dense-core (neuritic) plaque (C), and cerebral amyloid angiopathy (A) in the frontal lobe (Wippold et al., 2008).*

Although associated with a range of deposited proteins, the main component of amyloid plaques is the amyloid-beta (Aβ) peptide (Masters et al., 1985). Aβ peptides are natural products of metabolism (Haass et al., 1992), and part of a group of peptides produced by proteolytic cleavage of the larger transmembrane amyloid precursor protein (APP) (Kang et al., 1987). APP is ubiquitously expressed in mammalian cells, and can undergo amyloidogenic or non-amyloidogenic processing via cleavage by different secretases (Ling et al., 2003), as illustrated in Figure 1.2. The non-amyloidogenic APP

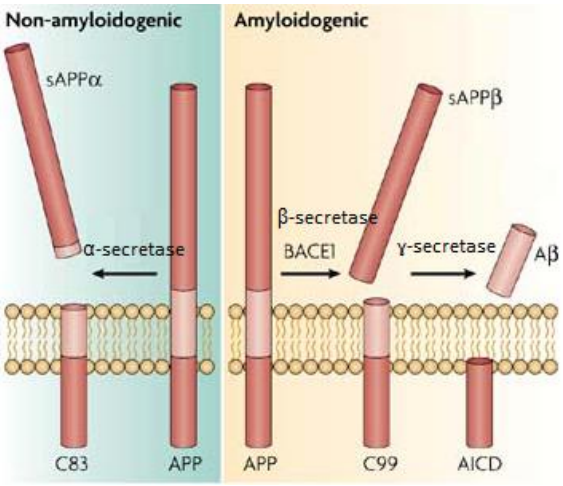

Figure 1.2 *Proteolytic processing of the amyloid precursor protein (APP) and the resulting cleavage products. Figure modified from LaFerla et al. (2007).*

processing pathway involves sequential proteolytic cleavages by α- and γ-secretases resulting in the generation of a soluble secreted form of APP (sAPPα in Figure 1.2) which, in contrast to Aβ, may be neuroprotective by promoting neurogenesis and survival (Furukawa et al., 1996). Proteolysis leading to Aβ production results from the alternative amyloidogenic APP processing pathway. APP is first cleaved by β-secretase, allowing its large ectodomain (sAPPβ) to be shed into the extracellular fluid. In the brain, β-site APP cleaving enzyme-1 (BACE1) has been found to be the main β-secretase (Vassar et al., 1999). The 99 amino acid long C-terminal stub left in the membrane is subsequently cleaved by ɣ-secretase, causing different isoforms of Aβ to be released, depending on the exact point of cleavage. The ɣ-secretase protein complex is member of a family of unusual proteases that are able to perform intramembrane cleavage of peptide bonds. The multipass transmembrane proteins called presenilin 1 (PS1) and 2 (PS2), are part of the ɣ-secretase protein complex, of which they possess the active site (Wolfe et al., 1999, Steiner et al., 2002).

The Aβ isoforms only differ in the length of their C-terminal, and the two species that have received the most interest are those that are 40 and 42 amino acids long (Aβ40 and Aβ42). Monomers of the Aβ40-species are more abundantly produced than Aβ42, but the longer Aβ42 is more hydrophobic and far more prone to spontaneous self-aggregation (Jarrett et al., 1993). Aβ42 is therefore the predominating form of Aβ in amyloid plaques. The pathogenic mechanisms that allow Aβ monomers to self-aggregate are largely unknown, but it is clear that Aβ can exist as monomers, dimers, trimers, oligomers, fibrils and the fibrillar aggregates of amyloid plaques (Walsh and Selkoe, 2007), as illustrated in Figure 1.3.

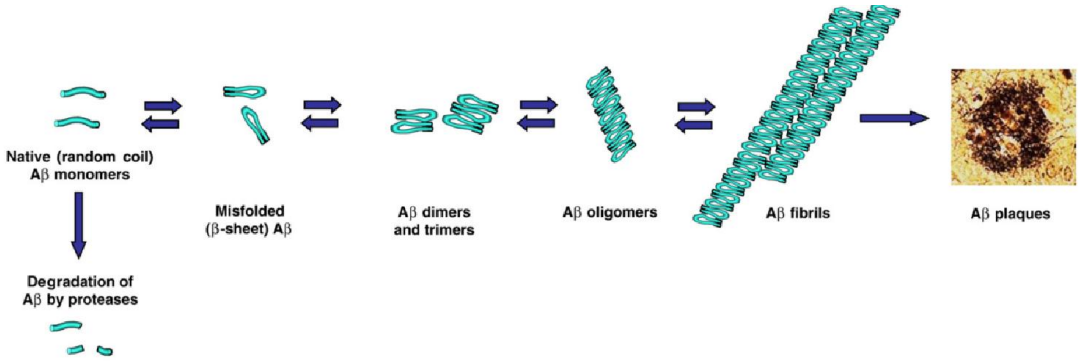

Figure 1.3 *Misfolded amyloid-beta (Aß) peptides self-aggregate into oligomeric and ultimately polymeric structures (Hampel et al., 2010).*

1.4.1.2 Neurofibrillary tangles

Neurofibrillary tangles are primarily composed of abnormally hyperphosphorylated forms of the protein tau (Grundke-Iqbal et al., 1986). Tau is a microtubule-associated protein normally located to the axon. By binding to tubulin in the axonal microtubules, tau promotes microtubule assembly and stability, which is important for axonal function and transport. Tau is a phosphoprotein, with more than 30 potential phosphorylation sites, regulated by the balance between multiple kinases and phosphatases (Iqbal et al., 2005). In AD, tau is translocated to the somatodendritic compartment and undergoes hyperphosphorylation, misfolding, and aggregation, giving rise to neurofibrillary tangles, as illustrated in Figure 1.4.

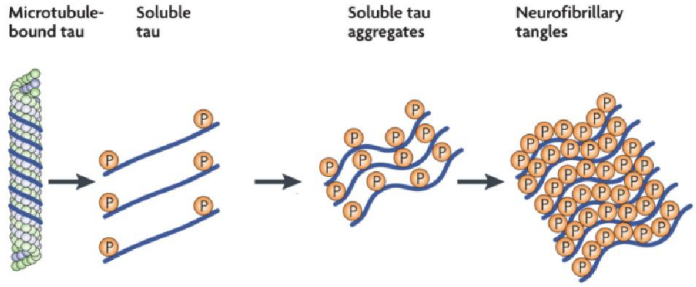

Figure 1.4 *Microtubule-bound soluble tau supports axonal transport. In Alzheimer's disease, tau is hyperphosphorylated which in turn leads to misfolding, aggregation, and ultimately neurofibrillary tangles. Figure modified from Citron (2010).*

In its hyperphosphorylated state, tau also loses its ability to bind to the microtubules, causing them to become unstable and disassemble, thereby collapsing the neuron's transport system, and disrupting structure and function in neurons which can be fatal (Iqbal et al., 2005). Hyperphosphorylated tau is also found in dystrophic neurites of the neuritic plaques. Figure 1.5 shows neurofibrillary tangles and neuritic plaques in the hippocampus.

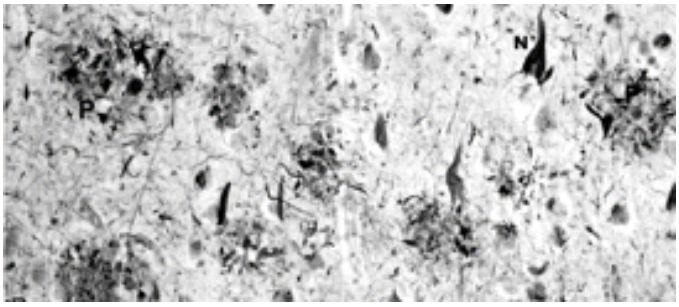

Figure 1.5 *Neurofibrillary tangles (N) and neuritic plaques (P) in the hippocampus (Wippold et al., 2008).*

Tau pathology has a rather stereotypical and predictable progression. The first neurofibrillary tangles seem to consistently appear in neurons in the transentorhinal region. Subsequently, the neurofibrillary tangles spread to the hippocampus and amygdala, and later to the neocortical association areas, relatively sparing primary sensory, motor and visual areas (Braak and Braak, 1991).

1.4.1.3 Neuronal and synaptic loss

The neurodegeneration that characterizes AD is initially manifested by decreased neuronal function with subsequent synaptic loss and neuronal death, ultimately leading to extensive atrophy. Knowledge of brain regions selectively vulnerable to AD was initially obtained from examination of post-mortem brain tissue (Brun and Gustafson, 1976, Braak and Braak, 1991), and could later be visualized *in vivo* by the means of neuroimaging, such as structural magnetic resonance imaging (MRI) (Bobinski et al., 2000, Dickerson et al., 2009). A symmetric pattern of cortical atrophy, with widening of the sulci and enlarged ventricles is typical. The atrophy is widespread, yet to a great extent confined to specific areas. As illustrated in Figure 1.6, the tissue loss in the hippocampus and entorhinal area is particularly profound, and often the first regions affected. Extensive degeneration also affects the cholinergic innervations to the neocortex, and the neocortex itself. However, primary motor and sensory cortices are often preserved even in advanced AD, and stand out as appearing almost normal in contrast to severe atrophy of frontal, parietal, and temporal association cortices.

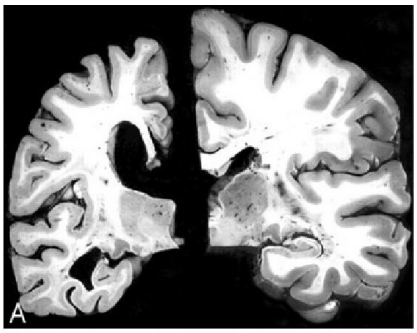

Figure 1.6 *On the left is a section of the hemibrain of a 70-year-old patient with Alzheimer's disease, showing severe atrophy. On the right, a brain section from a healthy individual of similar age (Wippold et al., 2008)*.

1.4.2 Disease mechanism

Besides the hallmarks, several other pathophysiological changes occur in the AD brain such as depletion of neurotrophins and neurotransmitters, abnormal lipid metabolism, oxidative stress and mitochondrial failure, and activation of inflammatory processes (Querfurth and LaFerla, 2010). Ultimately, the biochemical processes involved in the development of AD converge upon widespread death of neurons, likely through apoptosis. However, a major challenge consists in determining the role of a given pathological finding linked to the disease process; whether it is a cause, consequence, or just a neutral bystander. To be able to develop disease-modifying treatments, a detailed understanding of the disease process is necessary. Although the disease mechanism remains unclear, recent research progress has given a considerable amount of knowledge on the molecular basis of AD. There has been an intense search for the initial trigger(s) of the pathological cascade leading to neurodegeneration and cognitive decline, and several theories have been proposed.

1.4.2.1 The cholinergic hypothesis was the first theory of the cause of AD

In addition to other hallmarks, AD is characterized by a profound loss of cortical cholinergic innervation, attributed to degeneration of cholinergic projection neurons in the nucleus basalis of Meynert, the major source of cholinergic innervation of the cerebral cortex (Arendt et al., 1983). The cholinergic depletion was discovered during the heyday of neurotransmitter research in the 1970s, when the molecular basis of AD was still unknown (Davies and Maloney, 1976). The *cholinergic hypothesis* of AD became the dominant theory, stating that AD, including the clinical symptoms and neuropathological lesions, is caused by a deficiency in the production of the vital neurotransmitter acetylcholine. AD was claimed to be a cholinergic disease in the same way that Parkinson's disease is often described as a dopaminergic disease (Coyle et al., 1983), and all the first-generation anti-Alzheimer medications were based on this theory. These medications work to preserve acetylcholine by inhibiting acetylcholinesterases, enzymes that break down acetylcholine, but only serve to treat symptoms in some patients, and neither halt nor reverse the disease. Even though it may contribute to the severity of the cognitive and behavioral deficits (Mesulam, 2004), the cholinergic lesion is a result of neuronal degeneration, which today is known to happen later in the disease process (Jack et al., 2010, Perrin et al., 2009). It is therefore no longer viewed as the initial event in AD pathogenesis.

More recent hypotheses are centred on the effects of the proteins of plaques and tangles. AD and many other neurodegenerative disorders share common pathogenic mechanisms that are linked to the misfolding and progressive aggregation of otherwise soluble proteins. The protein abnormalities are thought to initiate pathological cascades involving downstream processes such as inflammation and oxidative stress, which in turn contribute to energy failure and synaptic dysfunction, and ultimately, neurodegeneration (Soto, 2003). Since the revelation of the molecular composition of plaques and tangles in the mid-1980s, a great amount of research has been done to further elucidate their role in the disease process.

1.4.2.2 The amyloid cascade hypothesis is the leading theory of AD

The amyloid cascade hypothesis suggests that accumulation of Aβ in the brain is the primary influence driving AD pathogenesis. An imbalance between production and clearance of Aβ, causing increased levels of Aβ42, is thought to initiate a series of pathogenic events (illustrated in Figure 1.7), including tau phosphorylation and formation of neurofibrillary tangles, ultimately leading to synaptic and neuronal dysfunction, and degeneration with subsequent cognitive disturbances (Hardy and Selkoe, 2002). Support for the amyloid hypothesis is largely based on genetic studies. Major clues came from families suffering from the autosomal dominantly inherited form of the disease. The first identified mutation causing familial AD was found in the gene encoding APP on chromosome 21 (Goate et al., 1991). Mutations in the PS1 and PS2 genes were also found in affected people, and

account for most cases of familial disease (Sherrington et al., 1995, Levy-Lahad et al., 1995). The familial form of AD is thus caused by mutations in genes both for the substrate (APP) and the enzyme (presenilin) for Aβ generation, which in turn lead to increased production of Aβ, in some cases specifically Aβ42, or an increased tendency of Aβ to aggregate (St George-Hyslop, 1999). Moreover, AD-like neuropathology is invariably seen in Down's syndrome (trisomy of chromosome 21) (Olson and Shaw, 1969, Motte and Williams, 1989), where triplication of the APP gene leads to increased APP expression and consequent higher levels of Aβ throughout life. Combined with the observation that duplication of the APP locus on chromosome 21 caused early onset AD and/or cerebral amyloid angiopathy in five unrelated families (Rovelet-Lecrux et al., 2006), the genetic data clearly point out the processing of APP and the production of Aβ peptides as a central part of the disease process.

Another supportive factor for the amyloid hypothesis is the fact that Aβ assemblies are neurotoxic. Synthetically produced Aβ42 monomers have been shown to be harmless to cultured neurons, but become neurotoxic upon self-aggregation (Pike et al., 1991). Initially, the neurotoxicity, and ultimately neurodegeneration, were attributed to the insoluble fibrils of the amyloid plaques, despite conflicting evidence. The major weaknesses included the fact that amyloid plaque burden correlates poorly with AD severity (Terry et al., 1991), and that a number of cognitively normal elderly individuals also display significant amounts of amyloid plaques (Katzman et al., 1988). Additionally, in some transgenic and cell culture models, pathological changes are observed before the onset of amyloid plaque accumulation (Billings et al., 2005). Later discoveries showed that fibrils are not the only toxic form of Aβ, and probably not most significant for AD pathogenesis.

Aβ oligomers are considered the primary toxic species

It now appears that soluble oligomeric forms of Aβ are the primary toxic species in AD (Kirkitadze et al., 2002). Findings suggest that soluble, oligomeric Aβ assemblies cause substantial neuronal dysfunction before the appearance of amyloid deposits (Klein et al., 2001). It has even been suggested that deposition of Aβ into fibrillar forms may serve as a protective mechanism against the more neurotoxic Aβ oligomers (Lee et al., 2004, Selkoe, 2002). With their smaller size, and because they are relatively soluble and diffusible, Aβ oligomers are more able to exert a toxic effect on the neuronal plasma membrane. Varying in morphology and toxicity, Aβ oligomers have been reported to range in size from 2 to 20 monomers, as reviewed by Glabe (2008). Aβ oligomers exert their toxicity through binding at synapses, and it has been suggested that AD may be primarily a disorder of synaptic failure (Selkoe, 2002). Oligomers have been found to rapidly inhibit long-term potentiation, enhance long-term depression and reduce dendritic spine density in normal rodent hippocampal slices (Lambert et al., 1998, Shankar et al., 2008). Shankar et al. (2008) also showed that insoluble plaque cores from AD cortex did not impair long-term potentiation unless they were

first solubilized to release Aβ dimers, strengthening the idea that amyloid plaques are largely inactive but sequester Aβ dimers that attack synapses. In light of the findings made about toxic Aβ oligomers, the early clinical symptom of memory loss can be attributed to oligomer-induced disruption of synaptic plasticity, while later stages of dementia may be attributed to oligomer-induced cellular degeneration and death (Ferreira and Klein, 2011).

In both familial and sporadic AD, soluble Aβ is thought to undergo a conformational change that makes it prone to aggregation into soluble oligomers and the larger insoluble fibrils found in plaques. The underlying mechanisms leading to this conformational change are not well understood. Although an increase of either total Aβ, or the Aβ42 isoform, is well established in familial AD, the Aβ dysregulation in sporadic AD is less well understood. It is debated as to whether abnormal processing or impaired clearance of Aβ42 causes the Aβ accumulation (Mawuenyega et al., 2010).

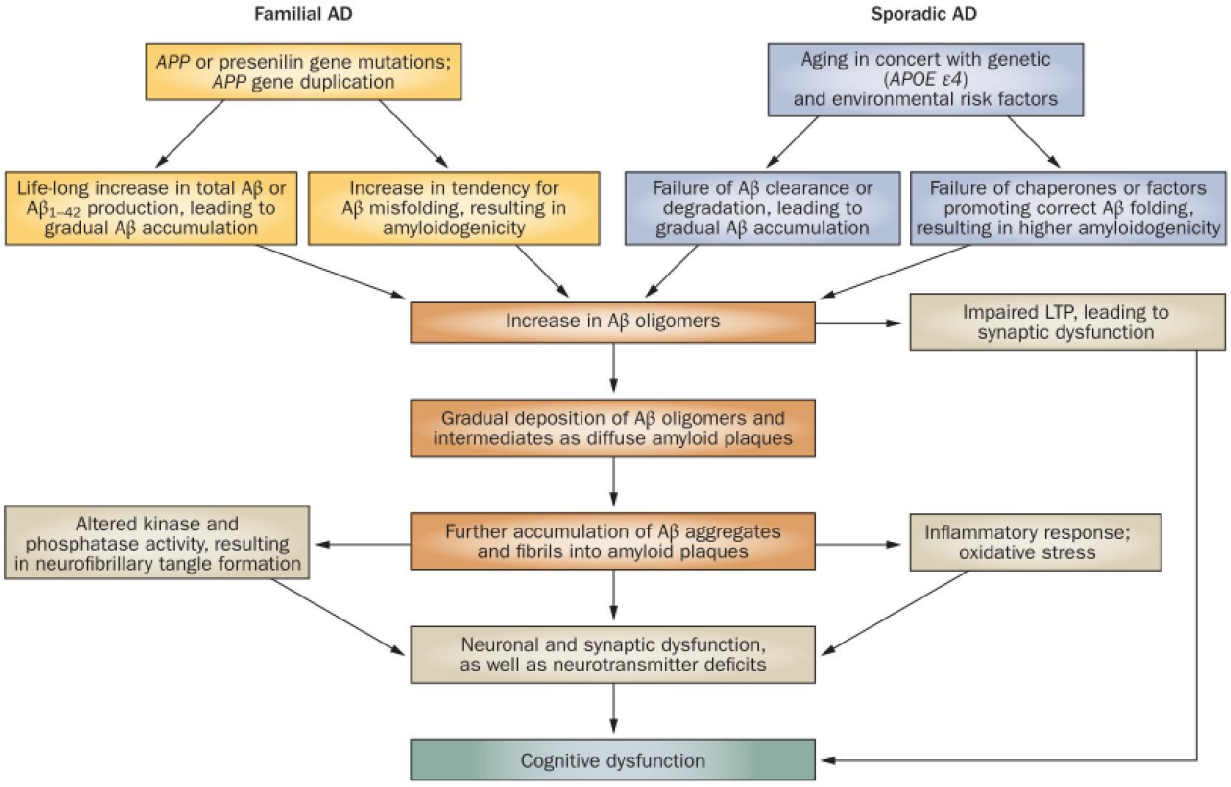

Figure 1.7 *The amyloid cascade hypothesis. According to the hypothesis, the initiating event in AD is an imbalance between Aб production and clearance in the brain, causing increased levels of the peptide, ultimately leading to neurodegeneration and dementia. Aб oligomers directly inhibit hippocampal long-term potentiation (LTP) and impair synaptic function, while aggregated and deposited Aб cause inflammatory and oxidative stress. Tau pathology with tangle formation is regarded to be a downstream event, contributing to neuronal dysfunction (Blennow et al., 2010).*

The role of ApoE in AD pathology

Even though the ε4 allele of *APOE* is the major genetic risk factor for sporadic AD, the underlying mechanism for the increased risk is not clear. *APOE* ε4 has been associated with several biochemical disturbances characteristic of AD, including Aβ deposition, tangle formation, oxidative stress, loss of synaptic plasticity, and cholinergic dysfunction, suggesting that ApoE is a key player in the pathogenesis of AD (summarized in the review by Cedazo-Minguez (2007)). ApoE is one of several proteins present in amyloid deposits, and it has been reported that Aβ deposition in the form of amyloid plaques is more abundant in *APOE* ε4 carriers than non-ε4 carriers (Schmechel et al., 1993). Despite numerous attempts to elucidate the role of ApoE in AD, exactly how the different ApoE isoforms contribute to disease pathogenesis has not been agreed upon. However, prevailing evidence suggests that the differential effects of ApoE isoforms on Aβ aggregation and/or clearance may play a major role, as reviewed by Kim et al. (2009). Suggestions have been made in which ApoE acts as an amyloid catalyst, enhancing Aβ aggregation, with ApoE4 being the strongest promoter of Aβ polymerization. An alternative hypothesis is that ApoE serves to clear Aβ from the brain, with ApoE4 being less efficient in this function compared to ApoE3 and E2 (Potter and Wisniewski, 2012).

1.4.2.3 Some have claimed that tau pathology is the initial disease trigger

While most investigators believe Aβ aggregation to be the key initial trigger of AD, some argue that hyperphosphorylation of tau plays the initial role. Neuropathological studies of cognitively normal individuals have shown that neurofibrillary tangles are fairly ubiquitous in the entorhinal cortex and other limbic structures by middle age, and precede amyloid disease in most people (Braak and Braak, 1991, Price and Morris, 1999). These observations, in addition to the fact that tangles have been reported to correlate more closely with the severity of AD compared to plaques, led some to suggest that tau-related pathology represents the origin of AD (Terry, 1996). Price and Morris (1999) noted that although tau disease progressed very slowly in cognitively normal individuals without amyloid disease, the severity and rate of accumulation of neurofibrillary tangles was markedly increased in individuals with accompanying Aβ disease, and concluded that age-related accumulation of neurofibrillary tangles is insufficient to cause significant neurodegeneration (Price and Morris, 1999). Biomarker data provide direct support for the hypothesis that altered Aβ metabolism precedes tau-related pathology and neurodegeneration (Buchhave et al., 2012). As summarized by Musiek and Holtzman (2012), findings suggest that tau deposition begins early in life and accumulates slowly with age, whereas the appearance of amyloid pathology occurs later in life, and acts as the key that triggers a cascade of events leading to AD. It seems that Aβ interacts with tau in a way that serves to accelerate tau disease and induce neurodegeneration (Bloom, 2014). Indeed, neuritic plaques, which

contain both hyperphosphorylated tau and Aβ fibrils, correlate more closely with neuronal loss and dementia in AD than either tangles or plaques alone (Tiraboschi et al., 2004).

Based on the prevailing evidence, the amyloid cascade hypothesis remains a robust model of AD neurodegeneration, and retains significant support among researchers. Yet the etiology of AD remains uncertain, and the possibility that there could be even earlier changes involved, should not be excluded (Pimplikar et al., 2010). Advances in the understanding of molecular mechanisms underlying AD pathology have provided new insight for interventions to modify disease progression. Many trials in the development of disease-modifying treatments for AD deal with Aβ-targeting compounds, such as secretase inhibitors or Aβ immunotherapy (Citron, 2010). So far, Aβ immunotherapy trials in humans involving clearance of Aβ from the brain have not improved cognition in patients with mild-to-moderate AD (Holmes et al., 2008, Doody et al., 2014, Salloway et al., 2014). BACE1, the first enzyme cleaving APP in the production of Aβ, is a major therapeutic target for the development of inhibitor drugs, and several promising BACE1 inhibitors have recently entered human clinical trials (Yan and Vassar, 2014).

1.5 Biomarkers for AD

In the broadest definition, a biomarker is any measurable biologic feature that can be used to diagnose or predict a physiologic or pathologic condition.

> "A biomarker can be defined as a physiologic, biochemical, or anatomic parameter that can be objectively measured as an indicator of normal biologic processes, pathologic processes, or responses to a therapeutic intervention."
>
> - *Biomarkers Definitions Working Group 2001*

Biomarkers have many valuable applications in monitoring of health status and detection of disease. They can be used for disease diagnosis and prognosis, that is identify patients with disease, or indicate the future course of a disease, respectively. Biomarkers can also be used as a tool for staging of the disease, monitoring a response to targeted treatment, or providing a basis for the selection of candidates for clinical trials (BDWG, 2001). The ideal biomarker for AD should reflect or indicate AD pathology and be validated by autopsy-confirmed cases; be measurable as early as possible in the course of the disease, ideally at preclinical stages; and it should be precise in terms of sensitivity and specificity (>80%) (defined in section 3.4). Additionally, a good biomarker for AD should be non-invasive, simple to perform, inexpensive, reliable and suitable for large-scale screenings (The

RNRRIAA & NIA Working group, 1998). A candidate biomarker also needs to be validated by further studies, in which the results must be reproduced by other researchers (Humpel, 2011).

Current laboratory and neuroimaging procedures can identify AD pathology, and can therefore serve as *in vivo* biomarkers of AD. The biomarkers can constitute a biological signature that indicates specific pathological features characterizing AD. In other words, biomarkers can function as surrogates for pathophysiological lesions in AD. Biomarkers for AD have been described using a range of tools, including neuroimaging, genotyping of genetic polymorphisms known to be associated with disease risk (e.g. *APOE* ε4), and quantification of the abundance of specific proteins in cerebrospinal fluid (CSF) or in blood. At present, the most widely studied and well-established AD biomarkers are the brain imaging measures amyloid positron emission tomography (PET), [^{18}F]-fluorodeoxyglucose (FDG)-PET, and structural MRI, in addition to the CSF proteins Aβ42 and tau. Together, these markers are considered the five major biomarkers of AD at present (Jack, 2012), and will be further discussed in the following sections.

1.5.1 Neuroimaging biomarkers

Neuroimaging provides a non-invasive set of methods for obtaining visual information about the topography and extent of brain pathology in AD. Two types of imaging biomarkers can be distinguished; pathophysiological and topographical markers (Dubois et al., 2010). The first category corresponds to specific pathological changes (amyloid plaques, neurofibrillary tangles) characterizing AD, and includes amyloid PET. Topographical markers are used to assess the less specific changes, measuring neuronal dysfunction and brain atrophy, particularly in regions that are the most vulnerable to the pathophysiological process. These include FDG-PET and structural MRI.

1.5.1.1 Structural MRI: imaging brain atrophy as a biomarker for AD neurodegeneration

Structural MRI is the most widely used neuroimaging technique to investigate *in vivo* structural changes and neurodegeneration associated with AD. As mentioned in section 1.4.1.3, structural MRI can provide measures of cerebral atrophy in AD, reflecting loss of neurons and synapses (Bobinski et al., 2000). Atrophy shown on MR images is not specific for AD, and does not reveal the underlying pathology. Yet, because distinct regions of the brain are primarily affected, whereas other parts of the brain are spared at least at the early stages, the specific patterns of atrophy are consistent with AD. As reviewed by Jagust (2006), many studies have shown that MRI measurements of hippocampal atrophy can distinguish AD patients from cognitively normal elderly controls with 80-90% accuracy.

1.5.1.2 FDG-PET: imaging brain glucose uptake as a biomarker for synaptic dysfunction

FDG is an analog of glucose, with the positron-emitting radioactive isotope fluorine-18 substituted for a normal hydroxyl group in the glucose molecule. After injecting this metabolic tracer into a

patient, a PET scanner can form images of cerebral glucose metabolism, known to be closely coupled to neuronal function. Although cerebral glucose metabolism clearly involves many neural and glial functions, FDG-PET measures have been suggested to predominantly indicate synaptic activity (Attwell and Laughlin, 2001). Synaptic and neuronal dysfunction lead to a reduced energy demand, reflected by reduced glucose metabolism in the affected parts of the brain. FDG-PET studies in AD patients show a typical pattern of reduced glucose uptake in the parietal and temporal association cortices, particularly in the region of the posterior cingulate cortex, a pattern often distinct from normal aging and other dementias (Minoshima et al., 1997, Silverman et al., 2001, Herholz et al., 2002, Langbaum et al., 2009). More impaired AD patients also show hypometabolism in the frontal lobe and prefrontal cortex relative to less impaired patients and healthy elderly individuals (Mosconi, 2005). Combined imaging and autopsy studies have demonstrated good correlation between ante-mortem FDG-PET diagnosis of AD and post-mortem confirmation (Hoffman et al., 2000). For distinction of AD patients from healthy individuals by FDG-PET measurements, a sensitivity and specificity of 93% have been reported (Herholz et al., 2002).

1.5.1.3 Amyloid PET: imaging fibrillar Aβ as a biomarker for AD plaque deposition

The radioactive tracer named [^{11}C]-Pittsburgh compound B (PiB) can be used in PET scans to image Aβ deposition *in vivo*. PiB crosses the blood-brain barrier rapidly after intravenous administration, and binds with high affinity and high specificity to insoluble, fibrillar Aβ in neuritic plaques (Klunk et al., 2004, Ikonomovic et al., 2008). AD patients typically show increased retention of PiB compared with normal elderly controls (Klunk et al., 2004, Rowe et al., 2007), illustrated in Figure 1.8.

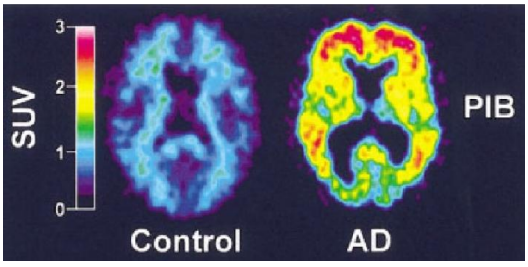

Figure 1.8 *Amyloid imaging in AD. High retention of [^{11}C]-Pittsburgh compound B (PiB) recorded in a 79-year-old with Alzheimer's disease (right), while a 67-year-old healthy control subject (left) exhibited low retention of the radioligand. Standardized uptake values (SUV) are expressed in a colour scale, with red indicating high retention (Klunk et al., 2004).*

The retention of PiB in brains of AD patients shows a regional distribution that is very similar to the distribution of Aβ deposits observed post-mortem, supporting the validity of PiB-PET imaging as a method for *in vivo* evaluation of Aβ plaque burden (Ikonomovic et al., 2008). In addition to PiB, several other PET tracers have been developed and used to image amyloid in AD patients, such as [^{18}F]-florbetapir (Clark et al., 2011). The ^{11}C-labeled compounds such as PiB have limitations for use in the clinic because of their short half-life. ^{18}F-labeled tracers have a longer half-life, and are therefore more suitable for clinical use, and to make amyloid PET imaging more broadly available (Nordberg et al., 2010).

1.5.2 Core CSF biomarkers for AD

CSF is a translucent bodily fluid that occupies the subarachnoid space and the ventricular system around the brain and spinal cord. Separating the ventricles from the nervous tissue of the brain is a single-cell layer epithelium of ependymal cells called the ependyma. By the means of modified tight junctions between these cells, the ependyma behaves like a selectively permeable sieve that allows fluid exchange between the CSF and nervous tissue of the brain (Del Bigio, 1995). As a result, biochemical changes in the brain may be reflected in the CSF, making it a relevant source of AD biomarkers. Moreover, CSF can be obtained by lumbar puncture, and though invasive the risk of complication is low (Zetterberg et al., 2010). Potential CSF biomarkers for AD have been extensively studied. The most consistent findings have been obtained with the measurement of CSF concentrations of Aβ42, total tau (T-tau), and phosphorylated tau (P-tau), reflecting core pathophysiological features of the disease. AD patients characteristically display significantly low concentrations of Aβ42 and high concentrations of T-tau and P-tau in CSF (Blennow, 2004).

1.5.2.1 T-tau in CSF reflects the degree of neuronal and axonal degeneration

Enzyme-linked immunosorbent assays (ELISA) have been developed that measure the total levels of tau in CSF, independently of phosphorylation (Blennow et al., 1995, Mori et al., 1995). Numerous publications have consistently found that the CSF concentration of T-tau is increased approximately 300% in AD patients compared to levels in cognitively normal elderly subjects (Blennow et al., 2001). The increased levels could be due to the release of tau from degenerating neurons and its subsequent diffusion into the CSF (Mandelkow and Mandelkow, 1998), as illustrated in Figure 1.9. Since tau is a normal axonal protein, the increased levels are thought to reflect the degree of neuronal and axonal degeneration (Blennow et al., 1995). This suggestion is supported by several findings. First, a marked transient increase in CSF T-tau is found after acute ischemic stroke, which causes neuronal damage and death. A positive correlation between CSF T-tau and infarct size has also been reported (Hesse et al., 2000). Secondly, the degree of increase in CSF T-tau is higher in disorders with more extensive or rapid neuronal degeneration, as is the case in patients with Creutzfeldt-Jakob disease (Otto et al., 1997). A moderate to marked increase is found in AD with less intense neurodegeneration (Andreasen et al., 1999), while normal levels are found in patients with depression, where there is limited or no degeneration (Blennow et al., 1995).

CSF T-tau has consistently been found to have a high sensitivity and specificity, often 80-90%, for distinguishing AD from elderly healthy controls (Blennow et al., 2001). However, CSF T-tau has a limited potential to discriminate AD from other dementias, or neurodegenerative disorders in general, something that is not surprising given that the biomarker is thought to reflect the degree of neuronal damage (Hulstaert et al., 1999).

1.5.2.2 P-Tau is thought to reflect tangle pathology

Several different methods have been developed for measuring levels of tau phosphorylated at different amino acids, including ELISA. CSF concentration of P-tau has been found to be increased in AD using all of these different methods, with levels around 200% of controls, as summarized in a review by Blennow (2004). The most common ELISA assays for P-tau in CSF use antibodies specific for either tau phosphorylated at threonine 181 (P-tau_{181}) or threonine 231 (P-tau_{231}) (Kohnken et al., 2000, Vanmechelen et al., 2000). Whether there are any phosphorylation sites that are specific to AD and hence not found in other tauopathies, is not certain. At a specificity level of 91%, the mean sensitivity of CSF P-tau to discriminate AD from elderly controls is about 81% (Blennow, 2004). This marker is considered to be more specifically associated with AD, given the central role of tau hyperphosphorylation in the formation of neurofibrillary tangles. Indirect evidence suggests that the CSF level of P-tau probably reflects the phospohorylation state of tau, and thus possibly the formation of neurofibrillary tangles in the AD brain (Figure 1.9). Elevated CSF P-tau levels measured ante mortem have been shown to correlate with neurofibrillary tangle load post mortem (Buerger et al., 2006). Moreover, in contrast to a very marked increase in T-tau after acute stroke and in Creutzfeldt-Jakob disease, P-tau levels in these conditions are normal and remain largely unchanged (Hesse et al., 2001, Riemenschneider et al., 2003). It therefore seems that P-tau in CSF is not simply a marker for neuronal degeneration or damage, but that it specifically reflects the phosphorylation state of tau, and thus possibly the formation of neurofibrillary tangles. Potentially, CSF P-tau is thereby a more specific biomarker for AD than CSF T-tau, and may be useful in differential diagnostics compared to other dementias (Genius et al., 2012).

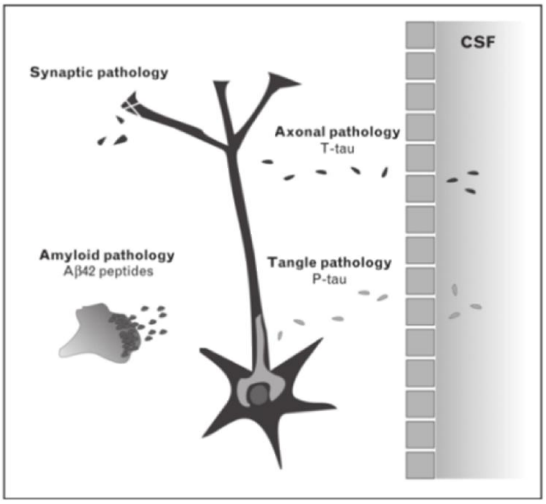

Figure 1.9 *The cerebrospinal fluid biomarkers total tau (T-tau), phosphorylated tau (P-tau) and amyloid-beta 42 (Aβ42) reflect the core pathologic features of Alzheimers's disease; axonal, tangle and amyloid pathology, respectively. Figure modified from Rosen and Zetterberg (2013).*

1.5.2.3 CSF Aβ42 reflects amyloid pathology

A decrease in the concentration of CSF Aβ42 to about 50% of the level in cognitively normal elderly subjects has been regularly reported in AD patients (Blennow, 2004). No major change has been detected in CSF Aβ40; some studies report unchanged Aβ40 levels, while other have demonstrated slightly increased levels in AD patients (Shoji et al., 1998, Mehta et al., 2000). However, a marked decrease has been observed in the Aβ42/Aβ40 ratio (Mehta et al., 2000, Hansson et al., 2007). The reduction in Aβ42 is thought to reflect the deposition of the peptide in plaques, with lower levels diffusing to the CSF. This is supported by the finding of an inverse relationship between *in vivo* amyloid brain load and CSF Aβ42. The greater the amyloid load, the lower the concentration of CSF Aβ42 (Fagan et al., 2006). Furthermore, the number of amyloid plaques at brain autopsy has been found to inversely correlate with CSF Aβ42 concentrations both post mortem (Strozyk et al., 2003) and ante mortem (Tapiola et al., 2009). As summarized by Blennow (2004), the mean sensitivity of CSF Aβ42 to discriminate between AD and healthy elderly controls is 86%, at a specificity level of 89%. Normal CSF Aβ42 is also found in depression, and in some chronic neurological disorders. However, a mild to moderate reduction in CSF Aβ42 is found in some patients with other dementias, indicating that the biomarker is somewhat unspecific for AD. Nevertheless, the combination of two or the three core biomarkers results in increased diagnostic performance compared with any one of them alone (Johansson et al., 2011).

1.6 Staging and progression of pathophysiological changes

1.6.1 The pathophysiological process starts long before clinical symptoms

Clinicopathological and biomarker studies have revealed that AD pathology can be detected more than a decade before the first symptoms appear, demonstrating that the pathological processes start long before the clinical onset of dementia (Price and Morris, 1999, Thal et al., 2002, Bateman et al., 2012). These findings suggest that dementia is a late stage of the disease process, and that there is a long *preclinical* phase before the presentation of cognitive decline. During this preclinical phase the pathological changes gradually accumulate in affected brain areas, and at a certain (currently undetermined) threshold the first symptoms appear, most often as impaired episodic memory (Small et al., 2000).

1.6.2 Biomarkers as a framework for *in vivo* staging of the disease

Advances in neuroimaging, and CSF biomarkers provide the ability to detect evidence of the AD pathophysiological process *in vivo*. Based on the idea that these processes may be temporally ordered, several biomarker-based models illustrating progression from normal ageing to AD have been proposed (Jack et al., 2009, Perrin et al., 2009, Jack et al., 2010, Jack et al., 2013). Figure 1.10

shows a hypothetical model of changes in CSF biomarkers in relation to the time course of pathological and clinical stages. During the asymptomatic, preclinical phase, plaques, and subsequently tangles, accumulate and there is a gradual neuronal loss. The accumulation of neurofibrillary tangles drives neurodegeneration during and just before the clinical phase. Only when substantial neuronal and synaptic loss have taken place do the earliest clinical symptoms become apparent. At this stage patients do not fulfil the criteria for dementia and may be diagnosed with mild cognitive impairment (MCI), which will be further discussed in section 1.7.2. When dementia is diagnosed, neuronal integrity is already severely compromised after years of gradual degeneration.

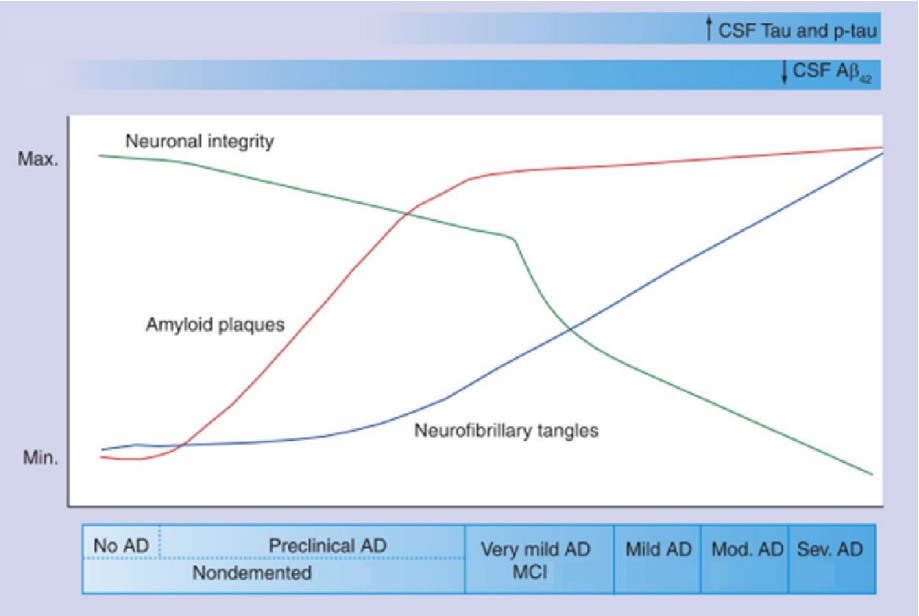

Figure 1.10 *Proposed changes in biomarkers in relation to time course of pathological and clinical stages in Alzheimer's disease (AD). In the preclinical phase, plaques, and subsequently neurofibrillary tangles, accumulate for many years before the synaptic and neuronal loss manifest as cognitive decline. The clinical stages of AD are associated with abundant amyloid plaques (red line), gradual accumulation of neurofibrillary tangles (blue line), and synaptic and neuronal loss in certain brain regions (green line). Figure modified from Fagan and Holtzman (2010).*

Jack et al. (2013) propose an expanded model that incorporates the five major AD biomarkers (Figure 1.11). The model describes the temporal evolution of AD biomarkers in relation to each other and to the progression of clinical symptoms. The five biomarkers are suggested to become abnormal in a temporally ordered manner. As illustrated in Figure 1.11, biomarkers reflecting Aβ deposition (amyloid PET and CSF Aβ42 measures) become abnormal first, before neurodegeneration and clinical symptoms occur. Biomarkers of neuronal injury, dysfunction, and neurodegeneration (CSF tau, FDG-PET and structural MRI) become abnormal later in the disease course, and correlate with clinical symptom severity. Jack and co-workers themselves acknowledge that the temporal courses in the figure may be modified as new data are available.

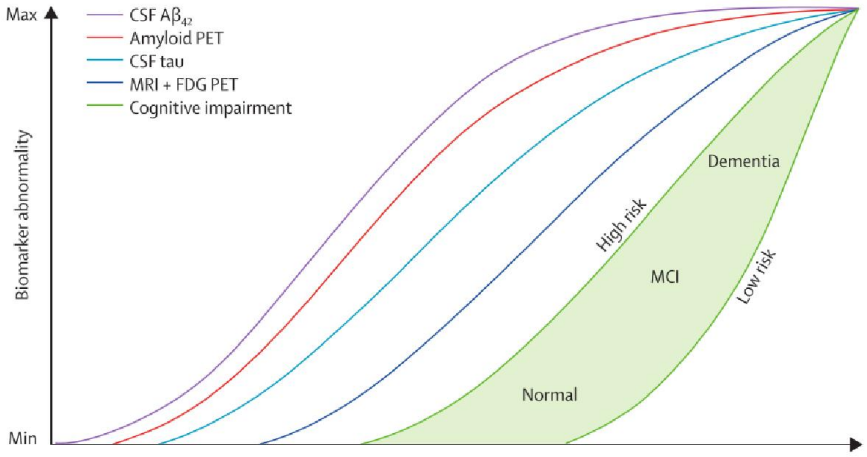

Figure 1.11 *Hypothetical model of dynamic biomarkers of the Alzheimer's disease pathological cascade. The horizontal axis expresses time. Cognitive impairment is illustrated as a zone (light-green-filled area) with low-risk and high-risk borders (Jack et al., 2013).*

This model takes several aspects into account; (1) the fact that time from disease onset to end, and the specific age of disease onset, vary among individuals, and (2) the fact that individuals respond differentially to pathological features of AD. As illustrated in Figure 1.11, the cognitive impairment curve is shifted to the left in time for people with at high risk of cognitive impairment due to AD pathology, meaning that they might carry more genetic risk alleles, have low cognitive reserve, or have other simultaneous pathological changes in the brain. On the contrary, low-risk individuals can display substantial AD pathology and still maintain cognitive function (Jack et al., 2013).

1.7 Characterizing the early stages of AD

1.7.1 Early detection of AD is crucial for early intervention

The acknowledgment that the pathophysiological process starts long before dementia has important implications for the development of AD therapeutic and diagnostic strategies. According to the 1984-criteria, AD can only be diagnosed clinically if a patient meets the criteria of having dementia. Based on preliminary findings from clinical trials that have failed to improve cognition (Holmes et al., 2008, Salloway et al., 2014, Doody et al., 2014), concerns have been made that anti-amyloid approaches in patients that have progressed to dementia might be "too little too late", owing to severe neuronal and synaptic loss at this stage of disease. Disease-modifying therapies are more likely to be effective if initiated during the early stages of AD, before significant neurodegeneration has occurred (Caselli and Reiman, 2013). Thus, there is an urgent need for methods to accurately identify individuals affected by AD in the pre-dementia stage (prodromal AD), or even in the asymptomatic phase of the disease (preclinical AD).

1.7.2 MCI as a prodromal condition for AD

In general, MCI refers to individuals who have some cognitive impairment but of insufficient severity to interfere with daily life or independent function, and thus do not meet diagnostic guidelines of dementia. As many patients will progress to dementia, MCI can be regarded as a transitional stage between normal aging and dementia. However, MCI is a heterogeneous syndrome and may be caused by several different disorders in addition to AD and other forms of dementia. People can also have a stable form of MCI, and some even return to normal over time. Several different subtypes of MCI exist; amnestic MCI (aMCI) and non-amnestic MCI (naMCI) each with single and multidomain subclasses. The amnestic subtype, involving a memory impairment, has a particularly high risk of progression to AD, and may be considered as the prodromal condition for AD (Petersen, 2004).

So far, there is no definite method to differentiate who will convert from MCI to AD dementia, but studies indicate that biomarkers can serve as tools to determine true prodromal AD cases. CSF biomarkers have been demonstrated to predict incipient AD with much higher accuracy than other established risk factors including age, sex, education and *APOE* genotype (Hansson et al., 2006). Studies with long clinical follow-up periods have shown that the combination of high CSF levels of T-tau and P-tau, and low levels of Aβ42, has sensitivity and specificity levels of about 80-90% for identifying cases of prodromal AD in individuals with MCI (Hansson et al., 2006, Buchhave et al., 2012, Hertze et al., 2010). Buchhave et al. (2012) performed an extended follow-up of the cohort from the Hansson et al. (2006) study, and showed that approximately 90% of patients with aMCI and pathologic CSF biomarker levels at baseline developed AD within 9 to 10 years. Imaging biomarkers have also proven to be very useful in the detection of early stages of AD. For instance, studies have shown that MRI measurements of hippocampal atrophy and reduced glucose metabolism detected by FDG-PET can predict conversion from aMCI to AD with high accuracy (Nordberg et al., 2010, Frisoni et al., 2010).

1.7.3 Preclinical AD is the long asymptomatic stage preceding cognitive impairment

The preclinical state of AD refers to the long asymptomatic period during which the pathophysiological process is progressing, but is not yet severe enough to affect cognition. Biomarkers can provide *in vivo* evidence of early AD. Individuals with biomarker evidence are at increased risk for developing cognitive decline and progression to AD dementia, but this does not mean that they necessarily will (Sperling et al., 2011). Two preclinical states of AD can be distinguished; “asymptomatic at-risk for AD” and “presymptomatic AD”. Asymptomatic at-risk for AD refers to individuals with biomarker evidence of AD pathology, whereas presymptomatic AD is designated to individuals who will develop AD because they carry familial genetic autosomal dominant mutations (Dubois et al., 2010). Based on current knowledge, it is hypothesized that the

earliest detectable pathological change is in the form of Aβ accumulation. Some studies have investigated whether CSF biomarkers may be useful to predict AD in the preclinical stage. Findings showed a significant reduction in CSF Aβ42 (in cognitively normal elderly that later developed dementia), but no significant change in CSF T-tau or P-tau (Gustafson et al., 2007, Skoog et al., 2003). Another clinical study also found that CSF Aβ42, but not T-tau and P-tau, predict cognitive decline in healthy elderly individuals (Stomrud et al., 2007). However, it is possible that Aβ accumulation is necessary, but not sufficient, to produce the clinical manifestations of AD (Sperling et al., 2011). In contrast to the model by Jack et al. (2013), findings suggest that early synaptic changes may be detected by PET even earlier than evidence of amyloid accumulation using currently available amyloid markers. FDG-PET measurements in young adults have revealed a pattern of reduced cerebral glucose metabolism that is topographically similar to FDG-PET patterns of AD itself but less severe, particularly in individuals carrying *APOE* ε4 (Reiman et al., 2004).

The preclinical stage provides a critical opportunity for therapeutic intervention. However, treating asymptomatic individuals because they might one day develop AD is challenging in many ways, not least of all ethical, and first demands a better understanding of the link between the appearance of any specific biomarker in asymptomatic individuals and the subsequent emergence of clinical symptoms (Sperling et al., 2011, Caselli and Reiman, 2013). Even though the preclinical phase of AD is currently not easily detected, the identification of pathological changes that have already taken place prior to the onset of aMCI must have occurred during the preclinical period. Identification of parameters that have altered during and prior to the prodromal period is therefore essential for future preventive therapy.

1.8 AD is more than dementia: revising research criteria for AD diagnosis and restating the definition of AD

According to the 1984-criteria, AD cannot be diagnosed clinically before the disease has progressed to dementia. This means that the symptoms must be severe enough to significantly interfere with daily life, such as work and social activities. For many years, research into AD focused on dementia as this was integral to the 1984-criteria. In the past three decades, there has been an exceptional growth of scientific knowledge and the understanding of the genetics, pathogenic events and course of AD has advanced greatly. The developments have led to the need for updated research criteria. Two sets of criteria and guidelines for the diagnosis of AD have been proposed; one set from the International Working Group (IWG) published in 2007 (Dubois et al., 2007) and revised in 2010 (Dubois et al., 2010), and one set published by the National Institute on Aging and the Alzheimer Association (NIA-AA) (McKhann et al., 2011).

Both sets of new criteria emphasize that the AD pathophysiological process precedes clinical dementia by years or decades, and that biomarkers can be used to detect underlying AD pathology. With the means of biological biomarkers, the diagnosis can be made on the basis of both clinical and *in vivo* biological evidence, with a very high level of sensitivity and specificity. The criteria constructed by Dubois et al. (2007) are based on a clinical core of early and significant episodic memory impairment (amnestic syndrome of the hippocampal type), together with the detection of one or more abnormal biomarkers, including MRI, PET, and CSF biomarkers. The presence of dementia will no longer be required. Important for the new proposed criteria are the fact they are not restricted to the dementia syndrome, but also capture the prodromal stage of AD. The revised criteria would allow diagnosis when symptoms first appear, thus supporting earlier intervention.

The new diagnostic framework proposed by Dubois et al. (2007) stimulated debate about the definition of AD and related conditions. In 2010, the International Working Group therefore published a new lexicon for AD, intended to clarify and restate the definition of AD and related states. They proposed to consider AD as a clinical symptomatic entity that encompasses both prodromal and dementia phases, where the diagnosis relies on both clinical and biological evidence, and the clinical phenotype can be *typical* or *atypical* (Table 1.1).

Table 1.1 *Comparative features of the different conditions described in the lexicon according to the new research criteria framework (Dubois et al., 2010).*

	AD diagnosis	**Presence of impairment on specific memory test**	**Evidence of biomarkers in vivo**	**Additional requirements**
Prodromal AD	Yes	Required	Required	Absence of dementia
AD dementia	Yes	Required	Required	Presence of dementia
Typical AD	Yes	Required	Required	None
Atypical AD	Yes	Not required	Required	Specific clinical presentation
Mixed AD	Yes	Required	Required	Evidence of comorbid disorders
Preclinical AD				
Asymptomatic at risk for AD	No	Not present	Required	Absence of symptoms of AD
Presymptomatic AD	No	Not present	Not required	Absence of symptoms of AD and presence of monogenic AD mutation

Typical AD represents individuals with the classic clinical phenotype of AD characterized by an early episodic memory loss, and who also have one or more positive biomarkers of AD pathology (Dubois et al., 2010). There are also less common, but well defined clinical phenotypic variant presentations of AD that do not follow the typical pattern, but still occur with AD pathology. These patients present with symptoms such as disturbances of language, spatial skills, vision and visual perception (Alladi et

al., 2007), and are therefore characterized as having an atypical form of AD. Moreover, some AD patients may exhibit a "frontal" behavioural picture which can be mistaken for frontotemporal dementia. These atypical presentations, where amnesia is not the prominent symptom, are frequently referred to as "focal" presentations of AD (Alladi et al., 2007, Snowden et al., 2007). Studies have suggested that 10-25% of patients will not follow the classic AD pattern of cognitive deficits (Lopez et al., 2000, Snowden et al., 2007). The International Working group also introduced the designation *mixed* AD, referring to patients who fulfil the diagnostic criteria for typical AD, but additionally present with clinical or biological evidence of other comorbid disorders (Dubois et al., 2010).

Because there are some substantial differences between the two proposed sets of *research* criteria published by the IWG and NIA-AA, efforts to harmonize the *diagnostic* criteria for AD have recently been made by a group in which both the IWG and NIA-AA were represented (Morris et al., 2014). New diagnostic criteria will in time replace the current criteria from 1984. The group recommended defining AD as a brain disorder regardless of clinical status, and to refer to the clinically expressed disorder, including its prodromal stages, as *symptomatic* AD. It was also suggested to allow non-amnestic, atypical presentations to be included as symptomatic AD, especially when supportive biomarker evidence exists. Lastly, the group recommended that the use of biomarkers in diagnosis should be considered after standardization of CSF and imaging biomarkers has been accomplished.

1.9 Biomarker discovery is a rapidly advancing area of AD research

In light of the suggested revisions to the diagnostic criteria for AD, biomarkers will become increasingly important in research, clinical trials, and clinical practice. Efforts to discover novel biomarkers that may aid in the early diagnosis of AD are ongoing. Among many promising candidate markers, none has so far fully met the criteria for an ideal AD biomarker.

1.9.1 CSF and neuroimaging biomarkers are most well-established, but there are limitations for clinical screening

Established biomarkers of AD from CSF (Aβ42, T-tau and P-tau) and neuroimaging (amyloid PET, FDG-PET, and structural MRI) meet several of the criteria for ideal AD biomarkers. Not only do they reflect key pathological changes characteristic of AD, but also compare well with results from studies performed on patients in which the diagnosis of dementia was confirmed at autopsy (Clark et al., 2003, Koopman et al., 2009, Shaw et al., 2009). They provide high diagnostic accuracy both for AD with dementia and to predict prodromal AD, and have been incorporated (once they are validated) into the suggested revision of the diagnostic guidelines for AD. Combining different biomarker modalities, such as imaging techniques and CSF analysis, provides even more accurate early and

differential diagnosis (Walhovd et al., 2010), and new biomarkers may support their diagnostic performance.

Even though the established CSF and neuroimaging biomarkers show the most promise, barriers for clinical applications exist. There has been a lack of standardization in the field of biomarkers, including methods for standardized extraction of quantitative information from images (Jack, 2012), and the application of standardized "cut-off" values for fluid-based biomarkers. As reviewed by Blennow et al. (2010), CSF biomarker levels between laboratories and studies vary, which could be due to variations in analytical procedures and/or batch-to-batch variation in the biomarker assays. Different assays often correlate but give different absolute concentrations of the protein, preventing the use of global reference limits and diagnostic cut-off values. Effort to establish standardized CSF biomarker measurements is ongoing (Carrillo et al., 2013). Furthermore, CSF measurements are time-consuming, and thereby expensive to perform. In addition, lumbar puncture is an invasive practice and impractical for screening populations at increased risk. Neuroimaging is also expensive to perform routinely, and there is a limited availability of PET scanners in many clinical settings. Thus, CSF and brain imaging biomarkers have limitations concerning application for large-scale screening. (Hampel et al., 2008, Henriksen et al., 2013). The remaining need for a reliable, minimally-invasive and inexpensive biomarker makes the possibility of finding biomarkers for AD in more easily-available fluids tempting.

1.9.2 Blood-based biomarkers are attractive

Because blood collection is simple and inexpensive, some researchers have suggested that blood-based biomarkers should be the first step in a multistage screening and diagnostic process for AD, to be followed by neuroimaging of the brain or CSF protein assessments (Schneider et al., 2009, Henriksen et al., 2013). The measurement of biomarkers for AD in blood is complicated by the presence of the blood-brain barrier, which limits the transportation of proteins between the brain and the blood. The small amounts of brain proteins that may enter the blood are diluted in the large plasma volume, and are exposed to degradation by proteases and clearance in the liver or kidneys. Thus, the obstacles to the identification of blood-based biomarkers for AD are many, and so far, no blood-based biomarkers have been validated (Henriksen et al., 2013).

1.9.3 Biomarker candidates in CSF and blood

Several candidate CSF and blood biomarkers have been investigated, but so far findings have often been difficult to verify in independent studies (Blennow et al., 2012). As reviewed by Blennow et al. (2010), plasma Aβ has been the most extensively studied peripheral biomarker for AD, but the findings are inconsistent. The variation in results might be due to the hydrophobic nature of Aβ,

increasing its binding to several plasma proteins (Kuo et al., 1999). Besides, Aβ is produced in the periphery by blood platelets (Chen et al., 1995), and there seems to be no correlation between plasma levels of Aβ40 or Aβ42 and CSF levels (Mehta et al., 2001). Some recent studies have found panels of multiple plasma biomarkers that successfully differentiated between AD patients and controls (Ray et al., 2007, Doecke et al., 2012) or were associated with MCI or AD (Hu et al., 2012). Although promising, some of these findings have been difficult to reproduce across studies (Bjorkqvist et al., 2012).

Because oligomeric forms of Aβ are suggested to be critical in the pathological cascade, there is ongoing work to develop CSF and plasma assays for Aβ oligomers. Attempts to measure oligomers in CSF have successfully been made with several methods, but with inconsistent results (Georganopoulou et al., 2005, Klyubin et al., 2008, Fukumoto et al., 2010). CSF level of Aβ oligomers have been demonstrated to be very low and thereby very difficult to quantify in a reliable manner. Also, in the wide range in size from dimers to protofibrils, it is important to determine which oligomers are pathologically relevant, and studies therefore need to be specific when addressing what species have been measured to make comparison of data between different research groups possible (Benilova et al., 2012). It has been suggested that the 43 amino acid Aβ species, Aβ43, is in addition to Aβ42, a pivotal species in the early pathogenesis of AD (Zou et al., 2013), and might therefore serve as an additional candidate CSF biomarker. Another potential CSF biomarker for AD is the cytoskeletal protein neurofilament-light (NF-L), further discussed in section 1.10.4.

APOE ε4 is the only firmly established genetic susceptibility marker for sporadic AD, but because it is neither sufficient nor necessary to develop AD, it has no diagnostic value as a biomarker. However, because *APOE* ε4 can affect the activity or level of expression of other biomarkers, it is included as a co-variable in many biomarker studies (Hampel et al., 2008). Results also indicate that peripheral blood levels of ApoE may reflect disease status, suggesting plasma or serum ApoE as a potential biomarker for AD (Wang et al., 2014). Another apolipoprotein that has been linked to the pathogenesis of AD, and proposed as a candidate biomarker, is apolipoprotein J (ApoJ), also called clusterin (Bhamra and Ashton, 2012). The list of potential candidates for genetic risk factors for AD besides *APOE* ε4 is long, and one of those suggested is the gene for angiotensin-converting enzyme (*ACE*). A potential relationship between *ACE* and AD was first suggested by a study reporting that an insertion(I)/deletion(D) polymorphism within intron 16 of the *ACE* gene was associated with AD (Kehoe et al., 1999). ApoE, clusterin, ACE, and NF-L levels in CSF and blood will be discussed in the following section.

1.10 CSF and serum or plasma levels of proteins implicated in the pathophysiology of AD

1.10.1 Apolipoprotein E and levels in blood

Various organs express ApoE, though the highest expression is found in the liver, followed by the brain where it is mostly synthesized by astrocytes (Mahley, 1988). ApoE exists mainly as a component of particles called lipoproteins, into which a variety of lipids can be packed for transportation in the blood or CSF (Roheim et al., 1979), as illustrated in Figure 1.12. ApoE is one of several different classes of apolipoproteins providing lipoprotein particles with stability, and directing their transport, delivery, and distribution from one tissue to another. ApoE serves as a ligand for low density lipoprotein receptors initiating endocytosis of lipoprotein particles (Mahley, 1988). Brain ApoE is believed to play a role in the redistribution of lipid and cholesterol during membrane repair and synaptic plasticity (Mauch et al., 2001).

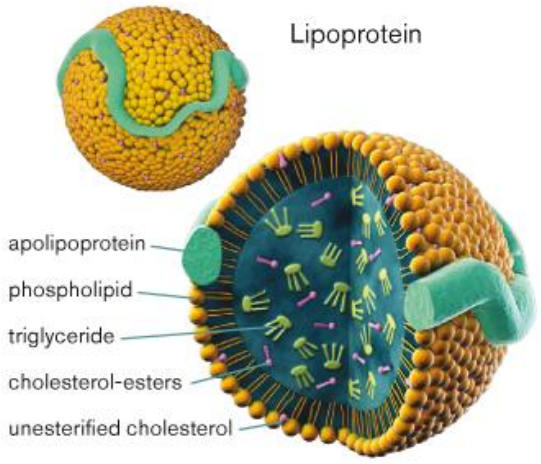

Figure 1.12 Apolipoproteins and phospholipids together form particles called lipoproteins. Lipoprotein particles function to package insoluble lipids for transportation in the blood or cerebrospinal fluid. *Figure from: https://www.mabtech.com/knowledge-center/applied-research/apolipoproteins.*

The strong effect of *APOE* alleles on the risk of developing AD has led many to investigate if ApoE protein levels are altered in AD. As summarized in a review by Kim et al. (2009), studies of CSF ApoE levels in humans remain inconsistent. The majority of studies reported on plasma or serum ApoE levels in AD patients have demonstrated lower levels than healthy controls, supported by a recent meta-analysis (Wang et al., 2014). When *APOE* genotype has been taken into consideration, studies have shown that *APOE* ε4 carriers were found to be associated with lower plasma ApoE levels whereas ε2 carriers were associated with higher levels (Soares et al., 2012, Gupta et al., 2011). It has also been demonstrated that *APOE* ε4 carriers have lower CSF Aβ42 and show more PiB binding on PET than do non-ε4 carriers (Prince et al., 2004, Head et al., 2012).

1.10.2 Clusterin and levels in CSF and blood

Clusterin is a ubiquitous glycoprotein that interacts with a wide variety of molecules and has multiple functions. Like ApoE, clusterin is present in lipoprotein particles and regulates cholesterol and lipid metabolism. The suggested main function of clusterin is to act as a chaperone molecule, primarily in the extracellular space but also in cytoplasmic and nuclear compartments during cellular stress (Wu et al., 2012). Important functions of chaperones are to stabilize stressed protein structures, and prevent both newly synthesized polypeptide chains and assembled subunits from aggregating into non-functional structures. As reviewed by Nuutinen et al. (2009), the expression of clusterin is up-regulated by a wide variety of stress and cellular injuries as well as cellular growth and differentiation. Increased expression of clusterin has repeatedly been observed in the brains of AD patients, and extensive literature has linked clusterin to the pathogenesis of AD (Figure 1.13).

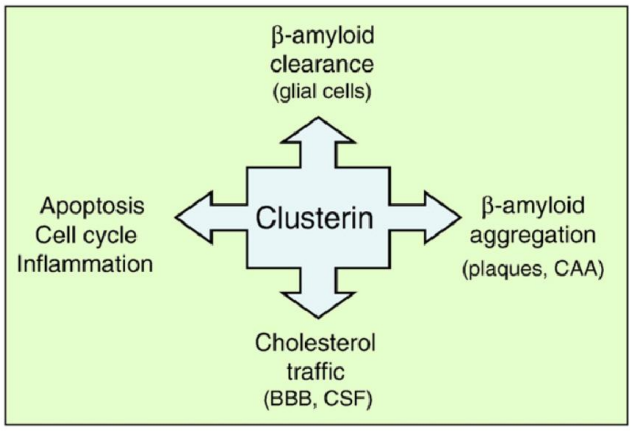

Figure 1.13 *The major functions of clusterin in Alzheimer's disease. BBB=blood-brain barrier, CAA=cerebral amyloid angiopathy, CSF=cerebrospinal fluid. Figure from Nuutinen et al. (2009).*

As reviewed by Nuutinen et al. (2009), clusterin has, like ApoE, been demonstrated to be co-deposited in amyloid plaques in the brain of AD patients. Studies have reported that clusterin can bind Aβ peptides and prevent their aggregation and fibril formation. Clusterin also enhances clearance of Aβ peptides, either by facilitating their transport across the blood-brain barrier or via local endocytosis and degradation within glial cells. Furthermore, clusterin is a complement inhibitor and can suppress the complement activation observed in AD. Activation of the complement system plays a key role in the normal inflammatory response to injury, but may cause substantial damage when activated inappropriately. In addition, intracellular clusterin can bind to proteins to inhibit neuronal apoptosis and reduce oxidative stress. In light of these findings, clusterin has been hypothesized to play a protective role in AD and neuroinflammation, but it is apparently unable to prevent the progressive neuropathology in AD (Nuutinen et al., 2009).

Studies have shown increased clusterin protein levels in affected areas of the AD brain (Oda et al., 1994, Bertrand et al., 1995, Lidstrom et al., 1998). Reports on levels of clusterin in CSF, however, have been inconclusive (Harr et al., 1996, Lidstrom et al., 2001, Nilselid et al., 2006). Plasma clusterin has been found to be both elevated (Schrijvers et al., 2011) and unchanged (Liao et al., 2007) in AD.

1.10.3 Angiotensin-converting enzyme polymorphism and levels in CSF and blood

ACE is a proteolytic peptidase normally expressed by endothelial, epithelial and neuronal cells. As reviewed by Coates (2003), ACE plays a key role in the renin-angiotensin system which controls blood pressure by regulating the volume of fluids in the body. By catalyzing the formation of the potent vasoconstrictor angiotensin II from its vasoinactive precursor angiotensin I, and degrading the vasodilator bradykinin, ACE causes blood vessels to constrict and thereby increase blood pressure (Coates, 2003). This activity can be blocked by ACE-inhibitors, which have thereby become one of the standard treatments for hypertension. The most well-documented polymorphism in the *ACE* gene involves the presence (insertion, I) or absence (deletion, D) of a sequence of DNA in intron 16 (Rigat et al., 1990), forming three possible genotypes: II, ID or DD. The researchers that first reported the polymorphism, also found that it contributed to the variability in circulating ACE levels. Serum ACE levels in DD carriers were approximately twice as high compared to the observed levels in II carriers, while subjects with genotype ID had intermediate levels (Rigat et al., 1990).

ACE has been implicated in AD, but the enzyme's role in AD pathophysiology remains controversial. The level and activity of ACE within the cerebral cortex tissue are generally found to be elevated in AD (Barnes et al., 1991, Miners et al., 2008). Findings concerning levels and activity of ACE in CSF are inconsistent (He et al., 2006, Nielsen et al., 2007, Miners et al., 2009). As suggested by Miners et al. (2010), increased activity and level of ACE in the cerebral cortex would be expected to increase production of angiotensin II, which could intensify cognitive dysfunction in AD because of its proinflammatory, anticholinergic and vasopressor effects. This indication is supported by studies showing that ACE-inhibitors and angiotensin receptor blockers, which inhibit binding of angiotensin II to its specific receptors, were associated with reductions in the incidence and rate of cognitive decline in MCI and AD (Hajjar et al., 2008, Rozzini et al., 2008, Li et al., 2010, O'Caoimh et al., 2014). Results are however, inconsistent. Some researchers reported that ACE-inhibitors, but not angiotensin II receptor blockers, were associated with an increased risk of mortality in patients with AD (Kehoe et al., 2013).

Furthermore, ACE has been shown to mediate cleavage of Aβ *in vitro* (Hu et al., 2001, Hemming and Selkoe, 2005, Oba et al., 2005). It has been demonstrated that ACE promoted degradation of both Aβ40 and Aβ42 in a cell model, and the reaction was reduced by the presence of an ACE-inhibitor

(Hemming and Selkoe, 2005). These findings are supported by mouse and human brain homogenates in which ACE was found to convert Aβ42 to the less aggregation-prone Aβ40 (Zou et al., 2007). These results suggest that ACE could have a role in AD via direct proteolysis of the Aβ peptide, modulating Aβ levels within the brain. Thus, it seems possible that patients taking ACE-inhibitors to treat hypertension could have a higher risk for increased Aβ deposition in the brain. In fact, ACE-inhibitors have been demonstrated to enhance brain Aβ deposition in an animal model (Zou et al., 2007).

A number of studies have investigated the association between *ACE* I/D polymorphism and AD. The study by Kehoe et al. (1999) first reported a positive association between the presence of the I-allele and AD, indicating an increased risk of AD. However, subsequent research results slightly vary or are even completely contradictory to the previous results, such as a large meta-analysis from 2005 (Lehmann et al., 2005), concluding that the D-allele gave a small reduced risk for AD. Zhang et al. (2012) investigated the relationship between *ACE* I/D polymorphism and serum ACE activity, and found that serum ACE level significantly differed among the three genotypes (DD > DI > II) in both patients with aMCI and healthy controls.

1.10.4 Neurofilament-light and levels in CSF

NF-L is one of the three subunits forming neurofilaments, neuron-specific intermediate filaments that together with microtubules and microfilaments constitute the main components of the neuronal cytoskeletal system. Neurofilaments provide mechanical strength, and help maintain neuronal shape and rigidity. Highly expressed in axons, a major function of neurofilaments is to maintain axonal calibre (Hoffman et al., 1987). In a similar fashion as described for the microtubule-associated tau protein, neuronal damage releases neurofilament proteins into the interstitial fluid from where they diffuse into, and can be detected in, the CSF (Van Geel et al., 2005). The concentration of NF-L in CSF may therefore reflect the degree of axonal degeneration and be a convenient marker of neuronal damage.

Since neurofilaments are particularly abundant in large calibre, myelinated axons (Friede and Samorajski, 1970), it is suggested that elevated CSF levels of NF-L probably reflect subcortical axonal injury and degeneration of white matter (Rosengren et al., 1996, Rosengren et al., 1999). Supportive of this is the fact that elevated levels of CSF NF-L have been demonstrated in patients with the demyelinating disease multiple sclerosis (Lycke et al., 1998), and CSF NF-L has been shown to correlate with increasing degrees of white matter changes in the brain (Sjogren et al., 2001). Elevated levels of CSF NF-L have also been found in patients with neurodegenerative disorders, including amyotrophic lateral sclerosis (Rosengren et al., 1996), frontotemporal dementia and AD (Sjogren et al., 2000, Norgren et al., 2003). In a meta-analysis from 2007 (Petzold et al., 2007), Petzold and

colleagues reviewed seven studies that compared 172 subjects with mild to severe AD dementia and 166 healthy age-matched controls, and found that overall CSF NF-L values were higher for AD subjects than controls.

As mentioned, CSF NF-L is suggested to be primarily a marker of subcortical axonal degeneration. AD is more commonly associated with cortical degeneration, but subcortical pathology has been reported to be present at a very early stage in the course of AD (Geula et al., 2008). CSF NF-L might therefore add to the diagnostic performance of the core CSF biomarkers in early stages of AD.

2 Aims and hypotheses of the study

2.1 Aims

There is an urgent need for biomarkers that can accurately detect AD in its earliest stages, preferably before symptoms appear. ApoE, ACE, clusterin and NF-L are proteins that in different ways have been implicated in AD pathology through an association with Aβ and tau, the main components of amyloid plaques and neurofibrillary tangles, respectively. This study was designed to assess:

- whether levels of these proteins altered significantly in early AD compared to levels in elderly control individuals healthy for their age,
- whether additional information could be obtained from comparisons with *ACE* and *APOE* polymorphisms,
- and consider their potential diagnostic value as early-stage biomarkers for AD compared to Aβ and tau protein.

2.2 Hypotheses

- If core biomarkers in CSF showed patterns typical for AD and healthy controls, other results could be considered more reliable even though this is a small pilot study.
- The kind of difference that a good biomarker will show between patients and controls means that high p-values, even in a small study, will indicate the substance under study to be a poor candidate biomarker.
- Even results that do not suggest suitability as a biomarker are useful to extend the characterization of the Trønderbrain material and contribute to the quality of the study.

3 Materials and methods

3.1 Subjects included in the study

3.1.1 Patients and controls from the SAMBA sub-study

The patients and controls included in the present study were participants of the SAMBA study, a longitudinal study begun in 2009 as a part of the TrønderBrain project (Genetic and metabolic studies of dementia) which has been in progress since 2003. The purpose of the SAMBA project is to develop AD biomarkers in CSF and/or blood. Patients diagnosed with amnestic mild cognitive impairment (aMCI) or probable AD, were recruited to the study, and samples taken every six months over a two-year period. The diagnosis of aMCI was made in accordance with criteria given by Winblad et al. (2004) and the diagnosis of probable AD according to the NINCDS-ADRDA criteria (McKhann et al., 1984). All participants were diagnosed by the same neurologist. Both patients and controls were ethnic Norwegians between 50-85 years of age. At each visit, patients underwent clinical examination, blood and CSF sampling, and a number of neuropsychological tests, of which only the mini mental state examination (MMSE) is considered in the present work. The MMSE is a simple test to roughly assess a number of different cognitive abilities, including a person's memory, attention and language (Folstein et al., 1975). The MMSE consists of a series of questions and tasks, each of which scores points if answered correctly. If every answer is correct, a maximum score of 30 points is possible (see Appendix 1). AD patients included in the present study did not have MMSE-scores below 20 (with one exception), because of the desire to study the early phases of the disease.

Age- and gender-matched healthy volunteers without first-degree relatives with dementia were assigned as control individuals. Like the patients, healthy controls underwent neurological examination including MMSE, but they provided blood and CSF samples only once, at baseline. Both patients and controls underwent MRI at inclusion and at the end of the two year follow-up period. In the present study, the clinical material consisted of a total of 40 individuals; 20 patients and 20 control individuals (Table 3.1).

Table 3.1 *Subjects included in the present study.*

20 patients with early AD
20 healthy control individuals

Twelve of the patients had a diagnosis of probable AD at inclusion, whereas eight were initially diagnosed with aMCI. During the two year follow up-period, the eight aMCI patients all progressed to AD dementia. Therefore, the total 20 patients are designated as having “early AD”.

3.1.2 Sampling of CSF and blood

CSF samples were provided by lumbar puncture, and collected directly into Corning Cryovials made of polypropylene. Polypropylene is a type of plastic that reduces adhesion of hydrophobic proteins to the walls of the tube. CSF collection was usually performed early in the morning. While being sent for storage, the CSF samples were kept on ice. The tubes were frozen within 30 minutes of lumbar puncture, and stored at -80°C until analysis.

Parallel blood samples were collected in tubes treated with the anticoagulant agent ethylene-diaminetetraacetic acid (EDTA) that prevents blood clotting. Some of the EDTA-blood was stored as whole blood for DNA isolation, and the rest was centrifuged (1500 *g* at room temperature for 10 minutes) and stored as plasma. In addition to the EDTA-tubes, blood was collected in gel glass tubes where blood is allowed to clot and then centrifuged (1500 *g* at room temperature for 10 minutes) to obtain serum. During centrifugation, the gel material incorporated in the tube forms an impermeable barrier between the serum and clot. Blood samples were kept at room temperature while being prepared, and subsequently stored at -80°C until analysis.

3.2. Ethical considerations

Written, informed consent was obtained from all patients and control individuals. The research project and biobank have been approved by the Regional Committee for Medical Research Ethics in central Norway.

3.3 Analysis of CSF and blood

3.3.1 Measuring levels of proteins in CSF, plasma and serum by ELISA

Levels of the proteins studied in this project in CSF, serum and plasma from patients and controls were determined using a technique called sandwich ELISA. Sandwich ELISA, one of several different types of ELISA, is a biochemical method that uses antibodies and colour change to detect and quantify a specific protein in a sample. The ELISA technique is widely used, including for the analysis of biomarkers for AD in CSF and blood (Blennow et al., 2010).

The analyses were performed using commercially-available ELISA kits. Table 3.2 lists the different proteins, the type of fluid they were analysed in, and the manufacturers of the ELISA kits. For the analyses in blood, plasma or serum was used dependent of the kit requirements.

Table 3.2 *Eight different proteins in CSF and/or serum or plasma from patients and controls were determined using commercially-available ELISA kits. Some of the assays required dilution of the samples prior to analysis.*

Protein	Fluid analysed	Manufacturer	Note/ dilution prior to assay onset
Aβ42	CSF Plasma	Innogenetics®	
Aβ40	CSF Plasma	IBL®	CSF diluted 1:500 Plasma diluted 1:50
T-tau	CSF	Innogenetics®	Measures all tau isoforms irrespective of phosphorylation status
P-tau$_{181}$	CSF	Innogenetics®	Measures tau phosphorylated at threonine 181
ApoE	Serum	Abcam®	Serum diluted 1:400
ACE	CSF Serum	R&D Systems®	Serum diluted 1:10
Clusterin	CSF Plasma	BioVendor Research and Diagnostic Products	CSF diluted 1:100 Plasma diluted 1:3000
NF-L	CSF	UmanDiagnostics NF-light®	CSF diluted 1:2

Prior to running of the assays, all samples were put in ice-water to thaw gently over time. As listed in Table 3.2, some samples required dilution before analysis. The assays were performed according to the manufacturers' instructions. Each ELISA kit had a slightly different procedure (see Appendices 2A-H for further details), but the general principle was the same, illustrated in Figure 3.1.

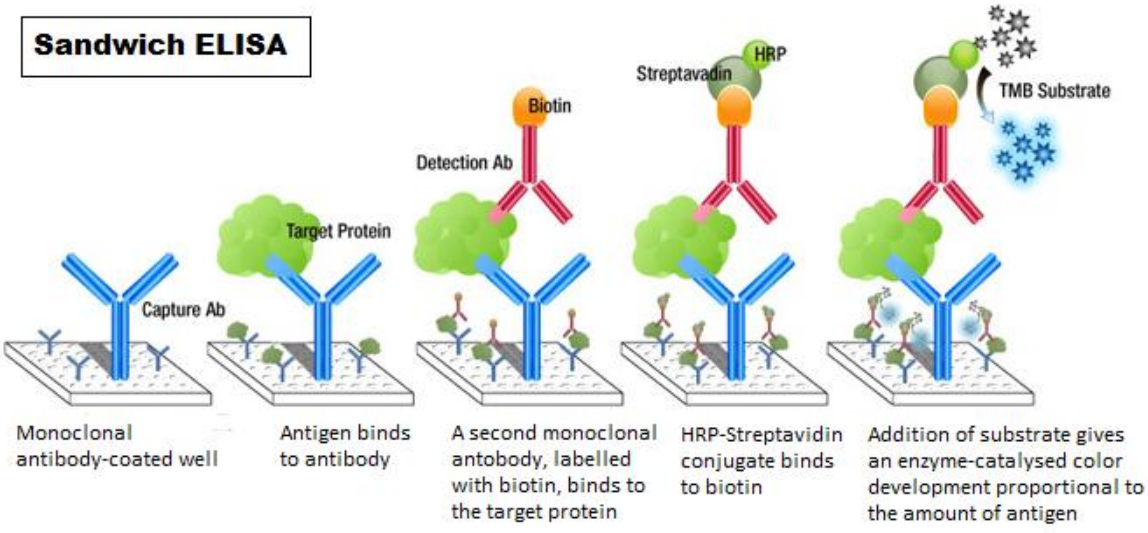

Figure 3.1 *Sandwich ELISA assays use antibodies and colour change to detect and quantify a specific protein in a sample. The cartoon illustrates the general principle behind the method, step by step. Although not illustrated here, between each step the wells are washed to remove unbound material. Figure modified from http://www.epitomics.com/products/products/c-Jun-antibody-6111-1.html#.*

The assays were performed in 96-well microtiter plates, in which the bottom of each well was coated with monoclonal antibodies specific for the protein to be measured. Samples were incubated in the wells allowing the target protein to bind to the antibodies, after which unbound sample material was washed away. To detect the bound antibodies, a secondary antibody was then added, which binds to a different epitope on the immobilized target protein. After an incubation period the wells are again washed to remove unbound material. The target protein is now "sandwiched" between two antibodies, hence the name of the assay. The secondary antibody was labelled with biotin, which provides an attachment point for the horseradish peroxidase (HRP)-streptavidin conjugate, which is added after another washing. HRP is an enzyme that can metabolize colourless substrates into coloured products. After the last washing step, the final addition of substrate gave an enzyme-catalysed colour development proportional to the amount of target protein in the sample. After a set time, the enzyme reaction was stopped by adding a stop solution, and absorbance of the resulting product was measured spectrophotometrically at a specific wavelength (Figure 3.2).

Figure 3.2 *The colour of the product changes from blue to yellow when stop solution is added to the 96-well microtiter plate. The picture to the right shows the spectrophotometric plate reader used to measure the absorbance of the yellow product.*

The absorbance is proportional to the concentration of the target protein, and therefore a measure for the amount of protein in the sample. A standard curve was constructed for each analyte on every plate by plotting absorbance values against concentrations of standards, and the concentration of unknown samples was automatically calculated using this standard curve. The dilutions performed prior to running of the assays yielded concentrations that fitted well into the standard curve.

To reduce analytic variance between samples from controls and patients, both were included on each ELISA plate. All samples, standards and blanks were run in duplicate. An example of a plate chart can be seen in Appendix 3. The analyses were carried out blinded to the diagnosis of individuals.

3.3.2 Isolation of DNA from whole blood

DNA isolation from whole blood was performed using the QIAamp DNA Blood Mini Kit (cat.no 16 107-50) from QIAGEN®, together with the spin protocol provided in the QIAamp® DNA Mini and Blood Mini Handbook (2010). The spin procedure is illustrated in Figure 3.3.

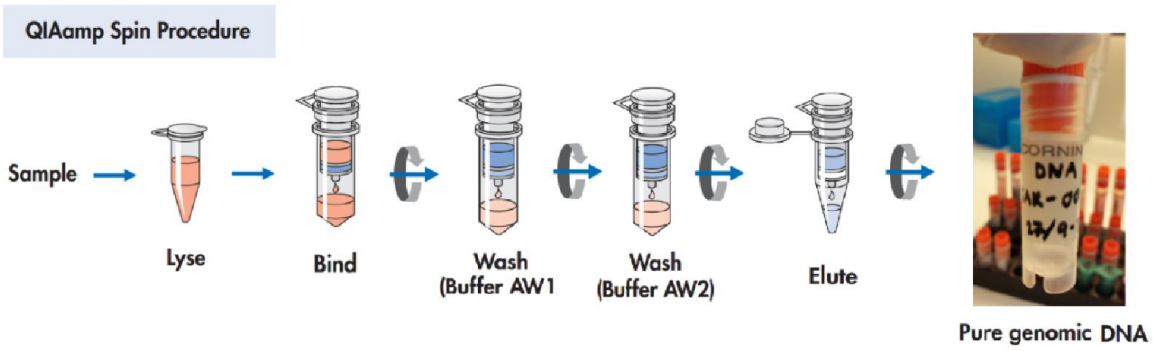

Figure 3.3 *QIAamp Spin Procedure for DNA isolation. Figure modified from QIAamp DNA Mini and Blood Mini Handbook 2010, p. 13: http://www.scribd.com/doc/56625169/QIAamp-DNA-Mini-and-Blood-Mini-Handbook.*

In short, extraction of DNA from whole blood involves digestion of proteins in the blood by a protease, cell lysis to expose the DNA, precipitation of DNA using ethanol, binding of the DNA to a membrane, washing for removal of residual contaminants, and finally the purified DNA is eluted in water. In between many of these steps are rounds of centrifugation using different centrifuge programs (Figure 3.3).

The DNA isolation was performed according to the procedure presented in Appendix 4. In step 1, it was optional to use either QIAGEN protease or protein kinase K, and the latter was chosen. Step 10 in the protocol was an optional, extra centrifugation, and was included in order to eliminate the possibility of carry-over from wash buffer “AW2”. In step 11, distilled water was added for the elution of the DNA, and not the optional “Buffer AE”. The purified DNA was transferred to 2 mL Corning Cryovials, and stored at -80°C.

3.3.3 *ACE* genotyping with the LightCycler® Real-time polymerase chain reaction system

3.3.3.1 The theoretical principle behind the method

Real-time polymerase chain reaction (PCR), also called quantitative PCR, is a gene analysis technique used for a broad range of applications, including genotyping. Whereas traditional PCR requires post-PCR processing using agarose gel electrophoresis for separation and analysis of PCR products, real-time PCR measures DNA amplification as it occurs by quantifying reaction products for each sample in every cycle. To manage this, real-time PCR systems rely upon the detection and quantification of a

fluorescent reporter, whose signal increases in direct proportion to the amount of PCR product in a reaction (Reece, 2004). SYBR® Green I is a commonly used fluorescent DNA-specific dye that binds to all double-stranded DNA (Wittwer et al., 1997). As the SYBR Green dye binds to double-stranded amplicons, it undergoes a conformational change and emits fluorescence at a greater intensity. Thus, as a PCR product accumulates, the fluorescence increases. Figure 3.4 illustrates the general principal behind SYBR Green I-based real-time PCR.

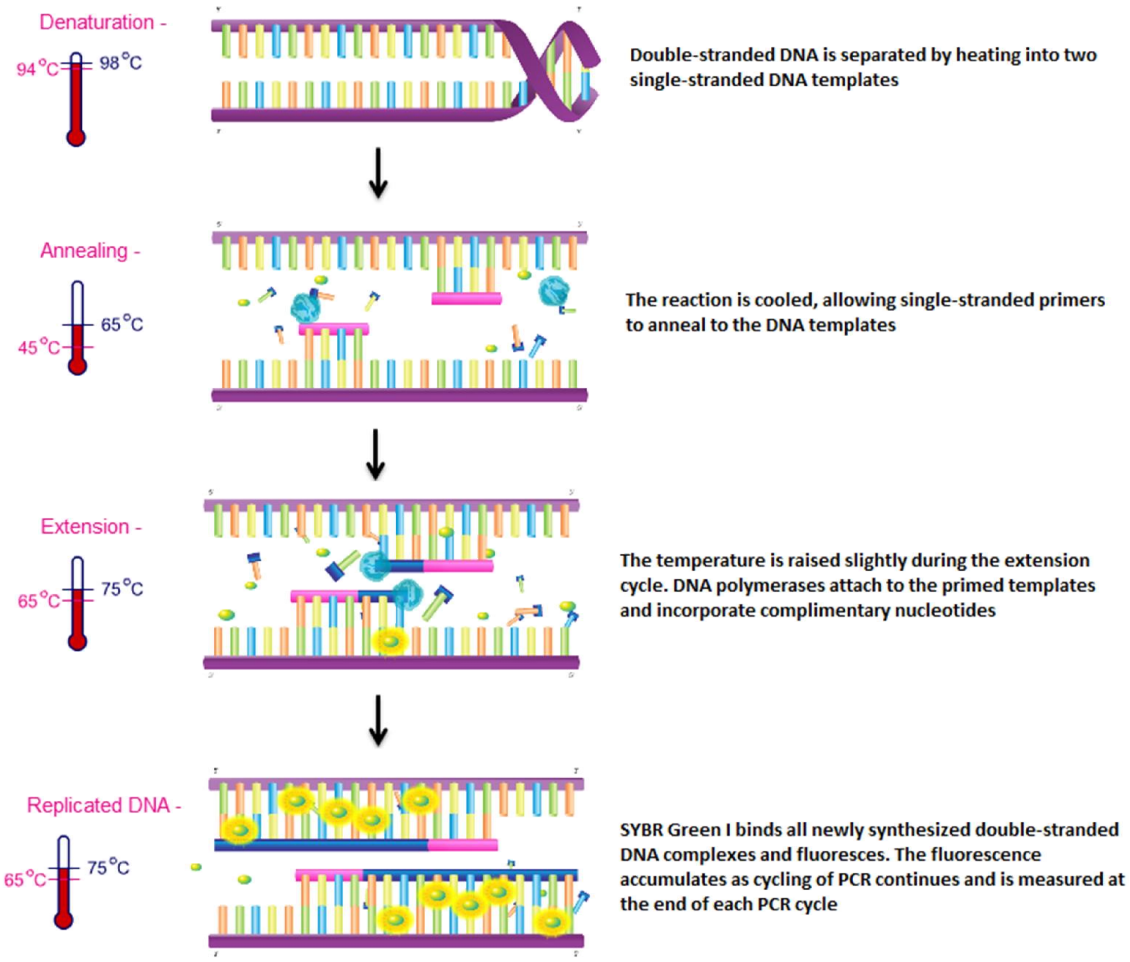

Figure 3.4 *The cartoon illustrates how SYBR® Green I can be used in real-time PCR for template DNA quantification. The figure has been made on the basis of the SYBR Green I-based qPCR technical animation by Sigma-Aldrich®: http://www.sigmaaldrich.com/life-science/molecular-biology/pcr/quantitative-pcr/sybr-green-based-qpcr.html.*

When monitoring the real-time PCR reaction continuously, the reaction progress can be plotted, illustrated in Figure 3.5. During heating to the denaturation temperature, fluorescence drops to zero as the double-stranded PCR products separate. Fluorescence increases during cooling as PCR products and primers anneal and extend, synthesizing more double-stranded DNA.

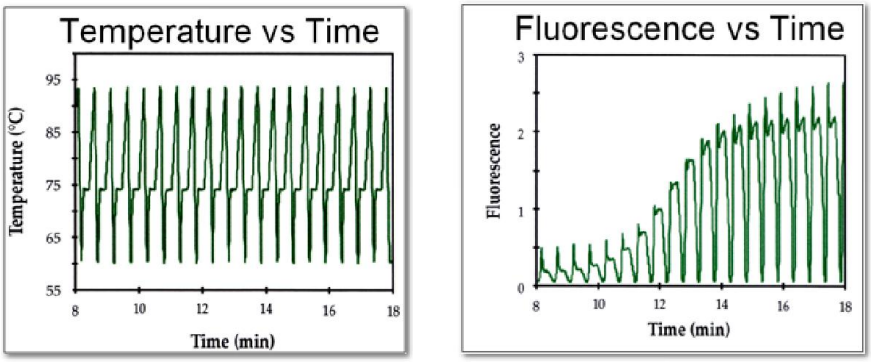

Figure 3.5 *To the left, a temperature versus time plot displaying the temperatures of the characteristic three steps of each PCR cycle: denaturation (~94°C), annealing (~60°C) and extension (~72°C). To the right, fluorescence versus time is plotted, showing fluorescence accumulating over time. Plots obtained from the Wittwer Lab for DNA Analysis: https://dna.utah.edu/LightCycler/Top_LightCycler.html.*

The LightCycler instrument performs rapid PCR with real-time detection and/or quantification of target DNA, as well as post-PCR analysis of the amplified DNA by melting curve analysis. The system allows a wide range of detection formats such as the DNA binding dye SYBR Green I, or fluorescently labelled hybridization probes. The instrument consists of a thermal cycler to drive DNA amplification, a photometer for excitation of the fluorescent dyes in the samples, detection of the emitted fluorescent light, and specialized software to collect and analyse the quantitative data generated. The PCR reaction is performed in glass capillaries, which give a high surface-to-volume ratio. The result is that a PCR cycle is finished in less than 30 seconds, and a complete run can be done in approximately 45 minutes (Roche, 2005).

The temperature at which double-stranded DNA melts (separates) when heated, varies greatly depending on a number of factors such as the sequence, length of the fragment, and GC content. The melting temperature (T_m) is defined as the point at which half the DNA is denatured, meaning that half of the dye is released. Because all double-stranded DNA fragments have a specific melting temperature (T_m), melting profiles can be used to identify and genotype DNA products (Roche, 2005). This is a lot faster and more precise than characterizing a PCR product by size on an agarose gel.

The melting point analysis is performed after the last PCR cycle, when the amplification of the target DNA is complete. The LightCycler instrument steadily increases the sample temperature while monitoring its fluorescence. During heating, sample fluorescence decreases as the double-stranded DNA separates and SYBR Green I molecules are released. Final results are visualized as a melting curve chart with one melting curve for each sample, displaying sample fluorescence versus temperature. The chart shows the downward curve in fluorescence for the samples as the double-stranded PCR-products separate. The melting curves are automatically converted into melting peaks by plotting the negative derivative of fluorescence versus temperature. Each peak represents the

melting temperature (T_m) of the individual samples. The following figure illustrates a melting curve chart with a melting peak chart below, from a melting temperature analysis.

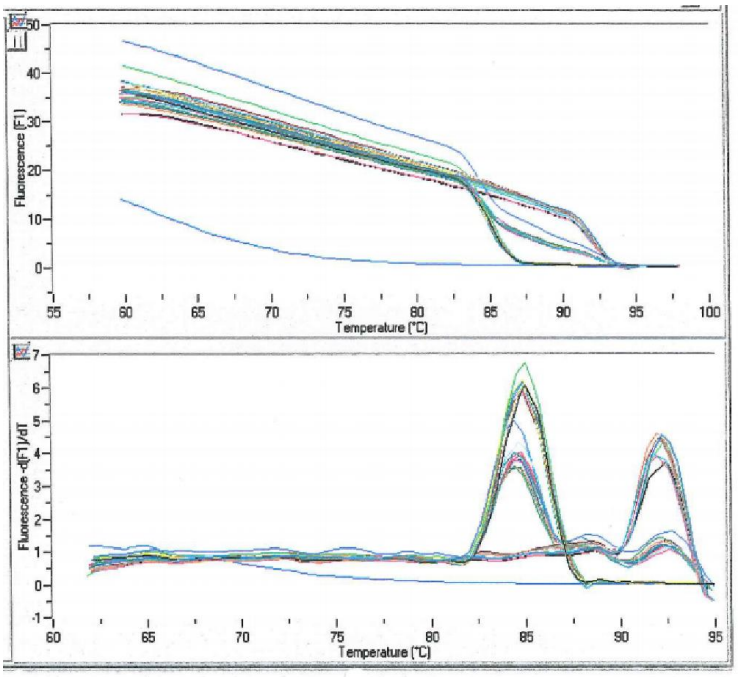

Figure 3.6. *Final results from a melting temperature analysis performed by a LightCycler® Real-time PCR instrument. The top chart displays melting curves for each sample, and the bottom chart displays peaks representing the individual samples melting temperature (T_m).*

After DNA amplification, a heterozygous sample contains two different DNA sequences, each with a different size, which therefore melt at different temperatures. Heterozygous samples are thus indicated by a two-peak curve in the melting peak chart, whereas homozygous samples display only one peak.

In a LightCycler run, a negative control is always run with the samples, in which template DNA is replaced with pure water. If the negative control is positive, the system is contaminated. Positive controls with known genotypes can also be included. The melting points of the unknown samples can then be compared with the controls, and the presence of the sequence of interest can be confirmed or disproved.

3.3.3.2 Specifics for the present study

Preparation of a LightCycler run

The experimental protocol for the LightCycler® 2.0 Instrument was used and the samples were run with Software 3.5. The programming of the LightCycler and the development of the experimental protocol for *ACE* genotyping had been developed in advance of the present study (Tronvik et al., 2008). The LightCycler carousel has a capacity for 32 samples. A negative control and two positive

controls (control *ACE* genotype I/D and control I/I) were included. Thus, a maximum of 29 unknown samples were analysed in each run.

DNA samples were thawed at room temperature, and reagents were thawed in a precooled cooling block. 32 disposable glass capillary tubes were placed in centrifuge adapters in the cooling block. The PCR reaction mix was then prepared using the Roche LightCycler® FastStart DNA Master SYBR Green I kit (cat.no. 3 003 230). The kit was designed specifically for real-time PCR assays using the SYBR® Green I detection format on the LightCycler® Carousel-Based System. The kit contained all the reagents needed for real-time PCR (Taq DNA polymerase, reaction buffer, deoxynucleotide triphosphate mix, SYBR® Green I dye, and $MgCl_2$), except the DNA samples and PCR primers. A set of two primers optimized for the *ACE* gene was provided from MedProbe AS:

- DCP1 deletion F: 5' – CTG-GAG-ACC-ACT-CCC-ATC-CTT-TCT – 3'
- DCP1 deletion R: 5' – GAT-GTG-GCC-ATC-ACA-TTC-GTC-AGA-T – 3'

The Master SYBR® Green I was prepared according to kit instructions (see Appendix 5). Reagents for the PCR reaction mix, listed in Table 3.3, were pipetted into a 1.5 mL microcentrifuge tube that was placed in the cooling block.

Table 3.3 *Reagents for PCR reaction mix for a full LightCycler® Carousel (32 samples). To make sure there was enough PCR reaction mix for a full carousel, volume for one additional reaction was prepared.*

Reagents	Volume for 32 samples + 1	For each reaction
PCR-grade H_2O	409.2 µL	12.4 µL
$MgCl_2$, stock 24 mM	52.8 µL	1.6 µL
Primer DCP1 deletion F	33.0 µL	1.0 µL
Primer DCP1 deletion R	33.0 µL	1.0 µL
LightCycler FastStart DNA Master SYBR Green	66.0 µL	2.0 µL

After gentle mixing and a short spin, 18 µL of the reagent mix was pipetted into the plastic reservoir at the top each of the 32 capillaries placed in the cooling block. 2 µL of the DNA samples, H_2O (negative control) and positive control samples, was then added. Each capillary was sealed with a plastic stopper using the LightCycler capping tool. With the help of the centrifuge adapters, the PCR reaction mix inside the capillaries was spun down using a standard benchtop centrifuge. The capillaries were only briefly centrifuged, and then placed in the LIghtCycler® Sample Carousel, keeping the capillaries in an upright position. The carousel was placed in the LightCycler instrument, and the run was started.

Interpretation of data

After the run was finished, which included amplification of a fragment of the human *ACE* gene and a melting point analysis, T_m peaks had to be registered manually. The melting temperatures can each be interpreted into two different *ACE* alleles (I=Insertion and D=deletion), giving three different *ACE* genotypes (Table 3.4).

Table 3.4 *ACE genotypes and the corresponding melting temperatures (T_m) for the different alleles.*

Genotype	Melting temperature (T_m)
Homozygote wild type I/I	Ca 91.8 °C
Homozygote polymorphic D/D	Ca 84.5 °C
Heterozygote I/D	Ca 91.8 °C and 84.5 °C

3.3.4 *APOE* genotyping

Information about the *APOE* genotypes was already obtained for all patients and control individuals according to the method described by Berge et al. (2014).

3.4 Statistical analysis

The statistical analysis was performed using the commercially available software program SPSS® Statistics Version 21 from IBM®. The distributions of the variables were investigated and found to be asymmetrical (not normally distributed), and outliers (defined below) were frequent. Given the asymmetry and presence of outliers, in addition to the small sample size, non-parametric statistical methods, which make fewer assumptions about the distributional shape, was considered to be the most appropriate statistical approach for the experimental data in the present study. In this approach, the actual values are replaced by rank scores from low to high, and the analyses are based on the distribution of ranks.

The Kruskal-Wallis test was used when comparing more than two groups, and the Mann-Whitney U-test was used when comparing two groups of independent samples. The Spearman correlation coefficient (r_s) was calculated. The association between two categorical variables was tested using the X^2- test. Quantitative variables are presented as the median and range. All reported p-values are two-sided with a significance level of 0.05, so $p<0.05$ was considered statistically significant. In addition, $0.05<p<0.10$ was considered a trend.

Boxplots are useful for visualization of how data are distributed and therefore frequently used for graphic presentation of results in the present study. The horizontal line in each box represents the median value. The top of the box corresponds to the upper quartile (75th percentile), whereas the

bottom of the box corresponds to the lower quartile (25th percentile). This means that 50% of cases have values that lie within the box. The T-bars that extend from the boxes are called whiskers. These extend to the minimum or maximum values, not including outlying values (Figure 3.7).

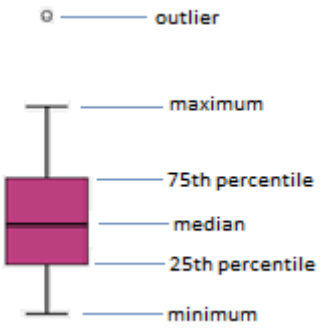

Figure 3.7 *Boxplot visualizing the distribution of experimental data.*

Outliers are values that seem to differ by a substantial amount from the rest of the data in the sample, and can be defined as a value x such that either

x > upper quartile + 1.5 x (upper quartile – lower quartile) or
x < lower quartile – 1.5 x (upper quartile – lower quartile).

Extreme outlying values represent cases that have values more than three times the height of the boxes, and are defined by the same equations as outliers, except that the factor 1.5 is replaced by 3 (Rosner, 2011). These values are identified on the box plot as cases below or above the end of each whisker. Boxplot outliers are marked by a ring and extreme outliers are marked by a star. In the present study, boxplot outliers have a number attached to them, referring to a sample's order in the database.

To evaluate the diagnostic performance of CSF protein levels in identifying AD patients, receiver operating characteristic (ROC) curve analyses were employed. A ROC curve is a plot of the sensitivity (true positive rate) versus 1- specificity (false positive rate) for different cut-off values used to designate test-positive (Rosner, 2011). Each point on the ROC curve represents a sensitivity/specificity pair corresponding to a particular decision threshold. The diagnostic accuracy of the test is measured by the area under the curve (AUC), and depends on how well a parameter separates the group being tested into those with and without the disease in question. The AUC corresponds to the probability that for a randomly selected pair of patients and controls, the test will correctly distinguish between the two diagnostic groups. When comparing two diagnostic tests for the same disease, the test with the higher AUC is considered the better test, unless some particular

level of sensitivity or specificity is especially important in comparing two tests (Rosner, 2011). An AUC of 1 represents a perfect test, while an area of 0.5 represents a worthless test.

The different coordinate points, or cut-off values, on the ROC curve are associated with a certain level of specificity and sensitivity. The selection of cut-off points depends to a large extent on how important sensitivity is versus specificity. If they are equally important, one should try to find the score that will maximize both sensitivity and specificity. Sensitivity, also called the true positive rate, measures the percentage of sick people who are correctly identified as having the condition. Specificity, also called true negative rate, measures the percentage of people who are correctly identified as *not* having the condition. Mathematically, sensitivity and specificity can be expressed as follows (The RNRRIAA & NIA Working group, 1998, Rosner, 2011):

- Sensitivity = P(disease|test is positive) = true positive cases/ (true positive cases + false negative cases)
- Specificity = P(no disease|test is negative) = true negative cases/ (true negative cases + false positive cases)

In terms of biomarkers for AD, sensitivity is often defined as the capacity of a biomarker to identify a substantial percentage of patients with the disease, while specificity refers to the capacity of a biomarker to differentiate AD patients from controls of the same age, other causes of cognitive disorders, and other forms of dementia (The RNRRIAA & NIA Working group, 1998).

4 Results

4.1 Demographic data

Descriptive statistics on gender, age, years of education, MMSE score and *APOE* genotype are presented in Table 4.1. The Mann-Whitney U-test was used for comparing age, years of education and MMSE score between patients with early AD and controls. No significant difference in age was found between patients and controls (p=0.698). However, MMSE scores were significantly reduced in the patient group compared to the control group (p<0.001), and years of education were significantly higher in the control group compared to early AD (p=0.024). The X^2- test was used for testing if the distribution of women and men was equal between groups, and no significant difference was found (p=0.507).

Table 4.1 *Patient and control group characteristics.*

	Controls (n=20)	Early AD (n=20)	p-value
Gender, Women/Men (n, %)	12/8 (60/40)	14/6 (70/30)	0.507
Age (y, median and range)	64.5 (57-77)	64 (57-78)	0.698
Years of education (median and range)	16 (8-21)	12 (8-18)	0.024*
MMSE score (median and range)	30 (28-30)	24.5 (14-28)	<0.001*
***APOE* ε4 carriers (n, %)**	8 (40)	15 (75)	0.025*
Heterozygote	8 (40)	9 (45)	
Homozygote	0	6 (30)	

*Significant difference between controls and patients with early AD

Data concerning *APOE* genotypes showed that none of the control individuals were homozygous for *APOE* ε4, but 40% were heterozygous carriers of one ε4 allele. For patients with early AD, carrier frequencies for the ε4 allele were much higher; 30% were homozygous and 45% were heterozygous for the *APOE* ε4 allele. Thus, a total of 75% of all patients with early AD carried one or two *APOE* ε4 alleles. Results from the X^2- test showed that there was a significantly higher occurrence of the *APOE* ε4 allele among patients with early AD compared to the control group (p=0.025).

4.2 Levels of proteins in CSF and blood

4.2.1 Aβ42, Aβ40, T-tau and P-tau in CSF

Results for the analysis of Aβ42, Aβ40, T-tau and P-tau, presented as the median and range, are shown in Table 4.2. Data were missing for one control individual. The Mann-Whitney U-test was used to compare levels of Aβ42, Aβ40, T-tau and P-tau between the controls and patients with early AD.

Table 4.2 *CSF levels of Aß42, Aß40, T-tau and P-tau (pg/ml) presented as the median (range).*

	Aβ42	Aβ40	T-tau	P-tau
Controls (n=19)	942.1 (499.8-1317.3)	17486 (11152-40852)	268.2 (147.4-1314.1)	49.4 (33.9-135.3)
Early AD (n=20)	476.1 (206.3-895.9)	14170 (6964-30851)	815.0 (153.7-1739.0)	106.7 (38.3-157.6)
p-value	<0.001*	0.149	<0.001*	<0.001*

*Significant difference between patients and controls

Patients with early AD had significantly decreased levels of CSF Aβ42 compared to controls (p<0.001). Boxplots illustrating CSF Aβ42 levels for controls and patients are shown in Figure 4.1. Two control samples (#4 and #18) were outliers with levels near the observed median among patients. One patient sample (#29) was an outlier with levels towards the observed median among controls.

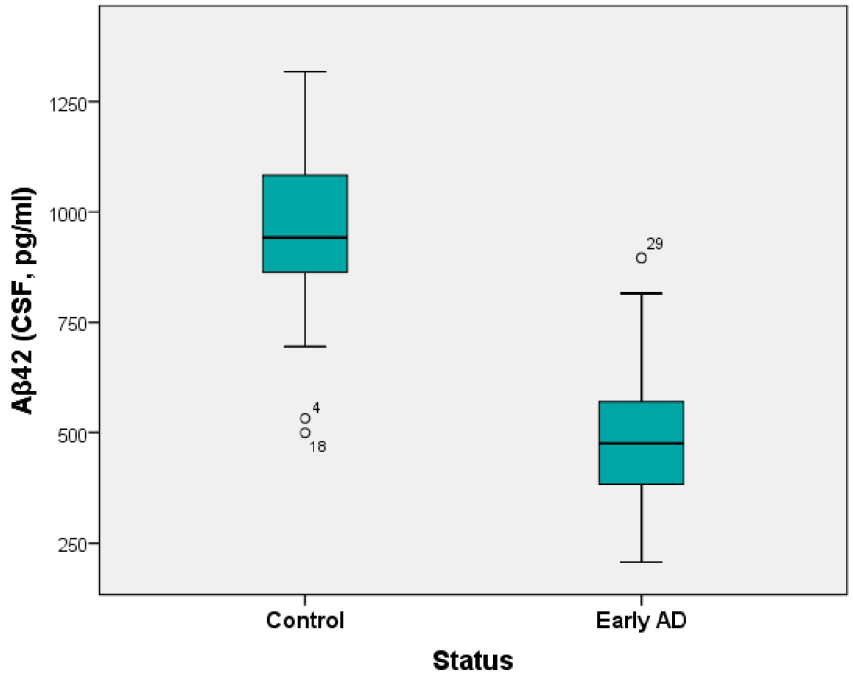

Figure 4.1 *Boxplots of CSF Aß42 levels in controls and patients with early AD.*

No significant difference in CSF Aβ40 was found between controls and patients with early AD (p=0.149). Boxplots illustrating CSF Aβ40 levels for controls and patients with early AD are shown in Figure 4.2. One control sample (#4) was an extreme outlier with the highest observed Aβ40 level among controls and patients. One patient sample (#23) was also an outlier with a substantially higher Aβ40 level than the rest of the patients with early AD.

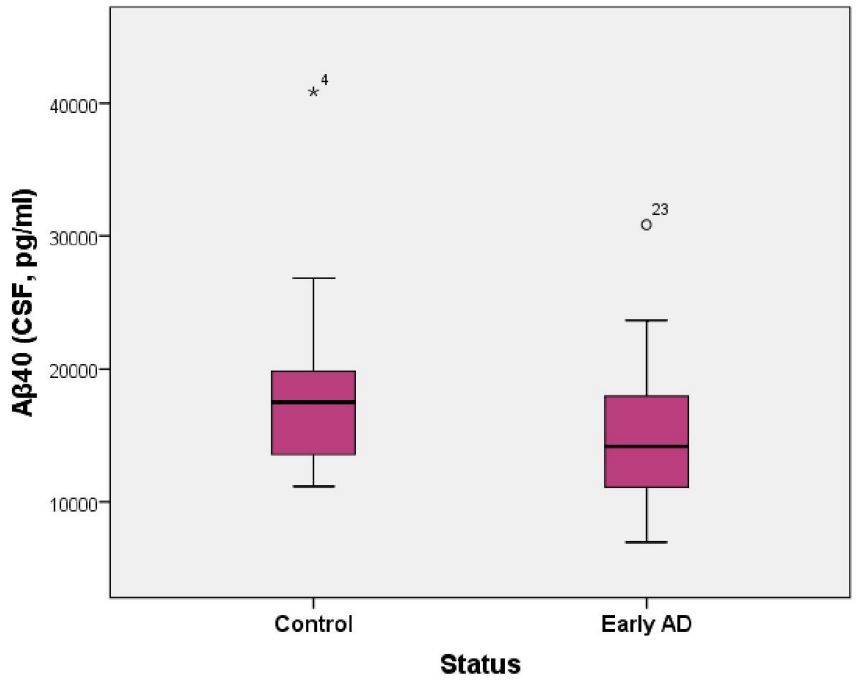

Figure 4.2 *Boxplots of CSF Aβ40 levels in controls and patients with early AD.*

Patients with early AD had significantly increased levels of CSF T-tau compared to controls ($p<0.001$). Boxplots illustrating CSF T-tau levels for controls and patients with early AD are shown in Figure 4.3. One control sample (#4) was an extreme outlier with a T-tau level well above the upper quartile of the levels for patients with early AD.

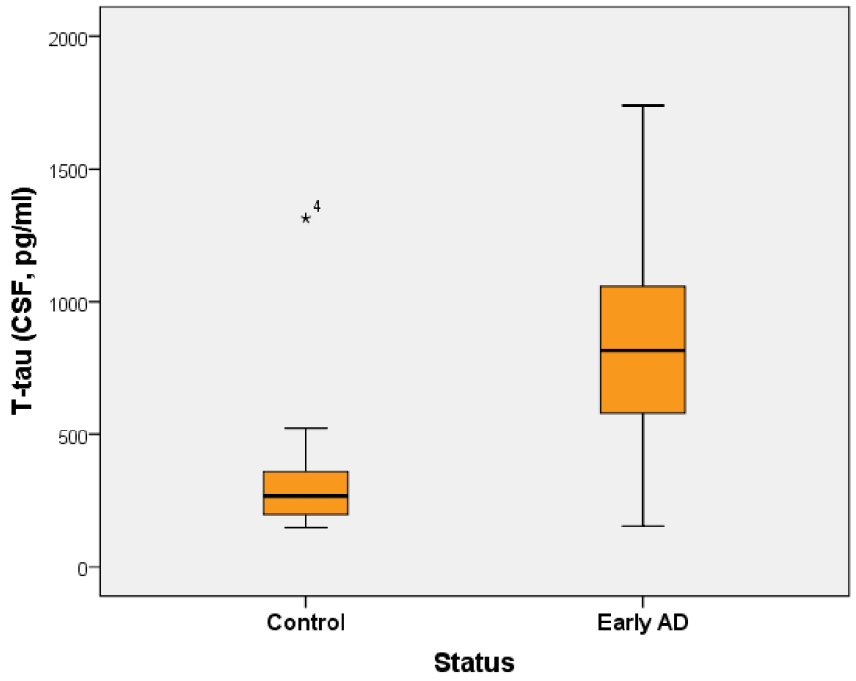

Figure 4.3 *Boxplots of CSF T-tau levels in controls and patients with early AD.*

Patients with early AD had significantly increased levels of CSF P-tau compared to controls (p<0.001). Boxplots illustrating CSF P-tau levels for controls and patients with early AD are shown in Figure 4.4. One control sample (#4) was an outlier with a P-tau level above the upper quartile of the levels for patients with early AD.

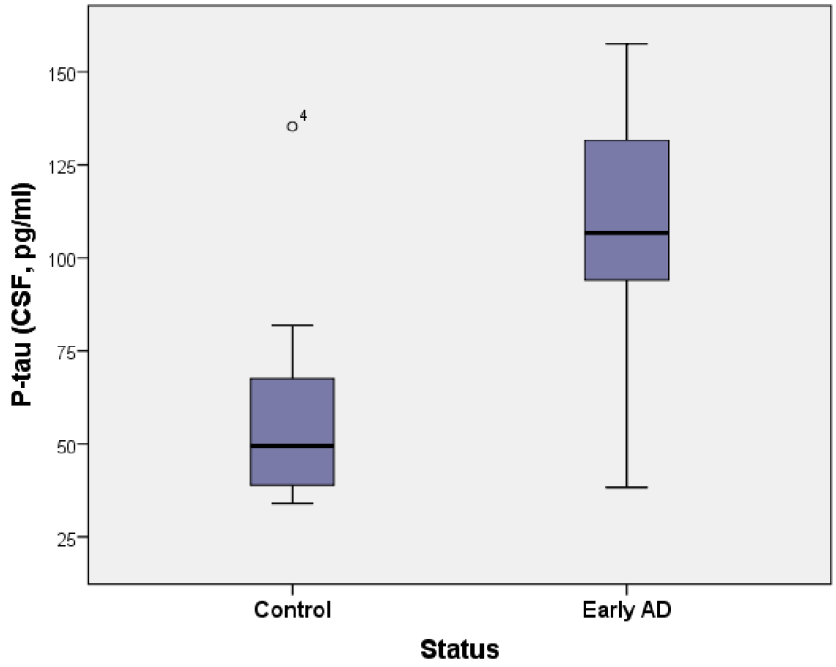

Figure 4.4 *Boxplots of CSF P-tau levels in controls and patients with early AD.*

4.2.1.1 Correlations between CSF Aβ42, Aβ40, T-tau and P-tau

Spearman's correlation coefficient (r_s) was calculated between CSF biomarker levels in the control and patient groups. Values of r_s are presented in Table 4.3.

Table 4.3 *Spearman's correlation coefficient (r_s) between CSF Aβ42, Aβ40, T-tau and P-tau (pg/ml) in the control and patient groups.*

	Controls			Patients with early AD		
	Aβ40	**T-tau**	**P-tau**	**Aβ40**	**T-tau**	**P-tau**
Aβ42	0.258	- 0.072	0.074	- 0.074	- 0.338	- 0.186
Aβ40		0.744**	0.591*		0.374	0.567*
T-tau			0.872**			0.905**

* p<0.01
** p<0.001

A significant, positive correlation was found between the levels of CSF Aβ40 and P-tau in both control (r_s=0.591, p=0.008) and patient groups (r_s=0.567, p=0.009), illustrated in Figure 4.5.

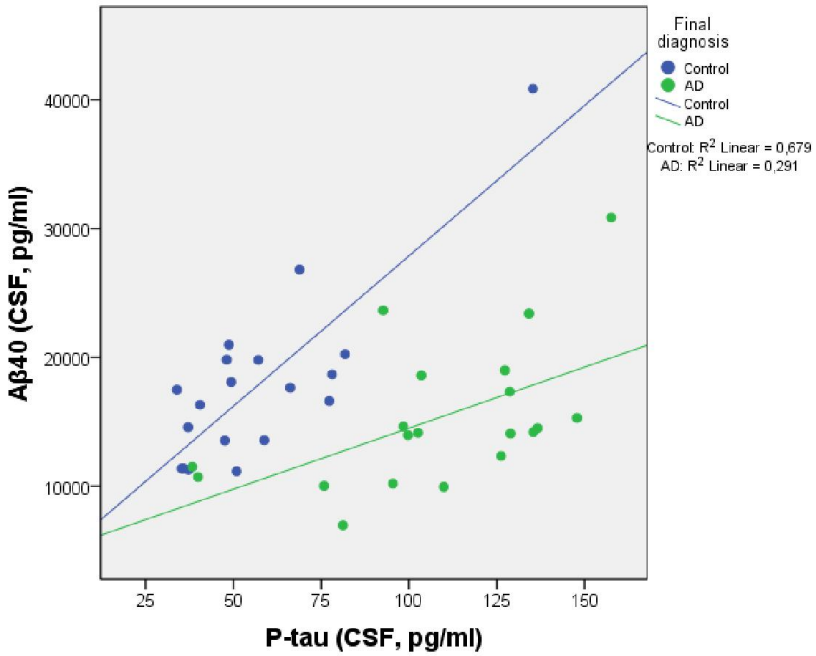

Figure 4.5 *Scatter plot showing relation between CSF levels of Aβ40 and P-tau in controls and patients with early AD. A best-fit line has been added to the specific subgroups.*

In the control group, Aβ40 was also found to positively correlate with T-tau (r_s=0.744, p<0.001), illustrated in Figure 4.6. This correlation was lost in the patient group.

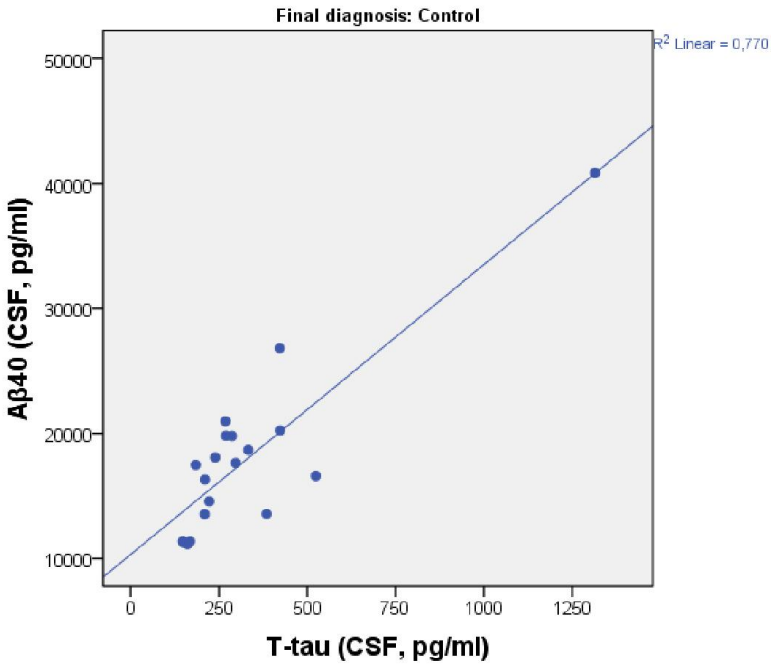

Figure 4.6 *Scatter plot showing the relation between CSF levels of Aβ40 and T-tau in controls. A best-fit line has been added.*

Levels of P-tau and T-tau in CSF were strongly, positively correlated in both control (r_s=0.872, p<0.001) and patient samples (r_s=0.905, p<0.001), as can be seen in Figure 4.7.

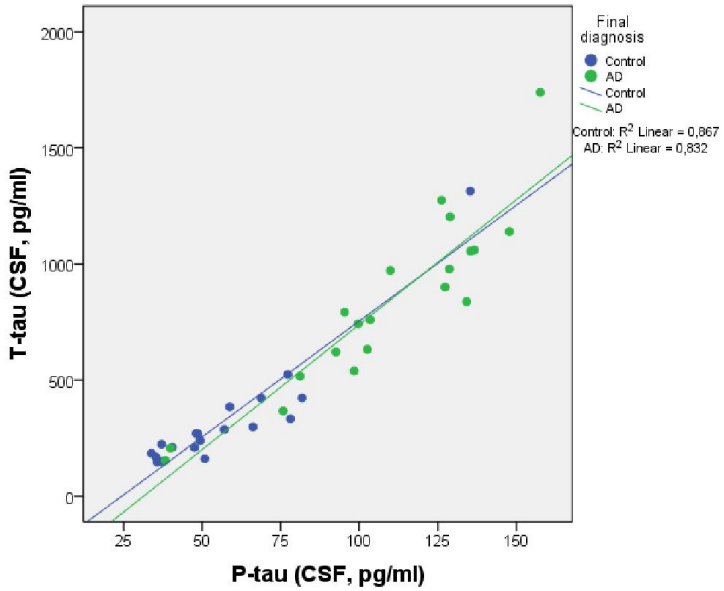

Figure 4.7 *Scatter plot showing the relation between CSF levels of T-tau and P-tau in controls and patients with early AD. A best-fit line has been added to the specific subgroups.*

4.2.1.2 Diagnostic performance of the core CSF biomarkers Aβ42, T-tau and P-tau

To evaluate the diagnostic performance of CSF Aβ42, T-tau, P-tau, and the ratios T-tau/Aβ42 and P-tau/Aβ42 as biomarkers for early AD in the present material, ROC curves were generated (Figure 4.8).

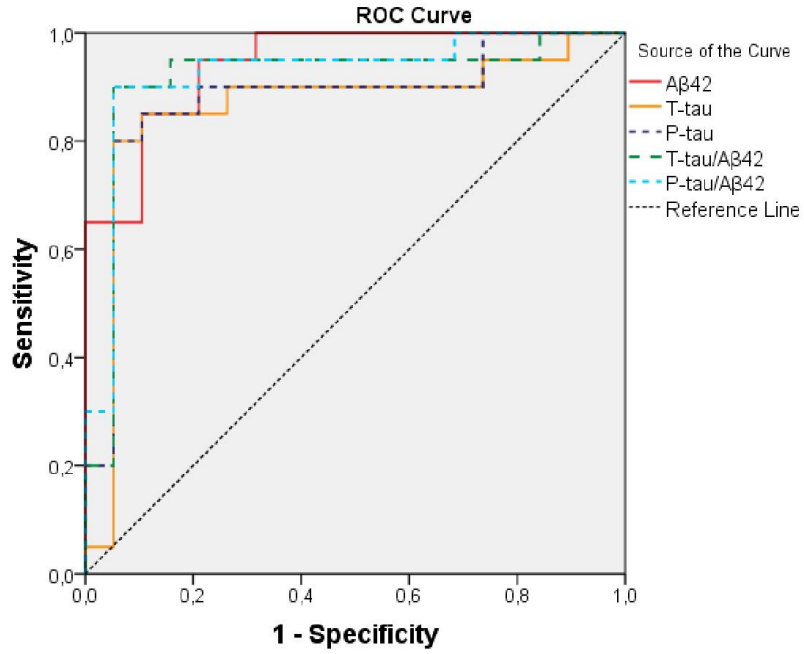

Figure 4.8 *Receiver operating characteristic (ROC) curves for the performance of the core CSF biomarkers (pg/ml) in distinguishing between patients with early AD and controls.*

Levels of sensitivity and specificity vary depending on the selected cut-off values. As can be seen in the ROC curves, there is a trade-off between sensitivity and specificity. Cut-off values maximizing sensitivity and/or specificity were selected from the ROC curves, and are presented in Table 4.4.

Table 4.4 *Area under the ROC curves (AUC), cut-off values and corresponding sensitivity and specificity levels for the core CSF biomarkers (pg/ml) in differentiating between patients with early AD and healthy controls.*

	AUC*	Cut-off (pg/ml)	Sensitivity	Specificity
Aβ42	0.942	830.1 698.1	95% 85%	79% 84%
T-tau	0.861	470.0	85%	90%
P-tau	0.879	72.3 77.7	90% 85%	79% 84%
T-tau/Aβ42	0.913	0.762 0.402	90% 95%	90% 84%
P-tau/Aβ42	0.924	0.141	90%	95%

*All p<0.001

Table 4.4 shows that the AUC was close to 0.9 or above for all of the core biomarkers and for ratios between them, meaning that they had a very good or excellent capability to correctly distinguish patients with early AD from healthy controls in the present study. The level of Aβ42 gave the highest AUC, and therefore had the highest diagnostic precision among the biomarkers. An AUC=0.942 means that there is a 94.2% probability of correctly distinguishing a person with early AD from a healthy age-matched individual based on the CSF level of Aβ42 in the present study. Figure 4.9 shows scatter plots visualizing the combination of T-tau and Aβ42, and P-tau and Aβ42.

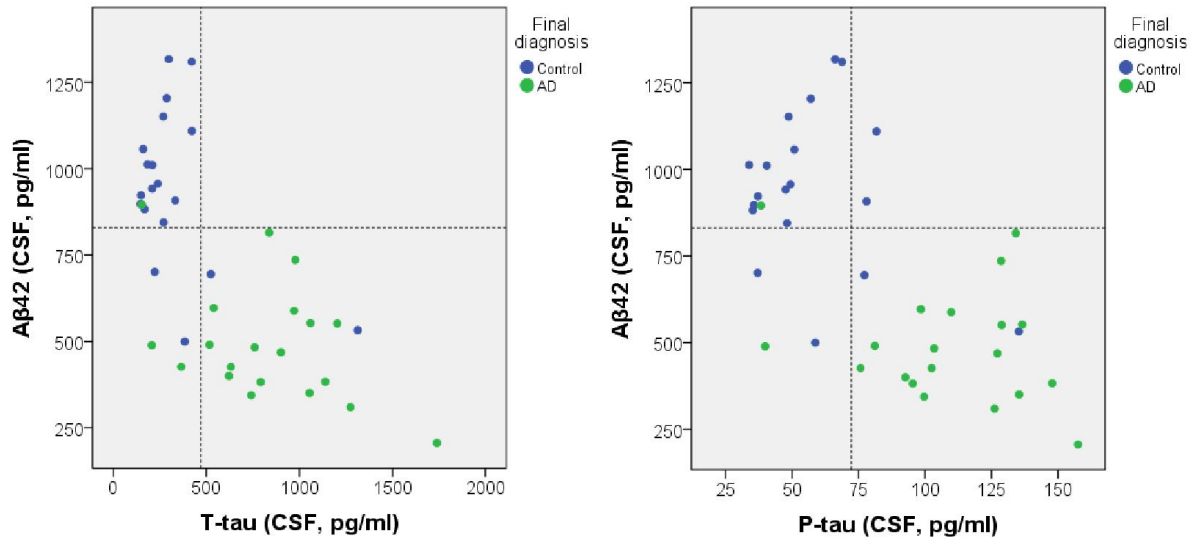

Figure 4.9 *Scatter plots showing the combination of T-tau and Aβ42 (left), and P-tau and Aβ42 (right) concentrations. Horizontal and vertical dotted lines represent the cut-off values; 830.1 pg/ml for Aβ42, 470.0 pg/ml for T-tau and 72.3 pg/ml for P-tau.*

4.2.2 Aβ42 and Aβ40 in plasma

No results for Aβ42 in plasma were obtained as levels were below the detection limit of the assay. More sensitive kits are therefore needed to obtain this information. Plasma Aβ40 was measured in samples diluted 1:50 as suggested by the manufacturer, but many samples were subsequently measured to be below the concentration of lowest standard, and some samples registered no value at all. These results are therefore unreliable and not shown.

4.2.3 Apolipoprotein E in serum

Results for the analysis of ApoE in serum, presented as the median and range, are shown in Table 4.5. The assay used for the analysis was not isoform-specific, but measured the total amount of ApoE in the serum samples. The Mann-Whitney U-test was used to compare levels of serum ApoE between controls and patients with early AD, and no significant difference was found (p=0.341).

Table 4.5 *Serum levels of ApoE presented as the median and range.*

	ApoE serum (µg/ml)
Controls (n=20)	63.8 (50.4-94.8)
Early AD (n=20)	59.0 (38.8-108.4)
p-value	0.341[a]

[a]No significant difference between controls and patients with early AD

Boxplots illustrating serum ApoE levels for controls and patients with early AD are shown in Figure 4.10.

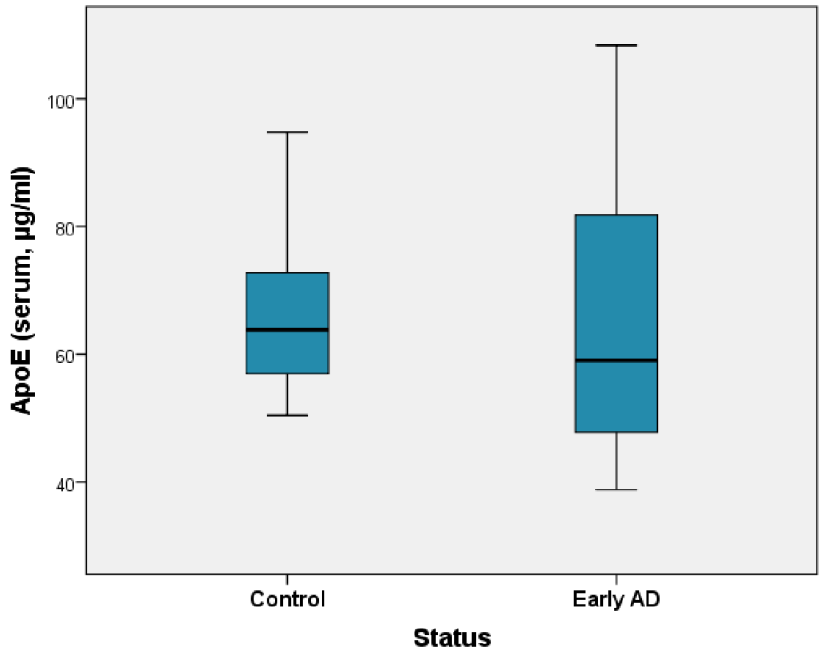

Figure 4.10 *Boxplots of serum ApoE levels in controls and patients with early AD.*

4.2.3.1 Serum ApoE level in relation to *APOE* genotype

APOE genotype frequencies and concentrations of serum ApoE in relation to the different genotypes are presented in Table 4.6 for the control and patient group.

Table 4.6 *APOE genotype frequencies and corresponding serum ApoE levels given as the median and range for controls and patients with early AD.*

	***APOE* genotype**					
	ε2/ε2	**ε3/ε3**	**ε4/ε4**	**ε2/ε3**	**ε2/ε4**	**ε3/ε4**
Controls						
Frequency (n, %)	0	12 (60)	0	0	1 (5)	7 (35)
ApoE serum (µg/ml)	-	69.6 (56.0-94.8)	-	-	63.2	56.4 (50.4-68.4)
Early AD						
Frequency (n, %)	0	5 (25)	6 (30)	0	0	9 (45)
ApoE serum (µg/ml)	-	98.0 (89.6-108.4)	47.8 (38.8-50.8)	-	-	62.0 (41.6-74.0)

Figure 4.11 shows boxplots illustrating the ApoE serum level in relation to *APOE* genotype for the controls and patients with early AD.

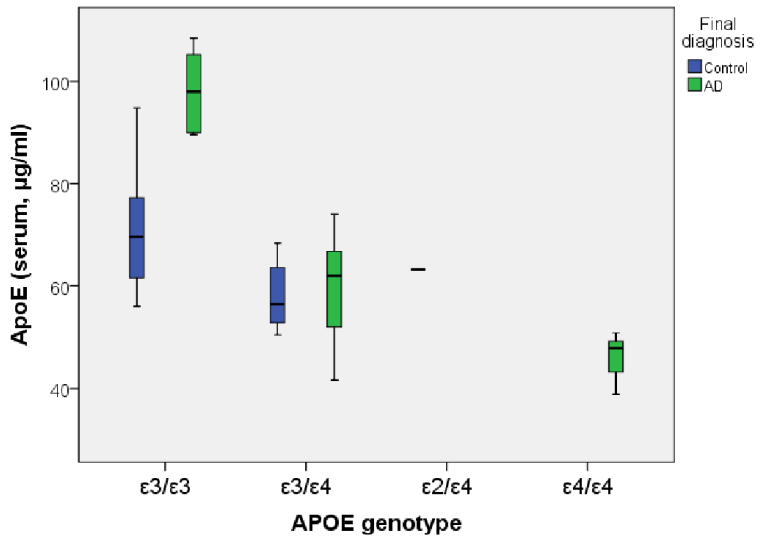

Figure 4.11 *Boxplots of serum ApoE levels versus APOE genotype for the controls and patients with early AD.*

The Kruskal Wallis test was used to compare levels of serum ApoE for individuals with different *APOE* genotypes in the controls and patients with early AD. A significant difference was found in the patient group ($p=0.001$), and a trend was observed in the control group ($p=0.07$). Pairwise comparisons were performed for the patient group. Patients with *APOE* genotype ε3/ε3 had significantly higher levels of serum ApoE than those with *APOE* genotype ε4/ε4 ($p<0.001$) and ε3/ε4 ($p=0.001$).

The levels of serum ApoE for *APOE* ε4 carriers and non-ε4 carriers are illustrated by boxplots in Figure 4.12. The boxplots indicate that *APOE* ε4 carriers tend to have a lower concentration of serum ApoE than non-ε4 carriers.

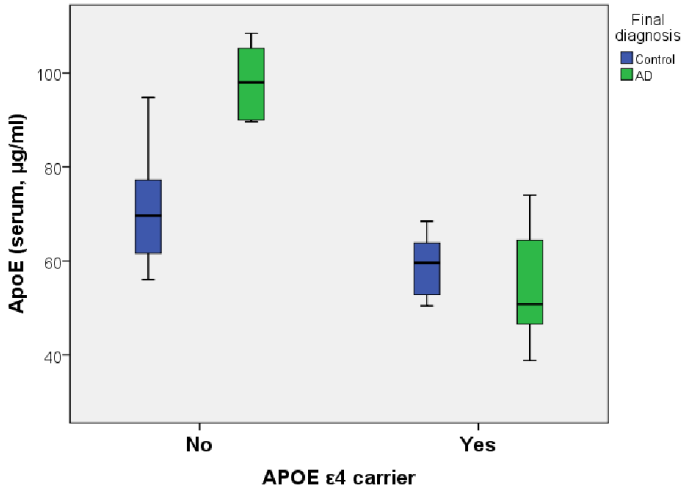

Figure 4.12 *Boxplots of serum ApoE levels for APOE ε4 carriers and non-ε4 carriers for the controls and patients with early AD.*

The Mann-Whitney U-test was used to compare serum ApoE level between *APOE* ε4 carriers and non-ε4 carriers. *APOE* ε4 carriers had significantly lower levels of serum ApoE compared to non-ε4 carriers in both the control (p=0.025) and patient (p<0.001) groups.

4.2.3.2 CSF Aβ42 in *APOE* ε4 carriers and non-ε4 carriers

The levels of CSF Aβ42 for *APOE* ε4 carriers and non-ε4 carriers are illustrated by boxplots in Figure 4.13. From the boxplots, there is no apparent difference between level of Aβ42 in CSF and *APOE* ε4 carrier status. This was confirmed by the Mann-Whitney U-test which showed no significant difference in CSF Aβ42 and *APOE* ε4 carrier status either among controls (p=0.902) or the patients with early AD (p=0.612).

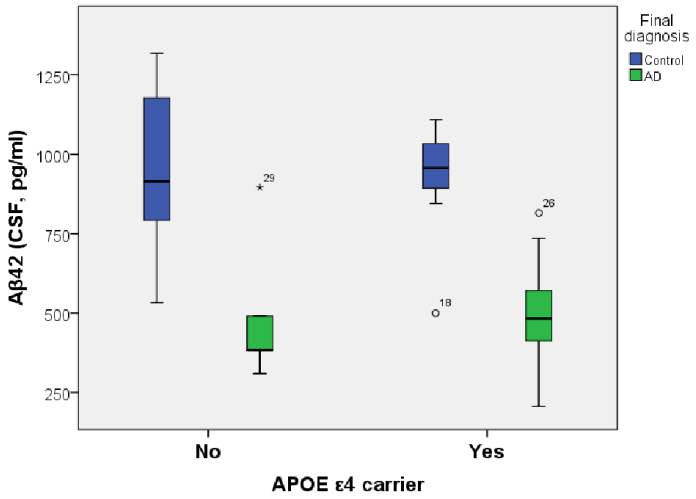

Figure 4.13 *Boxplots of CSF Aβ42 levels for APOE ε4 carriers and non-ε4 carriers for the controls and patients with early AD.*

4.2.3.3 Correlations between serum ApoE and other proteins in CSF and blood

Spearman's correlation coefficient (r_s) was calculated between serum ApoE levels in the control and patient groups and other proteins in CSF and blood. No significant correlations were found between serum ApoE and Aβ40, Aβ42, T-tau, P-tau, NF-L, clusterin or ACE in CSF, between serum ApoE and plasma clusterin, or between serum ApoE and serum ACE, either for controls or patients with early AD ($-0.4 < r_s < 0.3$, all $p > 0.1$).

4.2.4 Clusterin in CSF and plasma

Results for the analysis of clusterin in CSF and plasma, presented as the median and range, are shown in Table 4.7. Data were missing for one patient. The Mann-Whitney U-test was used to compare levels of CSF and plasma clusterin between controls and patients with early AD. No significant difference was found in CSF, but a trend towards higher levels of clusterin in plasma was observed in patients (p=0.074).

Table 4.7 *CSF and plasma levels of clusterin presented as the median and range.*

	Clusterin CSF (ng/ml)	Clusterin plasma (µg/ml)
Controls (n=20)	2799.1 (1982.4-4137.3)	79.1 (69.8-93.4)
Early AD (n=19)	2850.3 (2269.2-3747.5)	84.6 (72.2-98.2)
p-value	0.461[a]	0.074[a]

[a]No significant difference between controls and patients with early AD

Boxplots illustrating CSF clusterin levels for controls and patients with early AD are shown in Figure 4.14. Samples from two controls (#4 and #13) and two patients (#21 and #26) had outlying values with higher levels of CSF clusterin than the others in their respective group.

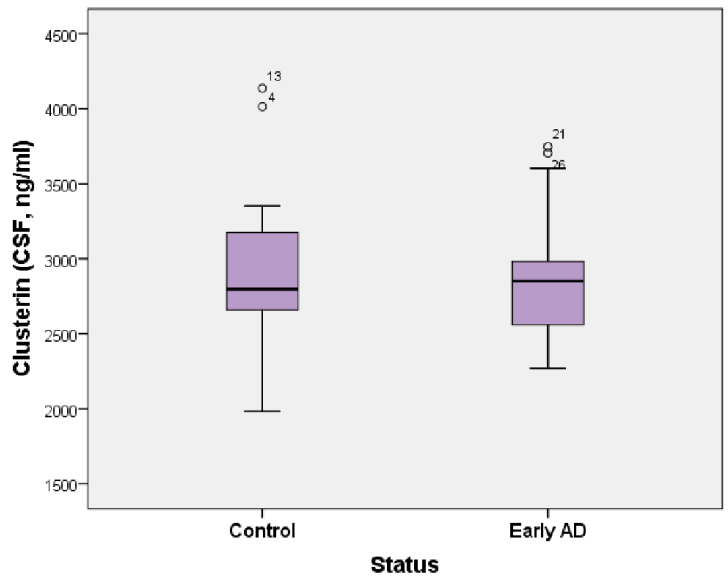

Figure 4.14 *Boxplots of CSF clusterin levels in controls and patients with early AD.*

Figure 4.15 shows boxplots illustrating plasma clusterin levels in samples from controls and patients with early AD, where a trend towards higher levels in patients can be observed.

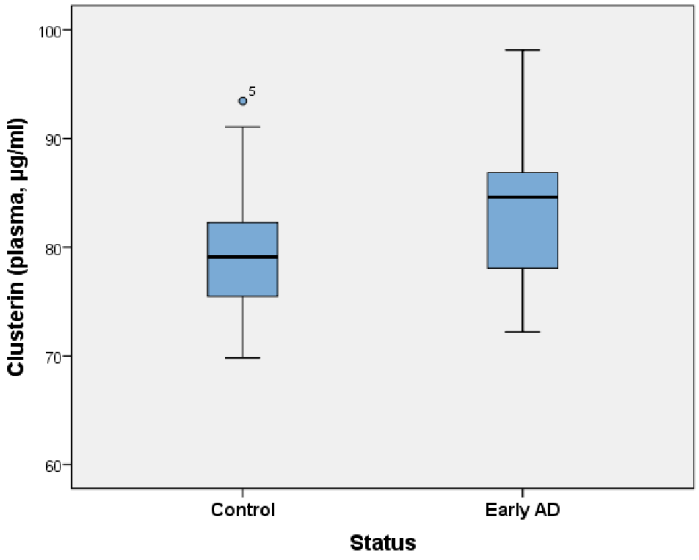

Figure 4.15 *Boxplots of plasma clusterin levels in controls and patients with early AD.*

4.2.4.1 CSF and plasma clusterin in *APOE* ε4 carriers and non-ε4 carriers

The levels of CSF clusterin for *APOE* ε4 carriers and non-ε4 carriers are illustrated by boxplots in Figure 4.16. From the boxplots, there is no apparent difference between the level of clusterin in CSF and *APOE* ε4 status. This was confirmed by the Mann-Whitney U-test which showed no significant difference in CSF clusterin and *APOE* ε4 carrier status either for controls (p=0.181) or the patients with early AD (p=0.754).

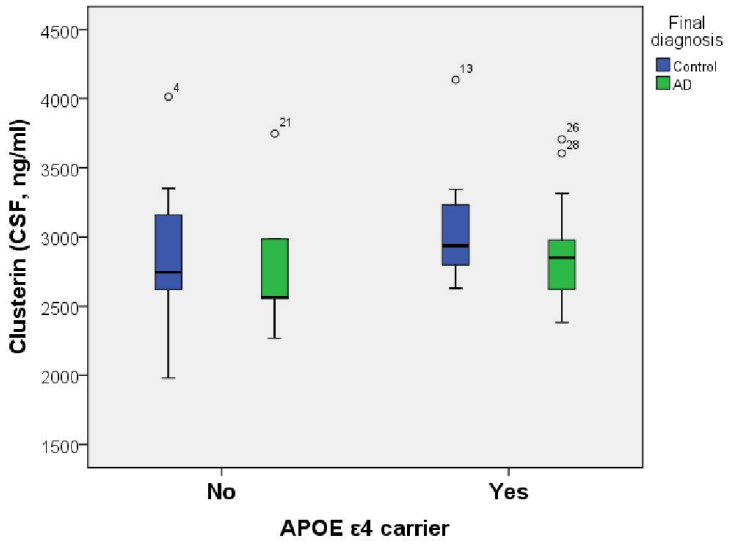

Figure 4.16 *Boxplots of CSF clusterin levels for APOE ε4 carriers and non-ε4 carriers for the controls and patients with early AD.*

The levels of clusterin in plasma for *APOE* ε4 carriers and non-ε4 carriers are illustrated by boxplots in Figure 4.17. From the boxplots, there seems to be a lower level of plasma clusterin among non-ε4

carriers in the control group. This was confirmed by the Mann-Whitney U-test which showed a significant difference in plasma clusterin and *APOE* ε4 carrier status among controls (p=0.039). No significant difference in plasma clusterin and *APOE* ε4 carrier status was found in the patient group (p=0.559).

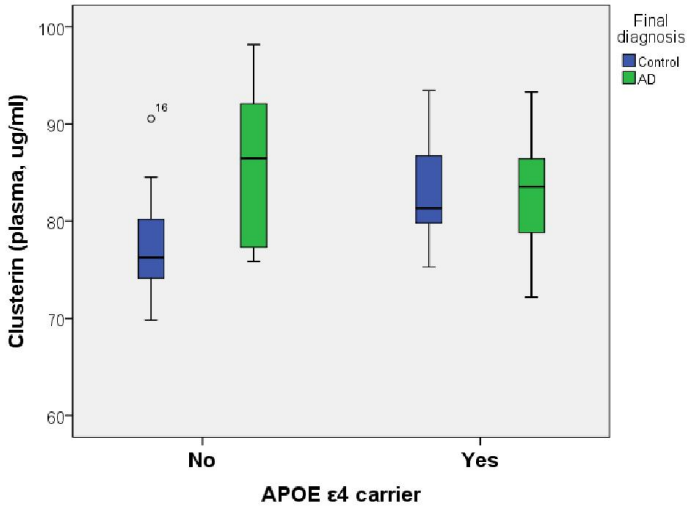

Figure 4.17 *Boxplots of plasma clusterin levels for APOE ε4 carriers and non-ε4 carriers for the controls and patients with early AD.*

4.2.4.2 Correlations between clusterin and other proteins in CSF and/or blood

Spearman's correlation coefficient (r_s) was calculated between CSF clusterin and levels of various proteins in CSF and/or blood, and between plasma clusterin and levels of various proteins in CSF and/or blood, in the control and early AD group. The only significant correlations were found between CSF clusterin and CSF cytoskeletal proteins, and between CSF clusterin and the level of ACE in CSF. These values are presented in Table 4.8.

Table 4.8 *Spearman's correlation coefficient (r_s) between CSF clusterin (ng/ml) and the CSF core biomarkers (pg/ml), CSF NF-L (pg/ml), and ACE in both CSF and serum (ng/ml).*

	Clusterin CSF	
	Controls	**Early AD**
Aβ42 CSF	0.147	0.305
Aβ40 CSF	0.416*	0.407*
T-tau CSF	0.604**	0.521**
P-tau CSF	0.746***	0.577**
NF-L CSF	0.502**	0.307
ACE CSF	0.781***	0.446*
ACE serum	-0.129	-0.051

* p<0.1 (trend)
** p<0.05
*** p<0.001

A significant, positive correlation was found between the levels of CSF clusterin and CSF T-tau in both controls (r_s=0.604, p=0.006) and patients with early AD (r_s=0.521, p=0.022), illustrated in Figure 4.18.

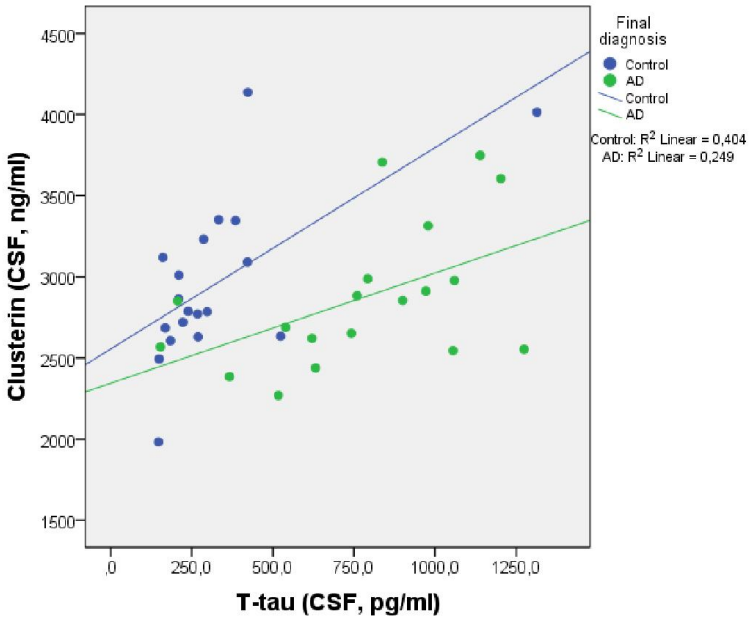

Figure 4.18 *Correlation between CSF levels of clusterin and T-tau in controls and patients with early AD. A best-fit line has been added to the specific subgroups.*

A significant, positive correlation was found between the level of CSF clusterin and CSF P-tau in both controls (r_s=0.746, p<0.001) and patients with early AD (r_s=0.577, p=0.010), illustrated in Figure 4.19.

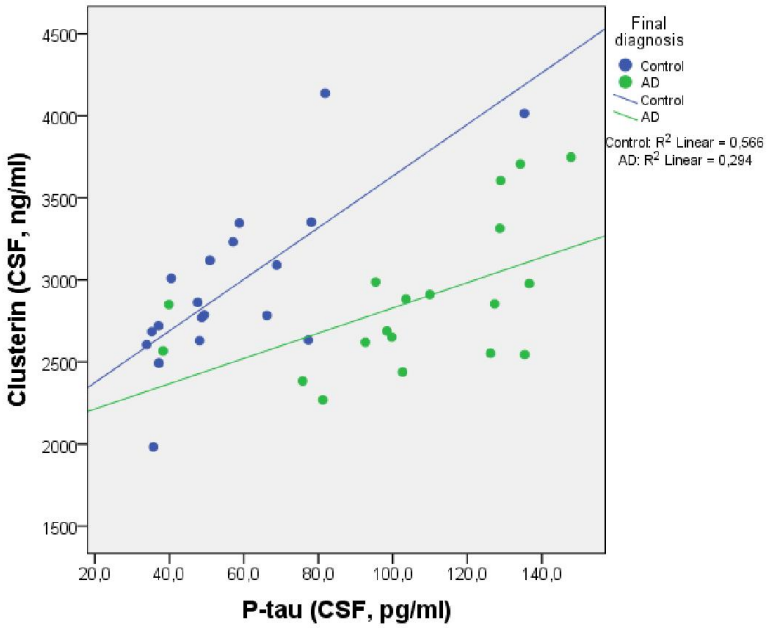

Figure 4.19 *Correlation between CSF levels of clusterin and P-tau in controls and patients with early AD. A best-fit line has been added to the specific subgroups.*

A significant, positive correlation was found between the levels of CSF clusterin and CSF NF-L in the control group (r_s=0.502, p=0.029), illustrated in Figure 4.20.

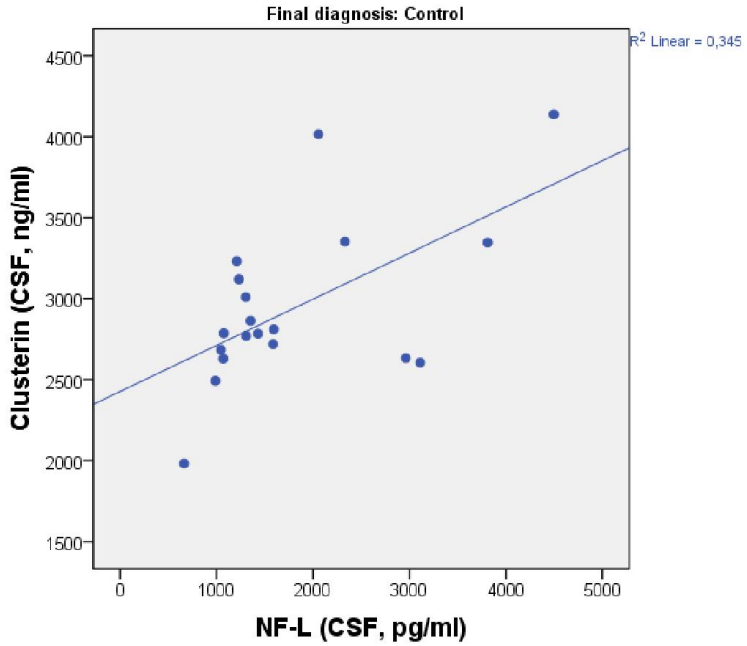

Figure 4.20 *Correlation between CSF clusterin and CSF NF-L in the control group. A best-fit line has been added.*

A significant, positive correlation was found between the levels of CSF clusterin and CSF ACE in controls (r_s=0.781 p<0.001), and a trend towards a significant, positive correlation was found in patients with early AD (r_s=0.446, p=0.056), illustrated in Figure 4.21.

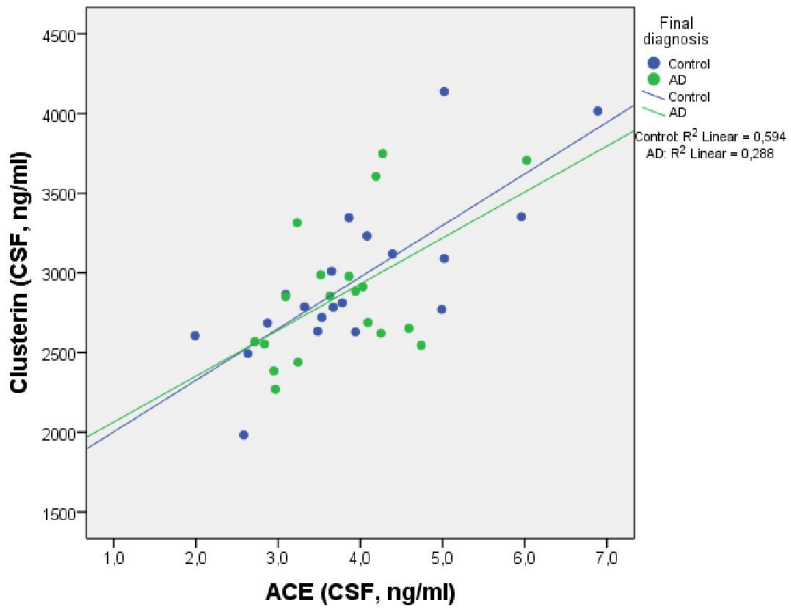

Figure 4.21 *Correlation between CSF levels of clusterin and ACE in controls and patients with early AD. A best-fit line has been added to the specific subgroups.*

4.2.5 Angiotensin-converting enzyme in CSF and serum

Results for the analysis of ACE in CSF and serum are listed in Table 4.9. The Mann-Whitney U-test was used to compare levels of CSF and serum ACE between controls and patients with early AD, and no significant difference was found in either CSF or serum.

Table 4.9. *CSF and serum levels of ACE presented as median and range.*

	ACE CSF (ng/ml)	ACE serum (ng/ml)
Controls (n=20)	3.7 (2.0-6.9)	133.7 (109.2-197.8)
Early AD (n=20)	3.9 (2.7-6.0)	138.2 (105.8-260.0)
p-value	0.925[a]	0.327[a]

[a]No significant difference between controls and patients with early AD

Boxplots illustrating CSF and serum ACE levels for controls and patients with early AD are shown in Figure 4.22. One patient sample (#26) had outlying values in both CSF and serum. Patient sample #35 also had an outlying, higher value of serum ACE than the other patients. In addition, two controls samples (#3 and #5) were outliers with higher levels of serum ACE than the other controls.

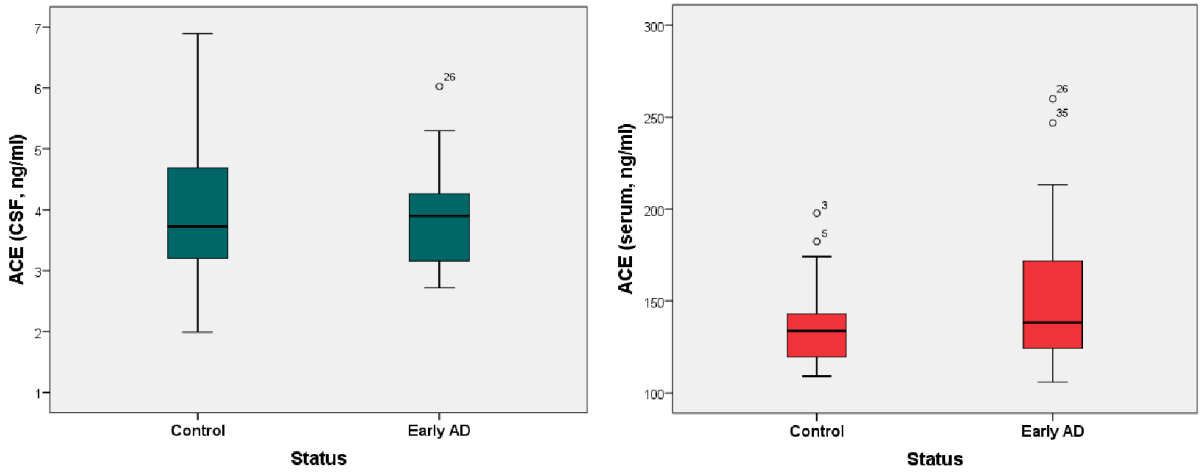

Figure 4.22 *Boxplots of ACE levels in CSF (left) and in serum (right) in controls and patients with early AD.*

4.2.5.1 *ACE* genotypes

DNA was isolated from control and patient blood samples, and *ACE* genotypes were obtained by means of the LightCycler instrument. The LightCycler melting analysis report obtained from the first LightCycler run is displayed in Appendix 5. *ACE* genotypes and allele distributions among controls and patients are presented in Table 4.10. Although it is quite clear from Table 4.10 that the distribution of *ACE* genotypes and alleles was rather similar among the controls and patients, the X^2- test was used

to test the association. As can be seen from the p-values listed in Table 4.10, no significant differences were found between controls and patients with regard to *ACE* genotype or allele distribution.

Table 4.10 *ACE genotype and allele distributions among controls and patients with early AD.*

	***ACE* genotypes**			**Alleles**	
	DD (%)	**ID (%)**	**II (%)**	**D (%)**	**I (%)**
Controls (n=20)	5 (25%)	9 (45%)	6 (30%)	19 (47.5%)	21 (52.5%)
Early AD (n=20)	5 (25%)	6 (30%)	9 (45%)	16 (40%)	24 (60%)
p-value	1.000[a]	0.327[a]	0.327[a]	0.549[a]	0.549[a]

[a]No significant difference between controls and patients

4.2.5.2 Relation between *ACE* genotype and ACE level in CSF and serum

Table 4.11 presents CSF and serum ACE in control and patient samples according to *ACE* genotype. The Kruskal Wallis test was used to compare levels of CSF and serum ACE between individuals with the different *ACE* genotypes, separately for the controls and patients with early AD. No significant differences were found in the CSF ACE level between individuals with the different *ACE* genotypes in the controls or the patients with early AD. However, a significant difference in serum ACE level was observed between control individuals with different *ACE* genotypes. No significant difference was found in serum ACE between patients with different *ACE* genotypes.

Table 4.11 *CSF and serum levels of ACE presented as median and range for controls (n=20) and patients with early AD (n=20) according to ACE genotype.*

	ACE CSF (ng/ml)		**ACE Serum (ng/ml)**	
***ACE* genotype**	**Controls**	**Early AD**	**Controls**	**Early AD**
DD	5.0 (2.6-6.9)	4.1 (3.1-4.7)	136.4 (116.1-197.8)	174.7 (125.8-246.8)
ID	3.8 (2.6-5.0)	3.9 (3.0-6.0)	139.9 (125.4-182.4)	142.0 (105.8-260.0)
II	3.6 (2.0-6.0)	3.9 (2.7-4.3)	117.2 (109.2-121.7)	127.6 (107.5-183.6)
p-value	0.518	0.331	0.009*	0.101

The ACE levels in CSF according to *ACE* genotype are illustrated by boxplots in Figure 4.23 for controls and patients with early AD. Levels of serum ACE in relation to *ACE* genotype can be seen in Figure 4.24.

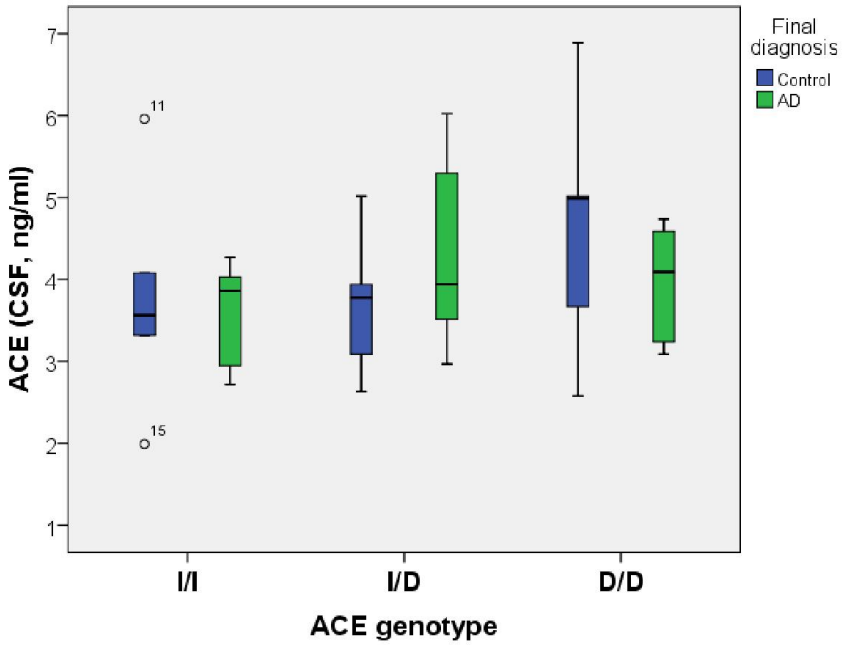

Figure 4.23 *Boxplots of ACE levels in CSF according to ACE genotype for controls and patients with early AD.*

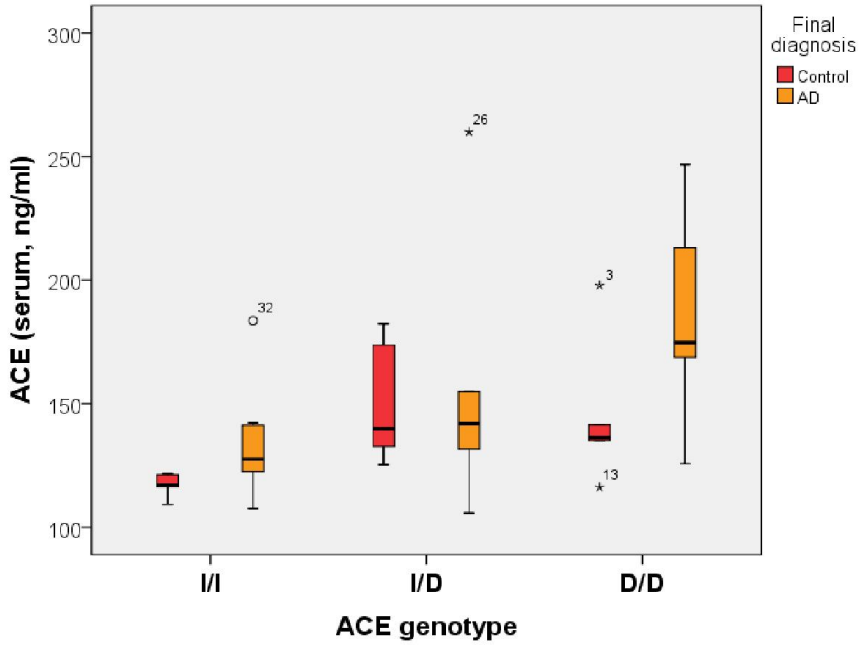

Figure 4.24 *Boxplots of ACE levels in serum according to ACE genotype for controls and patients with early AD.*

Pairwise comparisons for the control group were performed, and a significantly lower level of ACE in serum was found in II-carriers compared to ID-carriers (p=0.001). No significant difference was found between ID- and DD-carriers (p=0.947), but a trend towards a significantly lowered level in II-carriers was observed when compared to DD-carriers (p=0.068).

4.2.5.3 Correlations between CSF and serum ACE and other proteins in CSF

Spearman's correlation coefficient (r_s) was calculated between CSF ACE and levels of other proteins in CSF, between serum ACE and levels of other proteins in CSF, and between CSF ACE and serum ACE, in the control and patient groups. Significant correlations are presented in Table 4.12.

Table 4.12 *Spearman's correlation coefficient (r_s) between CSF ACE (ng/ml) and Aß, tau and NF-L in CSF (pg/ml), and between CSF and serum ACE (ng/ml).*

	ACE CSF	
	Controls	**Early AD**
Aβ42 CSF	0.175	- 0.218
Aβ40 CSF	0.679***	0.595**
T-tau CSF	0.699***	0.436*
P-tau CSF	0.805***	0.618**
NF-L CSF	0.368	0.202
ACE serum	0.014	0.522**

* p<0.1 (trend)
** p<0.05
*** p≤0.001

A significant, positive correlation was found between the levels of CSF ACE and CSF Aβ40 in samples from both controls (r_s=0.679 p=0.001) and patients with early AD (r_s=0.595, p=0.006), illustrated in Figure 4.25.

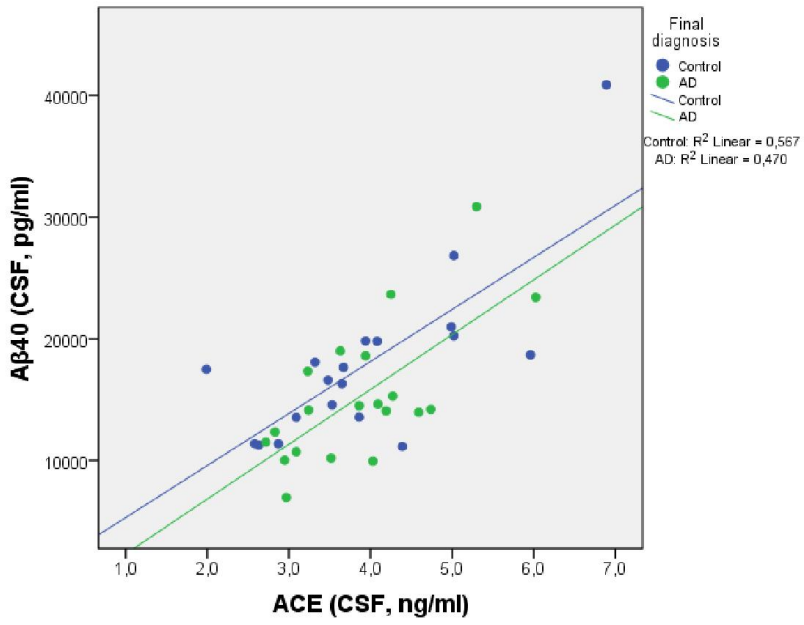

Figure 4.25 *Scatter plot showing the correlation between CSF levels of Aß40 and ACE in controls and patients with early AD. A best-fit line has been added to the specific subgroups.*

A significant, positive correlation was found between the levels of CSF ACE and CSF T-tau in controls (r_s=0.699 p=0.001), and a trend towards a significant, positive correlation was found in patients with early AD (r_s=0.436, p=0.055), illustrated in Figure 4.26.

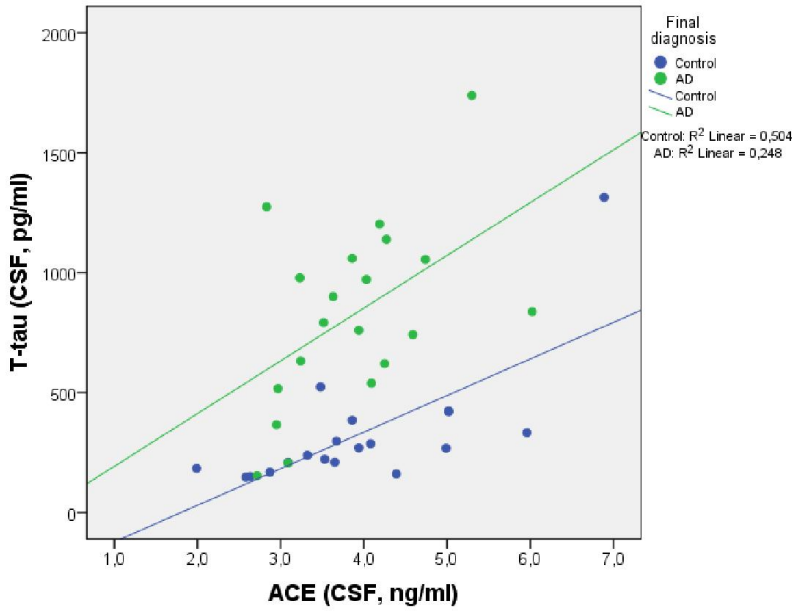

Figure 4.26 *Correlation between CSF levels of ACE and T-tau in controls and patients with early AD. A best-fit line has been added to the specific subgroups.*

A significant, positive correlation was also found between the levels of CSF ACE and CSF P-tau in samples from both controls (r_s=0.805 p<0.001) and patients with early AD (r_s=0.618, p=0.004), illustrated in Figure 4.27.

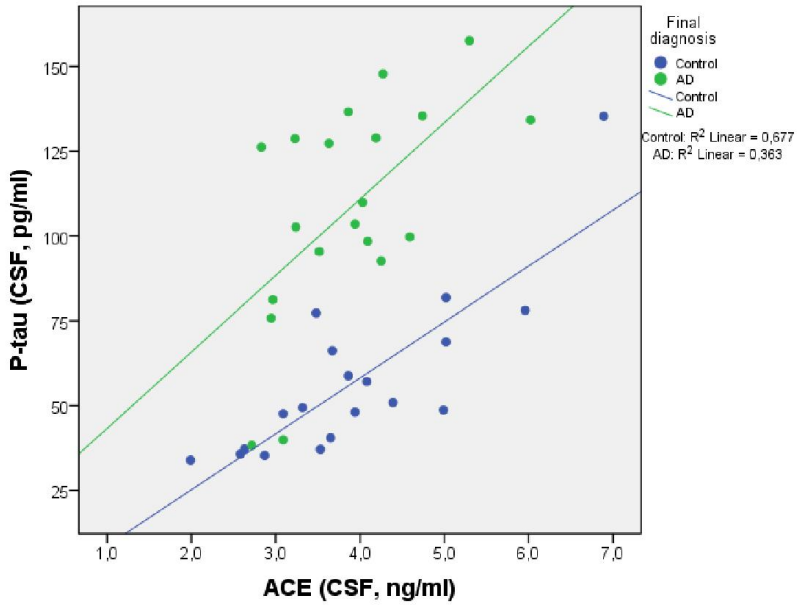

Figure 4.27 *Correlation between CSF levels of ACE and P-tau in controls and patients with early AD. A best-fit line has been added to the specific subgroups.*

A significant, positive correlation was found between the levels of ACE in CSF and serum for the patients with early AD (r_s=0.522, p=0.018), illustrated in Figure 4.28.

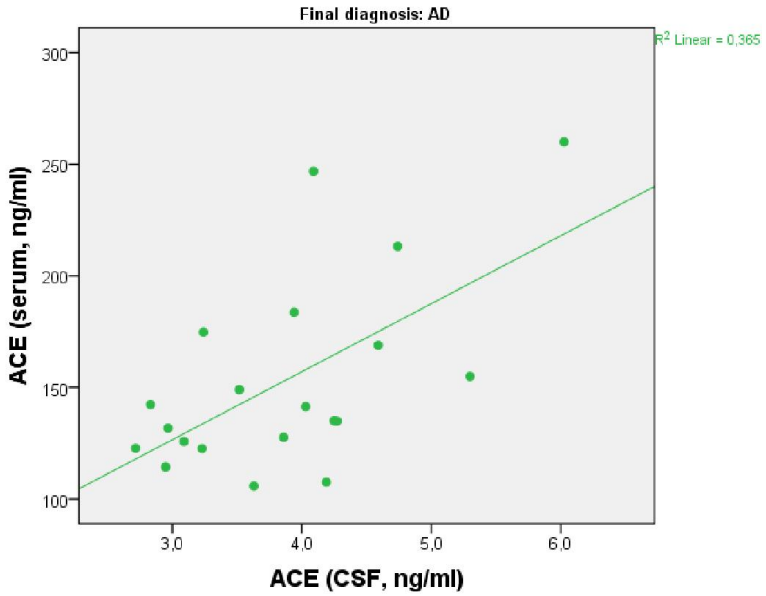

Figure 4.28 *Correlation between ACE in CSF and serum for patients with early AD. A best-fit line has been added.*

4.2.6 Neurofilament-light in CSF

Results for the analysis of NF-L in CSF, presented as the median and range, are shown in Table 4.13. Data were missing for one control. The Mann-Whitney U-test was used to compare levels of CSF NF-L between controls and patients with early AD. Patients with early AD had significantly increased levels of CSF NF-L compared to controls (p=0.002).

Table 4.13 *CSF levels of NF-L presented as the median and range.*

	NF-L (pg/ml)
Controls (n=19)	1351.4 (662.3-4496.5)
Early AD (n=20)	2303.0 (1320.9-7436.6)
p-value	0.002*

*Significant difference between controls and patients with early AD

Boxplots illustrating CSF NF-L levels for controls and patients with early AD are shown in Figure 4.29, where a significantly higher level can be observed among patients. Two control samples (#13 and #18) and two patient samples (#21 and #28) had outlying values that were substantially higher than the levels in the rest of their respective group.

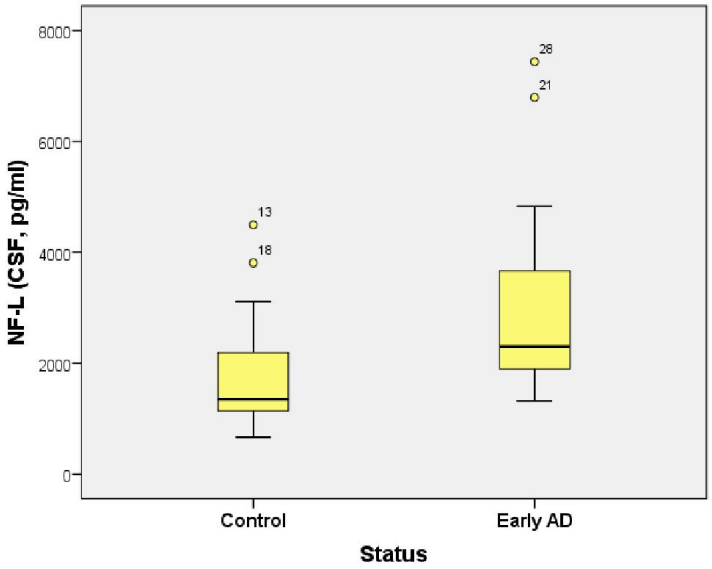

Figure 4.29 *Boxplots of CSF NF-L levels in controls and patients with early AD.*

4.2.6.1 Diagnostic performance of NF-L

To evaluate the diagnostic performance of the CSF level of NF-L as a potential diagnostic biomarker for early AD in the present study, a ROC curve was generated (Figure 4.30). A ROC curve for the ratio NF-L/Aβ42 is also presented in Figure 4.30, and the ROC curve for Aβ42 was added for comparison.

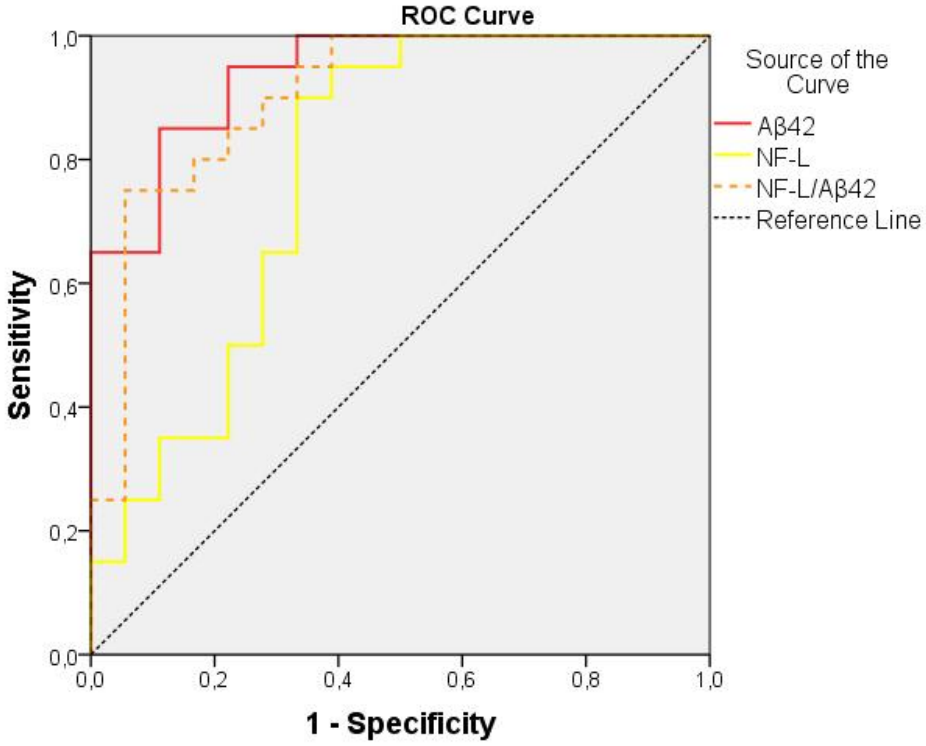

Figure 4.30 *Receiver operating characteristic (ROC) curves for the performance of CSF Aβ42, NF-L and the ratio NF-L/Aβ42 for distinguishing between patients with early AD and healthy controls.*

Cut-off values that maximized sensitivity and specificity were selected from the ROC curves, and are presented in Table 4.14.

Table 4.14 *Area under the ROC curves (AUC), cut-off values and corresponding sensitivity and specificity levels for CSF Aβ42, NF-L and the ratio NF-L/Aβ42, for differentiating between patients with early AD and healthy controls.*

	AUC	p-value	Cut-off (pg/ml)	Sensitivity	Specificity
Aβ42	0.942	<0.001	830.1 698.1	95% 85%	79% 84%
NF-L	0.787	0.002	1716.9	90%	68%
NF-L/Aβ42	0.903	<0.001	3.418 3.923	85% 80%	78% 83%

Table 4.14 shows that NF-L had a fairly good capability to distinguish between patients with early AD and healthy controls in the present study, but its diagnostic precision was well below the performance of Aβ42. However, the ratio between NF-L and Aβ42 differentiated very well between patients with early AD and healthy controls, with an AUC=0.903. The results indicate that NF-L had high sensitivity, but lower specificity than the core biomarkers. Figure 4.31 shows a scatter plot visualizing the combination of NF-L and Aβ42.

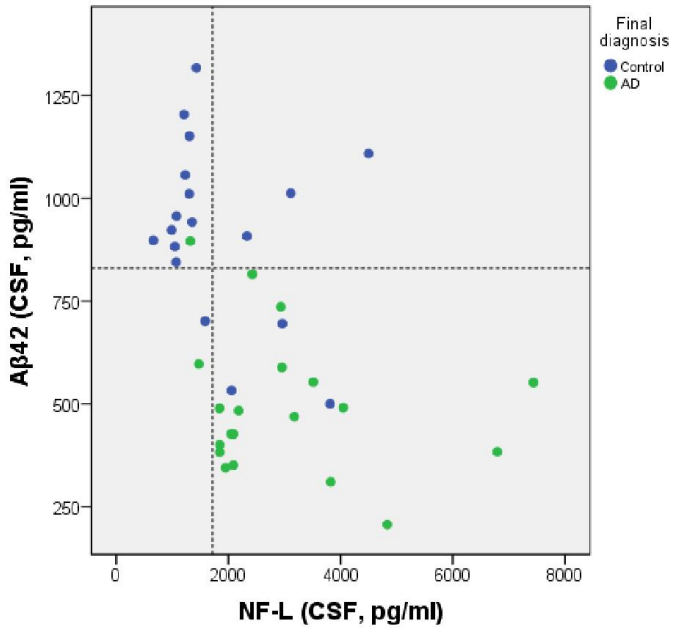

Figure 4.31 *Scatter plot showing the combination of NF-L and Aβ42 concentrations. The horizontal dotted line represents the cut-off value for Aβ42 (830.1 pg/ml), and the vertical dotted line represents the cut-off value for NF-L (1716.9 pg/ml).*

4.2.6.2 Correlations between NF-L and core biomarkers in CSF

Spearman's correlation coefficient (r_s) was calculated between CSF NF-L and CSF Aβ and tau, in the control and patient group. Data are presented in Table 4.15.

Table 4.15 *Spearman's correlation coefficient (r_s) between CSF NF-L and levels of Aβ and tau in CSF (pg/ml).*

	NF-L (CSF, pg/ml)	
	Controls	**Early AD**
Aβ42	- 0.088	- 0.153
Aβ40	0.364	0.176
T-tau	0.676**	0.759***
P-tau	0.521**	0.708***

** p<0.05
*** p<0.001

A significant, positive correlation was found between the levels of CSF NF-L and T-tau in both control (r_s=0.676, p=0.002) and patient samples (r_s=0.759, p<0.001), illustrated in Figure 4.32.

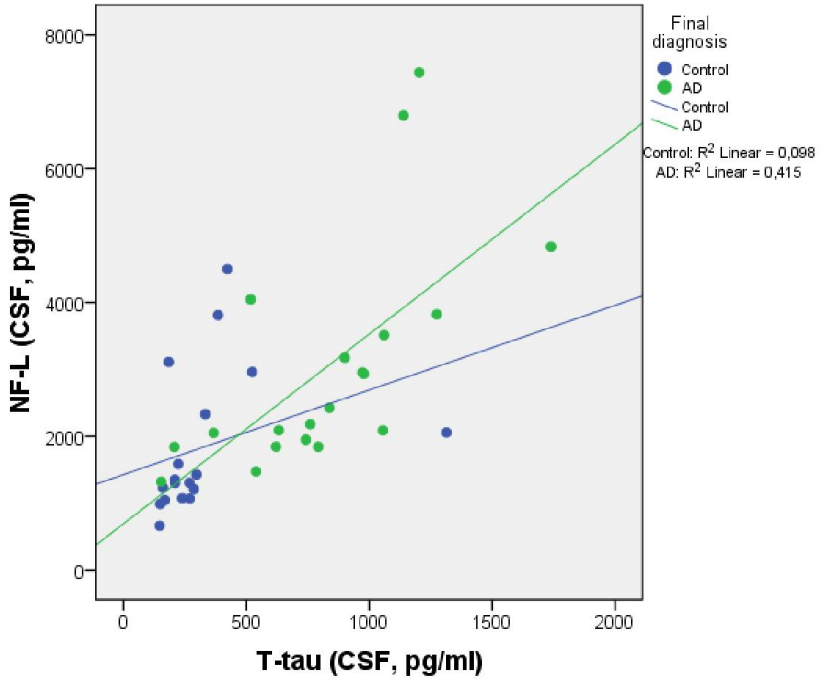

Figure 4.32 *Correlation between CSF levels of NF-L and T-tau in controls and patients with early AD. A best-fit line has been added to the specific subgroups.*

A significant, positive correlation was found between the levels of CSF NF-L and P-tau in both control (r_s=0.521, p=0.027) and patient samples (r_s=0.708, p<0.001), illustrated in Figure 4.33.

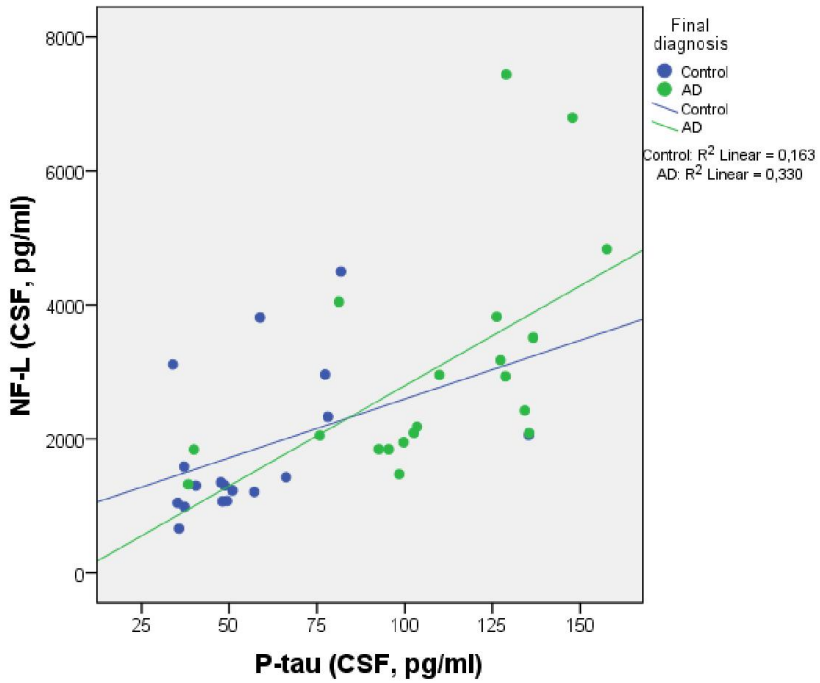

Figure 4.33 *Correlation between CSF levels of NF-L and P-tau in controls and patients with early AD. A best-fit line has been added to the specific subgroups.*

5 Discussion

The CSF biomarkers Aβ42, T-tau and P-tau, reflecting core pathological features of AD, have consistently been reported to have a high diagnostic accuracy in the discrimination between patients with AD and healthy elderly controls, also in early phases of the disease. This was also true in the present pilot study in which, despite the low number of samples, the core CSF biomarkers identified early AD with high levels of sensitivity and specificity. For decades, considerable efforts have focused on Aβ and tau, the main components of amyloid plaques and neurofibrillary tangles, respectively. Misfolding, accumulation and aggregation of the Aβ peptide have all been proposed to be the key events that initiate the pathological cascade leading to AD. Aβ has thereby been considered to be upstream of tau in AD pathogenesis and supposedly triggers the conversion of tau from a normal to a toxic state (Bloom, 2014). The putative key role of Aβ in pathogenesis of AD led to immunotherapeutic strategies to reduce levels of Aβ in the brain. Although successful in this respect, the clearance did not prevent progressive neurodegeneration or improve cognitive performance (Doody et al., 2014, Salloway et al., 2014). Therefore it is possible that Aβ accumulation is necessary to initiate, but not to maintain, progressive neurodegeneration. Although Aβ and tau undoubtedly play important roles in AD, little is known about the influence of other proteins, and we need to expand and look beyond these two molecules regarding the etiology of AD and development of new therapeutic strategies. Ultimately, it would be best to stop the disease process as early as possible before large numbers of neurons have been destroyed. This requires studying and understanding the earliest pre-dementia, and even pre-symptomatic phases of the disease. This will require biomarkers in addition to the CSF Aβ and tau species. This project sought to study, in CSF, and plasma or serum as suitable, a series of potentially useful additional substances.

5.1 Apolipoprotein E

The frequency of the *APOE* ε4 allele, the major genetic risk factor for sporadic AD, has consistently been shown to be dramatically increased in patients with AD (Sando et al., 2008b, Lovati et al., 2010). This was also true in the present study, in which 75% of the patients carried one or two *APOE* ε4 alleles, compared to the control group where 40% were carries of one *APOE* ε4 allele. The level in the control group was somewhat higher than found in a large study of the Trønderbrain material (Sando et al., 2008b), and probably an effect of studying a small group. Besides the genetic polymorphism, ApoE levels in plasma and serum have also been suggested to reflect disease status, and may therefore have potential as a diagnostic blood-based biomarker for AD (Wang et al., 2014). In the present study, no significant difference in serum ApoE was found between patients with early AD and healthy controls. However, in accordance with previous studies (Soares et al., 2012, Gupta et al.,

2011, Slooter et al., 1998), *APOE* ε4 carriers were found to have significantly lower levels of serum ApoE compared to non-ε4 carriers in both patients and controls, indicating that the serum ApoE level differs according to *APOE* genotype rather than the disease itself. If the serum ApoE level in fact depends on the distribution of *APOE* genotype irrespective of diagnosis, it would still be reasonable to expect lower levels of total ApoE in AD patients due to the higher percentage of *APOE* ε4-positive individuals. Although not statistically significant, the average level of serum ApoE was indeed lower in early AD patients compared to controls in the present study. The lack of significance may be attributed to the comparatively high frequency of the *APOE* ε4 allele in the control group in this material. Furthermore, the majority of previous studies have demonstrated significantly lower levels of serum or plasma ApoE in AD patients compared with controls, supported by a recent meta-analysis (Wang et al., 2014). The factors that influence ApoE levels in plasma and serum are unknown, but it has been suggested that the lower levels result from a more effective breakdown of lipoproteins in the liver of *APOE* ε4-positive individuals (Smit et al., 1988).

ApoE has been suggested to be fundamentally involved in the metabolism of Aβ (Potter and Wisniewski, 2012). In line with this notion, it has been demonstrated that *APOE* ε4 carriers have lower CSF Aβ42 and show more PiB binding on PET than non-ε4 carriers, indicating a greater burden of Aβ deposition in the brain of *APOE* ε4 carriers (Prince et al., 2004, Head et al., 2012). This seems to support the hypothesis that ApoE may act as a "pathological chaperone" that catalyzes Aβ aggregation, with ApoE4 being the strongest promoter of Aβ polymerization, or that ApoE serves to clear Aβ from the brain, with ApoE4 being less efficient in this function compared to the other isoforms. However, such indications could not be drawn from the present results where no significant difference was found between CSF Aβ42 and *APOE* ε4 carrier status. Although the number of participants might be too low in the present study to detect any statistically significant differences, this result has since been confirmed in a larger sample from the Trønderbrain study (unpublished results from Camilla Lauridsen). Since no direct disease-specific change in serum ApoE level was found, the present study does not support serum ApoE as a potential biomarker for early AD.

5.2 Clusterin (apolipoprotein J)

Nevertheless, because *APOE* ε4 has such a strong role as a risk factor for AD, it seems important to continue studying levels of ApoE in CSF in relation to other molecules that may have similar functions. Clusterin is another apolipoprotein that has demonstrated chaperone functions related to Aβ metabolism, and has also been linked to AD pathogenesis (Nuutinen et al., 2009). Studies have shown elevated levels of clusterin in affected areas of the AD brain (Lidstrom et al., 1998, Bertrand et al., 1995, Oda et al., 1994), and since the interstitial fluid of the brain is associated with the CSF, the

increased level of clusterin in AD brain tissue might also have been reflected in the CSF. However, initial small scale studies did not find altered levels of CSF clusterin in AD patients compared to healthy controls (Lidstrom et al., 2001, Harr et al., 1996). Considering the fact that clusterin is a highly glycosylated protein and the level of glycosylation can change, Nilselid et al. (2006) hypothesized that this might hamper the binding to clusterin antibody and thereby interfere with the quantification of clusterin in CSF. Based on this assumption, they performed a pilot study, wherein elevated clusterin levels in AD were found in deglycosylated samples, but not in native samples. When expanding the material of AD patients and controls, the CSF clusterin level was found to be significantly increased in AD, in *both* native and deglycosylated samples, indicating that the deglycosylation was not essential to demonstrate an elevated level of CSF clusterin in AD patients in a larger material (Nilselid et al., 2006). In accordance with previous reports on small scale material, no significant difference in CSF clusterin was found when comparing controls and patients with early AD in the present study. In light of the report by Nilselid et al. (2006), it seems that a larger patient material is needed to find any statistically significant differences regarding clusterin in CSF. However, even if differences were found, they would probably be too small to consider clusterin as a reliable biomarker.

Recently, there has been interest in the evaluation of levels of clusterin in plasma as a biomarker for AD. In the present study, plasma levels of clusterin in patients with early AD were not significantly different from levels in healthy controls, but a trend towards higher levels in patients was observed. There was also a small, but significant reduction in plasma clusterin in controls not carrying the *APOE* ε4 allele. Plasma levels of clusterin have previously been reported to be unchanged in AD patients compared to controls (Liao et al., 2007), but because only ten AD samples were included in this study, its reliability is questionable. However, a large study has demonstrated that patients with AD had significantly higher levels of plasma clusterin than controls (Schrijvers et al., 2011). Schrijvers et al. (2011) also reported that plasma clusterin levels were higher in more severe cases of AD, and that increased levels of clusterin did not precede the clinical onset of dementia. Based on these findings and the fact that the expression of clusterin is known to be up-regulated in a wide variety of cellular stress and injury, the elevated levels of clusterin in AD may represent a failed neuroprotective attempt triggered by the progressive neurodegenerative changes, rather than a preclinical event. This notion would be in agreement with the fact that CSF clusterin correlated positively with T-tau and P-tau in both control and patient groups in the present study, given that T-tau and P-tau in CSF are thought to reflect degree of neuronal degeneration or damage. Consequently, these findings altogether do not support clusterin as a potential biomarker for early AD, but rather suggest that clusterin should be considered as a non-specific cellular response to a wide variety of tissue insults.

5.3 Angiotensin-converting enzyme

ACE is a protease whose major function is to increase blood pressure by converting angiotensin I to angiotensin II, which causes blood vessels to constrict. ACE has also been demonstrated to mediate cleavage of Aβ *in vitro*, and there is some indication of an association between *ACE* I/D polymorphism and AD. In the present study, no significant differences were found between patients with early AD and controls concerning levels in CSF and serum, nor with regard to *ACE* genotype or allele distribution. However, the results seemed to indicate a relationship between *ACE* I/D polymorphism and level of serum ACE irrespective of diagnosis, where the I-allele was associated with lower serum levels of ACE whereas the D-allele associated with higher levels. Although not presented in the present study, this was recently tested in a larger study material where the association was even more evident (Camilla Lauridsen, unpublished results). This agrees with results from Zhang et al. (2012) who found that serum ACE level was significantly elevated according to D-allele-dose among the three genotypes (DD > DI > II) in both patients with aMCI and healthy controls, thus indicating that the increase is related to genotype rather than to the disease process.

Two patients in this study took ACE-inhibitors against high blood pressure and had the highest serum ACE levels (outliers in Figure 4.22). The proposed ability of ACE to mediate cleavage of Aβ suggests that reduced ACE activity, either by genetic mechanisms or pharmacological inhibition, could increase cerebral levels of Aβ deposition. Moreover, this could increase the risk of developing AD and/or contribute to its progression. This might seem to contradict the fact that ACE-inhibitors, with the aim of reducing ACE activity and thereby presumably increasing Aβ deposition, have been found to be associated with reductions in the incidence and rate of cognitive decline in AD (O'Caoimh et al., 2014). This is probably because patients with advanced AD usually have mixed pathology demonstrating vascular features (Kalaria and Ballard, 1999). Pharmacological reduction of such features may be beneficial in some patients regardless of Aβ deposition.

ACE did not demonstrate any disease-specific effect in the present study, and is therefore not considered to have potential as a biomarker for early AD. However, the potential of ACE-inhibitors for increasing deposition of Aβ suggests that elderly patients requiring control of blood pressure should be given angiotensin receptor blockers, rather than ACE-inhibitors (Hemming and Selkoe, 2005).

In accordance with its name, ACE is most often considered in terms of its effect on angiotensin and its role in blood pressure regulation. However, ACE is present in most tissues and bodily fluids, and can catalyse the hydrolysis of a wide distribution of peptides (Skidgel and Erdos, 1987), suggesting that it might have a variety of physiological roles other than those related to blood pressure

regulation. In the present study, ACE in CSF demonstrated positive correlations with several other proteins in CSF of both the control and patient groups (significant correlations or strong trends), including T-tau, P-tau, Aβ40 and clusterin, supporting the possibility that ACE has a broad substrate specificity. The absence of correlation with Aβ42 can probably be explained by its aggregation-prone features; oligomeric species of Aβ42 may not be a suitable substrate.

5.4 Neurofilament-light

As previously demonstrated in numerous studies (reviewed by Blennow et al. (2012)), highly increased levels of CSF T-tau and P-tau in AD patients compared to healthy individuals were found also in the present study. The elevated levels of tau in AD suggest that levels of other neuronal structural proteins like NF-L would show a similar pattern, and potentially improve the ability to distinguish patients from healthy individuals, and perhaps patients with early disease from such controls.

As expected, a significantly higher level of CSF NF-L was found in patients with early AD compared to age-matched healthy individuals, a finding in agreement with results for patients with mild to severe AD dementia in a meta-analysis (Petzold et al., 2007). Moreover, NF-L correlated positively with T-tau and P-tau in both patients and controls, although more strongly in the patient group. CSF NF-L demonstrated a fairly good capability to distinguish between patients with early AD and healthy controls, but its diagnostic precision was well below that of P-tau, T-tau, and especially far behind that of Aβ42. Although NF-L demonstrated a similar level of sensitivity as the other core biomarkers, the specificity level of CSF NF-L was comparatively lower than for the core biomarkers. It has been suggested that the destruction of myelinated axons is likely to contribute more to elevated CSF NF-L levels than breakdown of nerve cell bodies. In AD, the degeneration of cortical neurons dominates, whereas the subcortical white matter changes are less severe. Therefore, NF-L is probably more suitable as a biomarker for a disease like multiple sclerosis where there is greater destruction of myelinated axons (Lycke et al., 1998), than neurodegenerative diseases like AD. In addition, white matter changes are also observed in asymptomatic older healthy individuals (Fazekas et al., 1996), and may account for the low specificity of CSF NF-L in the present study. Nevertheless, the ratio of NF-L/Aβ42 differentiated very well between patients with early AD and healthy controls, and of the proteins tested in the present study, showed the best potential as a biomarker. However, it seems unlikely that NF-L will replace tau as a core biomarker for AD as it does not reduce the overlap between healthy controls and patients with early AD.

5.5 Aspects concerning methodology and future developments

The present study has both strengths and weaknesses. Due to the small sample size, the reliability of the study can be questioned. Given the low number of samples, asymmetric distributions of the variables and frequent presence of outliers in the material, non-parametric statistical tests were used. Making fewer assumptions about the distributional shape of the variables, non-parametric tests have generally less power than their parametric counterparts. A study with low statistical power has a reduced chance of detecting a true effect, but low power also reduces the likelihood that a statistically significant finding actually reflects a true effect (Button et al., 2013). However, the present study was intended as an exploratory pilot study, deliberately testing a low number of samples in order to evaluate the usefulness of further, more comprehensive investigation of certain proteins. Even non-significant trends were therefore considered worth reporting, as a trend in a small material may turn out to be significant in a larger material. Conversely, results that show high p-values are not likely to reach significance even in a much larger study, thus saving research time and resources.

Since the core biomarkers for AD distinguished the twenty patient samples from the twenty control samples so convincingly even in this small study, this supports the plausibility of the other results despite the size of the study. Even results that are not significant can provide useful information, and improve the quality of the Trønderbrain material overall.

Another major strength of the present study is the fact that all participants were clinically assessed and diagnosed by the same, experienced neurologist, who is specialized in dementia. This provides standardization within and between groups. However, the possibility that there might be presence of non-symptomatic AD patients among the controls cannot be excluded. In fact, one control individual in the present study was found to present with a typical “AD biomarker profile” in CSF, that is, low levels of Aβ42 and high levels of P-tau and T-tau (outlier #4 in Figure 4.1, 4.3 and 4.4). This indicates that the healthy individual included as a control, nevertheless might have been in a preclinical phase of AD at the time of sampling and may develop AD in time. The contract-based agreement with all study participants states that no feedback is to be given regarding results of biochemical testing, and there is therefore no contact with control individual #4 in this connection. Nevertheless, such samples may be extremely valuable for the future, because they may provide a means for studying the preclinical stage of AD.

If effective disease-modifying therapies become available in the future, diagnostic tools allowing early detection of AD in the general population will be essential for the prevention of the illness. Compared with CSF, blood analysis can be accessed with minimal discomfort to the subjects, making

it more suitable for screening of large populations. However, it is still unknown how the concentration of analytes in the blood directly correlates with pathological changes in the brain, especially in AD, and the results of the present study did not provide support for any of the proteins studied here as candidate blood-based biomarkers for AD.

6 Conclusion

No significant differences were found between patients with early AD and elderly control individuals regarding levels of ApoE in serum, clusterin in CSF or plasma, or ACE in CSF or serum. Nevertheless, the results indicated that levels of serum ApoE and ACE differ according, respectively, to *APOE* and *ACE* genotype. Since no disease-specific alteration was found in relation to ApoE, clusterin or ACE, this study does not support their potential as biomarker candidates for early AD. Patients with early AD demonstrated significantly higher levels of NF-L in CSF compared to the control group. However, as the diagnostic accuracy was well below that of Aβ and tau protein, it does not seem to provide improved discrimination as a biomarker. No candidate biomarkers for early AD were therefore identified in the present study. However, the data in the study seem to be robust and can improve the quality of the Trønderbrain material overall.

References

1987. About a peculiar disease of the cerebral cortex. By Alois Alzheimer, 1907 (Translated by L. Jarvik and H. Greenson). *Alzheimer Dis Assoc Disord,* 1**,** 3-8.

1998. Consensus report of the Working Group on: "Molecular and Biochemical Markers of Alzheimer's Disease". The Ronald and Nancy Reagan Research Institute of the Alzheimer's Association and the National Institute on Aging Working Group. *Neurobiol Aging.* 1998/04/29 ed.

2001. Biomarkers and surrogate endpoints: preferred definitions and conceptual framework. *Clin Pharmacol Ther,* 69**,** 89-95.

Alladi, S., Xuereb, J., Bak, T., Nestor, P., Knibb, J., Patterson, K. & Hodges, J. R. 2007. Focal cortical presentations of Alzheimer's disease. *Brain,* 130**,** 2636-45.

Andreasen, N., Minthon, L., Clarberg, A., Davidsson, P., Gottfries, J., Vanmechelen, E., Vanderstichele, H., Winblad, B. & Blennow, K. 1999. Sensitivity, specificity, and stability of CSF-tau in AD in a community-based patient sample. *Neurology,* 53**,** 1488-94.

Arendt, T., Bigl, V., Arendt, A. & Tennstedt, A. 1983. Loss of neurons in the nucleus basalis of Meynert in Alzheimer's disease, paralysis agitans and Korsakoff's Disease. *Acta Neuropathol,* 61**,** 101-8.

Attwell, D. & Laughlin, S. B. 2001. An energy budget for signaling in the grey matter of the brain. *J Cereb Blood Flow Metab,* 21**,** 1133-45.

Barnes, N. M., Cheng, C. H., Costall, B., Naylor, R. J., Williams, T. J. & Wischik, C. M. 1991. Angiotensin converting enzyme density is increased in temporal cortex from patients with Alzheimer's disease. *Eur J Pharmacol,* 200**,** 289-92.

Bateman, R. J., Xiong, C., Benzinger, T. L., Fagan, A. M., Goate, A., Fox, N. C., Marcus, D. S., Cairns, N. J., Xie, X., Blazey, T. M., Holtzman, D. M., Santacruz, A., Buckles, V., Oliver, A., Moulder, K., Aisen, P. S., Ghetti, B., Klunk, W. E., Mcdade, E., Martins, R. N., Masters, C. L., Mayeux, R., Ringman, J. M., Rossor, M. N., Schofield, P. R., Sperling, R. A., Salloway, S. & Morris, J. C. 2012. Clinical and biomarker changes in dominantly inherited Alzheimer's disease. *N Engl J Med,* 367**,** 795-804.

Benilova, I., Karran, E. & De Strooper, B. 2012. The toxic Abeta oligomer and Alzheimer's disease: an emperor in need of clothes. *Nat Neurosci,* 15**,** 349-57.

Berge, G., Sando, S. B., Rongve, A., Aarsland, D. & White, L. R. 2014. Apolipoprotein E {varepsilon}2 genotype delays onset of dementia with Lewy bodies in a Norwegian cohort. *J Neurol Neurosurg Psychiatry*.

Bertram, L., Lill, C. M. & Tanzi, R. E. 2010. The genetics of Alzheimer disease: back to the future. *Neuron,* 68**,** 270-81.

Bertrand, P., Poirier, J., Oda, T., Finch, C. E. & Pasinetti, G. M. 1995. Association of apolipoprotein E genotype with brain levels of apolipoprotein E and apolipoprotein J (clusterin) in Alzheimer disease. *Brain Res Mol Brain Res,* 33**,** 174-8.

Bhamra, M. S. & Ashton, N. J. 2012. Finding a pathological diagnosis for Alzheimer's disease: are inflammatory molecules the answer? *Electrophoresis,* 33**,** 3598-607.

Billings, L. M., Oddo, S., Green, K. N., Mcgaugh, J. L. & Laferla, F. M. 2005. Intraneuronal Abeta causes the onset of early Alzheimer's disease-related cognitive deficits in transgenic mice. *Neuron,* 45**,** 675-88.

Bjorkqvist, M., Ohlsson, M., Minthon, L. & Hansson, O. 2012. Evaluation of a previously suggested plasma biomarker panel to identify Alzheimer's disease. *PLoS One,* 7**,** e29868.

Blennow, K. 2004. Cerebrospinal fluid protein biomarkers for Alzheimer's disease. *NeuroRx,* 1**,** 213-25.

Blennow, K., Hampel, H., Weiner, M. & Zetterberg, H. 2010. Cerebrospinal fluid and plasma biomarkers in Alzheimer disease. *Nat Rev Neurol,* 6**,** 131-44.

Blennow, K., Vanmechelen, E. & Hampel, H. 2001. CSF total tau, Abeta42 and phosphorylated tau protein as biomarkers for Alzheimer's disease. *Mol Neurobiol,* 24**,** 87-97.

Blennow, K., Wallin, A., Agren, H., Spenger, C., Siegfried, J. & Vanmechelen, E. 1995. Tau protein in cerebrospinal fluid: a biochemical marker for axonal degeneration in Alzheimer disease? *Mol Chem Neuropathol,* 26**,** 231-45.

Blennow, K., Zetterberg, H. & Fagan, A. M. 2012. Fluid biomarkers in Alzheimer disease. *Cold Spring Harb Perspect Med,* 2**,** a006221.

Bloom, G. S. 2014. Amyloid-beta and Tau: The Trigger and Bullet in Alzheimer Disease Pathogenesis. *JAMA Neurol,* 71**,** 505-8.

Bobinski, M., De Leon, M. J., Wegiel, J., Desanti, S., Convit, A., Saint Louis, L. A., Rusinek, H. & Wisniewski, H. M. 2000. The histological validation of post mortem magnetic resonance imaging-determined hippocampal volume in Alzheimer's disease. *Neuroscience,* 95**,** 721-5.

Braak, H. & Braak, E. 1991. Neuropathological stageing of Alzheimer-related changes. *Acta Neuropathol,* 82**,** 239-59.

Brookmeyer, R., Johnson, E., Ziegler-Graham, K. & Arrighi, H. M. 2007. Forecasting the global burden of Alzheimer's disease. *Alzheimers Dement,* 3**,** 186-91.

Brun, A. & Gustafson, L. 1976. Distribution of cerebral degeneration in Alzheimer's disease. A clinico-pathological study. *Arch Psychiatr Nervenkr,* 223**,** 15-33.

Buchhave, P., Minthon, L., Zetterberg, H., Wallin, A. K., Blennow, K. & Hansson, O. 2012. Cerebrospinal fluid levels of beta-amyloid 1-42, but not of tau, are fully changed already 5 to 10 years before the onset of Alzheimer dementia. *Arch Gen Psychiatry,* 69**,** 98-106.

Buerger, K., Ewers, M., Pirttila, T., Zinkowski, R., Alafuzoff, I., Teipel, S. J., Debernardis, J., Kerkman, D., Mcculloch, C., Soininen, H. & Hampel, H. 2006. CSF phosphorylated tau protein correlates with neocortical neurofibrillary pathology in Alzheimer's disease. *Brain,* 129**,** 3035-41.

Button, K. S., Ioannidis, J. P., Mokrysz, C., Nosek, B. A., Flint, J., Robinson, E. S. & Munafo, M. R. 2013. Power failure: why small sample size undermines the reliability of neuroscience. *Nat Rev Neurosci,* 14**,** 365-76.

Carrillo, M. C., Blennow, K., Soares, H., Lewczuk, P., Mattsson, N., Oberoi, P., Umek, R., Vandijck, M., Salamone, S., Bittner, T., Shaw, L. M., Stephenson, D., Bain, L. & Zetterberg, H. 2013. Global standardization measurement of cerebral spinal fluid for Alzheimer's disease: an update from the Alzheimer's Association Global Biomarkers Consortium. *Alzheimers Dement,* 9**,** 137-40.

Caselli, R. J. & Reiman, E. M. 2013. Characterizing the preclinical stages of Alzheimer's disease and the prospect of presymptomatic intervention. *J Alzheimers Dis,* 33 Suppl 1**,** S405-16.

Cedazo-Minguez, A. 2007. Apolipoprotein E and Alzheimer's disease: molecular mechanisms and therapeutic opportunities. *J Cell Mol Med,* 11**,** 1227-38.

Chen, M., Inestrosa, N. C., Ross, G. S. & Fernandez, H. L. 1995. Platelets are the primary source of amyloid beta-peptide in human blood. *Biochem Biophys Res Commun,* 213**,** 96-103.

Citron, M. 2010. Alzheimer's disease: strategies for disease modification. *Nat Rev Drug Discov,* 9**,** 387-98.

Clark, C. M., Schneider, J. A., Bedell, B. J., Beach, T. G., Bilker, W. B., Mintun, M. A., Pontecorvo, M. J., Hefti, F., Carpenter, A. P., Flitter, M. L., Krautkramer, M. J., Kung, H. F., Coleman, R. E., Doraiswamy, P. M., Fleisher, A. S., Sabbagh, M. N., Sadowsky, C. H., Reiman, E. P., Zehntner, S. P. & Skovronsky, D. M. 2011. Use of florbetapir-PET for imaging beta-amyloid pathology. *JAMA,* 305**,** 275-83.

Clark, C. M., Xie, S., Chittams, J., Ewbank, D., Peskind, E., Galasko, D., Morris, J. C., Mckeel, D. W., Jr., Farlow, M., Weitlauf, S. L., Quinn, J., Kaye, J., Knopman, D., Arai, H., Doody, R. S., Decarli, C., Leight, S., Lee, V. M. & Trojanowski, J. Q. 2003. Cerebrospinal fluid tau and beta-amyloid: how well do these biomarkers reflect autopsy-confirmed dementia diagnoses? *Arch Neurol,* 60**,** 1696-702.

Coates, D. 2003. The angiotensin converting enzyme (ACE). *Int J Biochem Cell Biol,* 35**,** 769-73.

Corbo, R. M. & Scacchi, R. 1999. Apolipoprotein E (APOE) allele distribution in the world. Is APOE*4 a 'thrifty' allele? *Ann Hum Genet,* 63**,** 301-10.

Corder, E. H., Saunders, A. M., Strittmatter, W. J., Schmechel, D. E., Gaskell, P. C., Small, G. W., Roses, A. D., Haines, J. L. & Pericak-Vance, M. A. 1993. Gene dose of apolipoprotein E type 4 allele and the risk of Alzheimer's disease in late onset families. *Science,* 261**,** 921-3.

Coyle, J. T., Price, D. L. & Delong, M. R. 1983. Alzheimer's disease: a disorder of cortical cholinergic innervation. *Science,* 219**,** 1184-90.

Davies, P. & Maloney, A. J. 1976. Selective loss of central cholinergic neurons in Alzheimer's disease. *Lancet,* 2**,** 1403.

Del Bigio, M. R. 1995. The ependyma: a protective barrier between brain and cerebrospinal fluid. *Glia,* 14**,** 1-13.

Delaere, P., Duyckaerts, C., Masters, C., Beyreuther, K., Piette, F. & Hauw, J. J. 1990. Large amounts of neocortical beta A4 deposits without neuritic plaques nor tangles in a psychometrically assessed, non-demented person. *Neurosci Lett,* 116**,** 87-93.

Dickerson, B. C., Bakkour, A., Salat, D. H., Feczko, E., Pacheco, J., Greve, D. N., Grodstein, F., Wright, C. I., Blacker, D., Rosas, H. D., Sperling, R. A., Atri, A., Growdon, J. H., Hyman, B. T., Morris, J. C., Fischl, B. & Buckner, R. L. 2009. The cortical signature of Alzheimer's disease: regionally specific cortical thinning relates to symptom severity in very mild to mild AD dementia and is detectable in asymptomatic amyloid-positive individuals. *Cereb Cortex,* 19**,** 497-510.

Dickson, D. W., Crystal, H. A., Mattiace, L. A., Masur, D. M., Blau, A. D., Davies, P., Yen, S. H. & Aronson, M. K. 1992. Identification of normal and pathological aging in prospectively studied nondemented elderly humans. *Neurobiol Aging,* 13**,** 179-89.

Doecke, J. D., Laws, S. M., Faux, N. G., Wilson, W., Burnham, S. C., Lam, C. P., Mondal, A., Bedo, J., Bush, A. I., Brown, B., De Ruyck, K., Ellis, K. A., Fowler, C., Gupta, V. B., Head, R., Macaulay, S. L., Pertile, K., Rowe, C. C., Rembach, A., Rodrigues, M., Rumble, R., Szoeke, C., Taddei, K., Taddei, T., Trounson, B., Ames, D., Masters, C. L. & Martins, R. N. 2012. Blood-based protein biomarkers for diagnosis of Alzheimer disease. *Arch Neurol,* 69**,** 1318-25.

Doody, R. S., Thomas, R. G., Farlow, M., Iwatsubo, T., Vellas, B., Joffe, S., Kieburtz, K., Raman, R., Sun, X., Aisen, P. S., Siemers, E., Liu-Seifert, H. & Mohs, R. 2014. Phase 3 trials of solanezumab for mild-to-moderate Alzheimer's disease. *N Engl J Med,* 370**,** 311-21.

Dubois, B., Feldman, H. H., Jacova, C., Cummings, J. L., Dekosky, S. T., Barberger-Gateau, P., Delacourte, A., Frisoni, G., Fox, N. C., Galasko, D., Gauthier, S., Hampel, H., Jicha, G. A., Meguro, K., O'brien, J., Pasquier, F., Robert, P., Rossor, M., Salloway, S., Sarazin, M., De Souza, L. C., Stern, Y., Visser, P. J. & Scheltens, P. 2010. Revising the definition of Alzheimer's disease: a new lexicon. *Lancet Neurol,* 9**,** 1118-27.

Dubois, B., Feldman, H. H., Jacova, C., Dekosky, S. T., Barberger-Gateau, P., Cummings, J., Delacourte, A., Galasko, D., Gauthier, S., Jicha, G., Meguro, K., O'brien, J., Pasquier, F., Robert, P., Rossor, M., Salloway, S., Stern, Y., Visser, P. J. & Scheltens, P. 2007. Research criteria for the diagnosis of Alzheimer's disease: revising the NINCDS-ADRDA criteria. *Lancet Neurol,* 6**,** 734-46.

Fagan, A. M. & Holtzman, D. M. 2010. Cerebrospinal fluid biomarkers of Alzheimer's disease. *Biomark Med,* 4**,** 51-63.

Fagan, A. M., Mintun, M. A., Mach, R. H., Lee, S. Y., Dence, C. S., Shah, A. R., Larossa, G. N., Spinner, M. L., Klunk, W. E., Mathis, C. A., Dekosky, S. T., Morris, J. C. & Holtzman, D. M. 2006. Inverse relation between in vivo amyloid imaging load and cerebrospinal fluid Abeta42 in humans. *Ann Neurol,* 59**,** 512-9.

Farrer, L. A., Cupples, L. A., Haines, J. L., Hyman, B., Kukull, W. A., Mayeux, R., Myers, R. H., Pericak-Vance, M. A., Risch, N. & Van Duijn, C. M. 1997. Effects of age, sex, and ethnicity on the association between apolipoprotein E genotype and Alzheimer disease. A meta-analysis. APOE and Alzheimer Disease Meta Analysis Consortium. *JAMA,* 278**,** 1349-56.

Fazekas, F., Kapeller, P., Schmidt, R., Offenbacher, H., Payer, F. & Fazekas, G. 1996. The relation of cerebral magnetic resonance signal hyperintensities to Alzheimer's disease. *J Neurol Sci,* 142**,** 121-5.

Ferreira, S. T. & Klein, W. L. 2011. The Abeta oligomer hypothesis for synapse failure and memory loss in Alzheimer's disease. *Neurobiol Learn Mem,* 96**,** 529-43.

Folstein, M. F., Folstein, S. E. & Mchugh, P. R. 1975. "Mini-mental state". A practical method for grading the cognitive state of patients for the clinician. *J Psychiatr Res,* 12**,** 189-98.

Friede, R. L. & Samorajski, T. 1970. Axon caliber related to neurofilaments and microtubules in sciatic nerve fibers of rats and mice. *Anat Rec,* 167**,** 379-87.

Frisoni, G. B., Fox, N. C., Jack, C. R., Jr., Scheltens, P. & Thompson, P. M. 2010. The clinical use of structural MRI in Alzheimer disease. *Nat Rev Neurol,* 6**,** 67-77.

Fukumoto, H., Tokuda, T., Kasai, T., Ishigami, N., Hidaka, H., Kondo, M., Allsop, D. & Nakagawa, M. 2010. High-molecular-weight beta-amyloid oligomers are elevated in cerebrospinal fluid of Alzheimer patients. *FASEB J,* 24**,** 2716-26.

Furukawa, K., Sopher, B. L., Rydel, R. E., Begley, J. G., Pham, D. G., Martin, G. M., Fox, M. & Mattson, M. P. 1996. Increased activity-regulating and neuroprotective efficacy of alpha-secretase-derived secreted amyloid precursor protein conferred by a C-terminal heparin-binding domain. *J Neurochem,* 67**,** 1882-96.

Gatz, M., Reynolds, C. A., Fratiglioni, L., Johansson, B., Mortimer, J. A., Berg, S., Fiske, A. & Pedersen, N. L. 2006. Role of genes and environments for explaining Alzheimer disease. *Arch Gen Psychiatry,* 63**,** 168-74.

Genius, J., Klafki, H., Benninghoff, J., Esselmann, H. & Wiltfang, J. 2012. Current application of neurochemical biomarkers in the prediction and differential diagnosis of Alzheimer's disease and other neurodegenerative dementias. *Eur Arch Psychiatry Clin Neurosci,* 262 Suppl 2**,** S71-7.

Georganopoulou, D. G., Chang, L., Nam, J. M., Thaxton, C. S., Mufson, E. J., Klein, W. L. & Mirkin, C. A. 2005. Nanoparticle-based detection in cerebral spinal fluid of a soluble pathogenic biomarker for Alzheimer's disease. *Proc Natl Acad Sci U S A,* 102**,** 2273-6.

Geula, C., Nagykery, N., Nicholas, A. & Wu, C. K. 2008. Cholinergic neuronal and axonal abnormalities are present early in aging and in Alzheimer disease. *J Neuropathol Exp Neurol,* 67**,** 309-18.

Glabe, C. G. 2008. Structural classification of toxic amyloid oligomers. *J Biol Chem,* 283**,** 29639-43.

Glenner, G. G. & Wong, C. W. 1984. Alzheimer's disease: initial report of the purification and characterization of a novel cerebrovascular amyloid protein. *Biochem Biophys Res Commun,* 120**,** 885-90.

Goate, A., Chartier-Harlin, M. C., Mullan, M., Brown, J., Crawford, F., Fidani, L., Giuffra, L., Haynes, A., Irving, N., James, L. & Et Al. 1991. Segregation of a missense mutation in the amyloid precursor protein gene with familial Alzheimer's disease. *Nature,* 349**,** 704-6.

Greene, J. D., Baddeley, A. D. & Hodges, J. R. 1996. Analysis of the episodic memory deficit in early Alzheimer's disease: evidence from the doors and people test. *Neuropsychologia,* 34**,** 537-51.

Grundke-Iqbal, I., Iqbal, K., Tung, Y. C., Quinlan, M., Wisniewski, H. M. & Binder, L. I. 1986. Abnormal phosphorylation of the microtubule-associated protein tau (tau) in Alzheimer cytoskeletal pathology. *Proc Natl Acad Sci U S A,* 83**,** 4913-7.

Gupta, V. B., Laws, S. M., Villemagne, V. L., Ames, D., Bush, A. I., Ellis, K. A., Lui, J. K., Masters, C., Rowe, C. C., Szoeke, C., Taddei, K. & Martins, R. N. 2011. Plasma apolipoprotein E and Alzheimer disease risk: the AIBL study of aging. *Neurology,* 76**,** 1091-8.

Gustafson, D. R., Skoog, I., Rosengren, L., Zetterberg, H. & Blennow, K. 2007. Cerebrospinal fluid beta-amyloid 1-42 concentration may predict cognitive decline in older women. *J Neurol Neurosurg Psychiatry,* 78**,** 461-4.

Haass, C., Schlossmacher, M. G., Hung, A. Y., Vigo-Pelfrey, C., Mellon, A., Ostaszewski, B. L., Lieberburg, I., Koo, E. H., Schenk, D., Teplow, D. B. & Et Al. 1992. Amyloid beta-peptide is produced by cultured cells during normal metabolism. *Nature,* 359**,** 322-5.

Hajjar, I. M., Keown, M., Lewis, P. & Almor, A. 2008. Angiotensin converting enzyme inhibitors and cognitive and functional decline in patients with Alzheimer's disease: an observational study. *Am J Alzheimers Dis Other Demen,* 23**,** 77-83.

Hampel, H., Burger, K., Teipel, S. J., Bokde, A. L., Zetterberg, H. & Blennow, K. 2008. Core candidate neurochemical and imaging biomarkers of Alzheimer's disease. *Alzheimers Dement,* 4**,** 38-48.

Hampel, H., Shen, Y., Walsh, D. M., Aisen, P., Shaw, L. M., Zetterberg, H., Trojanowski, J. Q. & Blennow, K. 2010. Biological markers of amyloid beta-related mechanisms in Alzheimer's disease. *Exp Neurol,* 223**,** 334-46.

Hansson, O., Zetterberg, H., Buchhave, P., Andreasson, U., Londos, E., Minthon, L. & Blennow, K. 2007. Prediction of Alzheimer's disease using the CSF Abeta42/Abeta40 ratio in patients with mild cognitive impairment. *Dement Geriatr Cogn Disord,* 23**,** 316-20.

Hansson, O., Zetterberg, H., Buchhave, P., Londos, E., Blennow, K. & Minthon, L. 2006. Association between CSF biomarkers and incipient Alzheimer's disease in patients with mild cognitive impairment: a follow-up study. *Lancet Neurol,* 5**,** 228-34.

Hardy, J. & Selkoe, D. J. 2002. The amyloid hypothesis of Alzheimer's disease: progress and problems on the road to therapeutics. *Science,* 297**,** 353-6.

Harr, S. D., Uint, L., Hollister, R., Hyman, B. T. & Mendez, A. J. 1996. Brain expression of apolipoproteins E, J, and A-I in Alzheimer's disease. *J Neurochem,* 66**,** 2429-35.

He, M., Ohrui, T., Maruyama, M., Tomita, N., Nakayama, K., Higuchi, M., Furukawa, K. & Arai, H. 2006. ACE activity in CSF of patients with mild cognitive impairment and Alzheimer disease. *Neurology,* 67**,** 1309-10.

Head, D., Bugg, J. M., Goate, A. M., Fagan, A. M., Mintun, M. A., Benzinger, T., Holtzman, D. M. & Morris, J. C. 2012. Exercise Engagement as a Moderator of the Effects of APOE Genotype on Amyloid Deposition. *Arch Neurol,* 69**,** 636-43.

Hemming, M. L. & Selkoe, D. J. 2005. Amyloid beta-protein is degraded by cellular angiotensin-converting enzyme (ACE) and elevated by an ACE inhibitor. *J Biol Chem,* 280**,** 37644-50.

Henriksen, K., O'bryant, S. E., Hampel, H., Trojanowski, J. Q., Montine, T. J., Jeromin, A., Blennow, K., Lonneborg, A., Wyss-Coray, T., Soares, H., Bazenet, C., Sjogren, M., Hu, W., Lovestone, S., Karsdal, M. A., Weiner, M. W. & Blood-Based Biomarker Interest, G. 2013. The future of blood-based biomarkers for Alzheimer's disease. *Alzheimers Dement*.

Herholz, K., Salmon, E., Perani, D., Baron, J. C., Holthoff, V., Frolich, L., Schonknecht, P., Ito, K., Mielke, R., Kalbe, E., Zundorf, G., Delbeuck, X., Pelati, O., Anchisi, D., Fazio, F., Kerrouche, N., Desgranges, B., Eustache, F., Beuthien-Baumann, B., Menzel, C., Schroder, J., Kato, T., Arahata, Y., Henze, M. & Heiss, W. D. 2002. Discrimination between Alzheimer dementia and controls by automated analysis of multicenter FDG PET. *Neuroimage,* 17**,** 302-16.

Hertze, J., Minthon, L., Zetterberg, H., Vanmechelen, E., Blennow, K. & Hansson, O. 2010. Evaluation of CSF biomarkers as predictors of Alzheimer's disease: a clinical follow-up study of 4.7 years. *J Alzheimers Dis,* 21**,** 1119-28.

Hesse, C., Rosengren, L., Andreasen, N., Davidsson, P., Vanderstichele, H., Vanmechelen, E. & Blennow, K. 2001. Transient increase in total tau but not phospho-tau in human cerebrospinal fluid after acute stroke. *Neurosci Lett,* 297**,** 187-90.

Hesse, C., Rosengren, L., Vanmechelen, E., Vanderstichele, H., Jensen, C., Davidsson, P. & Blennow, K. 2000. Cerebrospinal fluid markers for Alzheimer's disease evaluated after acute ischemic stroke. *J Alzheimers Dis,* 2**,** 199-206.

Hoffman, J. M., Welsh-Bohmer, K. A., Hanson, M., Crain, B., Hulette, C., Earl, N. & Coleman, R. E. 2000. FDG PET imaging in patients with pathologically verified dementia. *J Nucl Med,* 41**,** 1920-8.

Hoffman, P. N., Cleveland, D. W., Griffin, J. W., Landes, P. W., Cowan, N. J. & Price, D. L. 1987. Neurofilament gene expression: a major determinant of axonal caliber. *Proc Natl Acad Sci U S A,* 84**,** 3472-6.

Holmes, C., Boche, D., Wilkinson, D., Yadegarfar, G., Hopkins, V., Bayer, A., Jones, R. W., Bullock, R., Love, S., Neal, J. W., Zotova, E. & Nicoll, J. A. 2008. Long-term effects of Abeta42 immunisation in Alzheimer's disease: follow-up of a randomised, placebo-controlled phase I trial. *Lancet,* 372**,** 216-23.

Hu, J., Igarashi, A., Kamata, M. & Nakagawa, H. 2001. Angiotensin-converting enzyme degrades Alzheimer amyloid beta-peptide (A beta); retards A beta aggregation, deposition, fibril formation; and inhibits cytotoxicity. *J Biol Chem,* 276**,** 47863-8.

Hu, W. T., Holtzman, D. M., Fagan, A. M., Shaw, L. M., Perrin, R., Arnold, S. E., Grossman, M., Xiong, C., Craig-Schapiro, R., Clark, C. M., Pickering, E., Kuhn, M., Chen, Y., Van Deerlin, V. M., Mccluskey, L., Elman, L., Karlawish, J., Chen-Plotkin, A., Hurtig, H. I., Siderowf, A., Swenson, F., Lee, V. M., Morris, J. C., Trojanowski, J. Q. & Soares, H. 2012. Plasma multianalyte profiling in mild cognitive impairment and Alzheimer disease. *Neurology,* 79**,** 897-905.

Hulstaert, F., Blennow, K., Ivanoiu, A., Schoonderwaldt, H. C., Riemenschneider, M., De Deyn, P. P., Bancher, C., Cras, P., Wiltfang, J., Mehta, P. D., Iqbal, K., Pottel, H., Vanmechelen, E. & Vanderstichele, H. 1999. Improved discrimination of AD patients using beta-amyloid(1-42) and tau levels in CSF. *Neurology,* 52**,** 1555-62.

Humpel, C. 2011. Identifying and validating biomarkers for Alzheimer's disease. *Trends Biotechnol,* 29**,** 26-32.

Ikonomovic, M. D., Klunk, W. E., Abrahamson, E. E., Mathis, C. A., Price, J. C., Tsopelas, N. D., Lopresti, B. J., Ziolko, S., Bi, W., Paljug, W. R., Debnath, M. L., Hope, C. E., Isanski, B. A., Hamilton, R. L. & Dekosky, S. T. 2008. Post-mortem correlates of in vivo PiB-PET amyloid imaging in a typical case of Alzheimer's disease. *Brain,* 131**,** 1630-45.

Iqbal, K., Alonso Adel, C., Chen, S., Chohan, M. O., El-Akkad, E., Gong, C. X., Khatoon, S., Li, B., Liu, F., Rahman, A., Tanimukai, H. & Grundke-Iqbal, I. 2005. Tau pathology in Alzheimer disease and other tauopathies. *Biochim Biophys Acta,* 1739**,** 198-210.

Jack, C. R., Jr. 2012. Alzheimer disease: new concepts on its neurobiology and the clinical role imaging will play. *Radiology,* 263**,** 344-61.

Jack, C. R., Jr., Knopman, D. S., Jagust, W. J., Petersen, R. C., Weiner, M. W., Aisen, P. S., Shaw, L. M., Vemuri, P., Wiste, H. J., Weigand, S. D., Lesnick, T. G., Pankratz, V. S., Donohue, M. C. & Trojanowski, J. Q. 2013. Tracking pathophysiological processes in Alzheimer's disease: an updated hypothetical model of dynamic biomarkers. *Lancet Neurol,* 12**,** 207-16.

Jack, C. R., Jr., Knopman, D. S., Jagust, W. J., Shaw, L. M., Aisen, P. S., Weiner, M. W., Petersen, R. C. & Trojanowski, J. Q. 2010. Hypothetical model of dynamic biomarkers of the Alzheimer's pathological cascade. *Lancet Neurol,* 9**,** 119-28.

Jack, C. R., Jr., Lowe, V. J., Weigand, S. D., Wiste, H. J., Senjem, M. L., Knopman, D. S., Shiung, M. M., Gunter, J. L., Boeve, B. F., Kemp, B. J., Weiner, M. & Petersen, R. C. 2009. Serial PIB and MRI in normal, mild cognitive impairment and Alzheimer's disease: implications for sequence of pathological events in Alzheimer's disease. *Brain,* 132**,** 1355-65.

Jagust, W. 2006. Positron emission tomography and magnetic resonance imaging in the diagnosis and prediction of dementia. *Alzheimers Dement,* 2**,** 36-42.

Jarrett, J. T., Berger, E. P. & Lansbury, P. T., Jr. 1993. The carboxy terminus of the beta amyloid protein is critical for the seeding of amyloid formation: implications for the pathogenesis of Alzheimer's disease. *Biochemistry,* 32**,** 4693-7.

Jellinger, K. A. 2004. Head injury and dementia. *Curr Opin Neurol,* 17**,** 719-23.

Johansson, P., Mattsson, N., Hansson, O., Wallin, A., Johansson, J. O., Andreasson, U., Zetterberg, H., Blennow, K. & Svensson, J. 2011. Cerebrospinal fluid biomarkers for Alzheimer's disease: diagnostic performance in a homogeneous mono-center population. *J Alzheimers Dis,* 24**,** 537-46.

Kalaria, R. N. & Ballard, C. 1999. Overlap between pathology of Alzheimer disease and vascular dementia. *Alzheimer Dis Assoc Disord,* 13 Suppl 3**,** S115-23.

Kang, J., Lemaire, H. G., Unterbeck, A., Salbaum, J. M., Masters, C. L., Grzeschik, K. H., Multhaup, G., Beyreuther, K. & Muller-Hill, B. 1987. The precursor of Alzheimer's disease amyloid A4 protein resembles a cell-surface receptor. *Nature,* 325**,** 733-6.

Katzman, R., Terry, R., Deteresa, R., Brown, T., Davies, P., Fuld, P., Renbing, X. & Peck, A. 1988. Clinical, pathological, and neurochemical changes in dementia: a subgroup with preserved mental status and numerous neocortical plaques. *Ann Neurol,* 23**,** 138-44.

Kehoe, P. G., Davies, N. M., Martin, R. M. & Ben-Shlomo, Y. 2013. Associations of angiotensin targeting antihypertensive drugs with mortality and hospitalization in primary care patients with dementia. *J Alzheimers Dis,* 33**,** 999-1008.

Kehoe, P. G., Russ, C., Mcilory, S., Williams, H., Holmans, P., Holmes, C., Liolitsa, D., Vahidassr, D., Powell, J., Mcgleenon, B., Liddell, M., Plomin, R., Dynan, K., Williams, N., Neal, J., Cairns, N. J., Wilcock, G., Passmore, P., Lovestone, S., Williams, J. & Owen, M. J. 1999. Variation in DCP1, encoding ACE, is associated with susceptibility to Alzheimer disease. *Nat Genet,* 21**,** 71-2.

Kim, J., Basak, J. M. & Holtzman, D. M. 2009. The role of apolipoprotein E in Alzheimer's disease. *Neuron,* 63**,** 287-303.

Kirkitadze, M. D., Bitan, G. & Teplow, D. B. 2002. Paradigm shifts in Alzheimer's disease and other neurodegenerative disorders: the emerging role of oligomeric assemblies. *J Neurosci Res,* 69**,** 567-77.

Klein, W. L., Krafft, G. A. & Finch, C. E. 2001. Targeting small Abeta oligomers: the solution to an Alzheimer's disease conundrum? *Trends Neurosci,* 24**,** 219-24.

Klunk, W. E., Engler, H., Nordberg, A., Wang, Y., Blomqvist, G., Holt, D. P., Bergstrom, M., Savitcheva, I., Huang, G. F., Estrada, S., Ausen, B., Debnath, M. L., Barletta, J., Price, J. C., Sandell, J., Lopresti, B. J., Wall, A., Koivisto, P., Antoni, G., Mathis, C. A. & Langstrom, B. 2004. Imaging brain amyloid in Alzheimer's disease with Pittsburgh Compound-B. *Ann Neurol,* 55**,** 306-19.

Klyubin, I., Betts, V., Welzel, A. T., Blennow, K., Zetterberg, H., Wallin, A., Lemere, C. A., Cullen, W. K., Peng, Y., Wisniewski, T., Selkoe, D. J., Anwyl, R., Walsh, D. M. & Rowan, M. J. 2008. Amyloid beta protein dimer-containing human CSF disrupts synaptic plasticity: prevention by systemic passive immunization. *J Neurosci,* 28**,** 4231-7.

Kohnken, R., Buerger, K., Zinkowski, R., Miller, C., Kerkman, D., Debernardis, J., Shen, J., Moller, H. J., Davies, P. & Hampel, H. 2000. Detection of tau phosphorylated at threonine 231 in cerebrospinal fluid of Alzheimer's disease patients. *Neurosci Lett,* 287**,** 187-90.

Koopman, K., Le Bastard, N., Martin, J. J., Nagels, G., De Deyn, P. P. & Engelborghs, S. 2009. Improved discrimination of autopsy-confirmed Alzheimer's disease (AD) from non-AD dementias using CSF P-tau(181P). *Neurochem Int,* 55**,** 214-8.

Kuo, Y. M., Emmerling, M. R., Lampert, H. C., Hempelman, S. R., Kokjohn, T. A., Woods, A. S., Cotter, R. J. & Roher, A. E. 1999. High levels of circulating Abeta42 are sequestered by plasma proteins in Alzheimer's disease. *Biochem Biophys Res Commun,* 257**,** 787-91.

Laferla, F. M., Green, K. N. & Oddo, S. 2007. Intracellular amyloid-beta in Alzheimer's disease. *Nat Rev Neurosci,* 8**,** 499-509.

Lambert, M. P., Barlow, A. K., Chromy, B. A., Edwards, C., Freed, R., Liosatos, M., Morgan, T. E., Rozovsky, I., Trommer, B., Viola, K. L., Wals, P., Zhang, C., Finch, C. E., Krafft, G. A. & Klein, W. L. 1998. Diffusible, nonfibrillar ligands derived from Abeta1-42 are potent central nervous system neurotoxins. *Proc Natl Acad Sci U S A,* 95**,** 6448-53.

Langbaum, J. B., Chen, K., Lee, W., Reschke, C., Bandy, D., Fleisher, A. S., Alexander, G. E., Foster, N. L., Weiner, M. W., Koeppe, R. A., Jagust, W. J. & Reiman, E. M. 2009. Categorical and correlational analyses of baseline fluorodeoxyglucose positron emission tomography images from the Alzheimer's Disease Neuroimaging Initiative (ADNI). *Neuroimage,* 45**,** 1107-16.

Launer, L. J., Andersen, K., Dewey, M. E., Letenneur, L., Ott, A., Amaducci, L. A., Brayne, C., Copeland, J. R., Dartigues, J. F., Kragh-Sorensen, P., Lobo, A., Martinez-Lage, J. M., Stijnen, T. & Hofman, A. 1999. Rates and risk factors for dementia and Alzheimer's disease: results from EURODEM pooled analyses. EURODEM Incidence Research Group and Work Groups. European Studies of Dementia. *Neurology,* 52**,** 78-84.

Lee, H. G., Casadesus, G., Zhu, X., Takeda, A., Perry, G. & Smith, M. A. 2004. Challenging the amyloid cascade hypothesis: senile plaques and amyloid-beta as protective adaptations to Alzheimer disease. *Ann N Y Acad Sci,* 1019**,** 1-4.

Lehmann, D. J., Cortina-Borja, M., Warden, D. R., Smith, A. D., Sleegers, K., Prince, J. A., Van Duijn, C. M. & Kehoe, P. G. 2005. Large meta-analysis establishes the ACE insertion-deletion polymorphism as a marker of Alzheimer's disease. *Am J Epidemiol,* 162**,** 305-17.

Levy-Lahad, E., Wasco, W., Poorkaj, P., Romano, D. M., Oshima, J., Pettingell, W. H., Yu, C. E., Jondro, P. D., Schmidt, S. D., Wang, K. & Et Al. 1995. Candidate gene for the chromosome 1 familial Alzheimer's disease locus. *Science,* 269**,** 973-7.

Li, N. C., Lee, A., Whitmer, R. A., Kivipelto, M., Lawler, E., Kazis, L. E. & Wolozin, B. 2010. Use of angiotensin receptor blockers and risk of dementia in a predominantly male population: prospective cohort analysis. *BMJ,* 340**,** b5465.

Liao, P. C., Yu, L., Kuo, C. C., Lin, C. & Kuo, Y. M. 2007. Proteomics analysis of plasma for potential biomarkers in the diagnosis of Alzheimer's disease. *Proteomics Clin Appl,* 1**,** 506-12.

Lidstrom, A. M., Bogdanovic, N., Hesse, C., Volkman, I., Davidsson, P. & Blennow, K. 1998. Clusterin (apolipoprotein J) protein levels are increased in hippocampus and in frontal cortex in Alzheimer's disease. *Exp Neurol,* 154**,** 511-21.

Lidstrom, A. M., Hesse, C., Rosengren, L., Fredman, P., Davidsson, P. & Blennow, K. 2001. Normal levels of clusterin in cerebrospinal fluid in Alzheimer's disease, and no change after acute ischemic stroke. *J Alzheimers Dis,* 3**,** 435-442.

Lill, C. M. & Bertram, L. 2011. Towards unveiling the genetics of neurodegenerative diseases. *Semin Neurol,* 31**,** 531-41.

Ling, Y., Morgan, K. & Kalsheker, N. 2003. Amyloid precursor protein (APP) and the biology of proteolytic processing: relevance to Alzheimer's disease. *Int J Biochem Cell Biol,* 35**,** 1505-35.

Lopera, F., Ardilla, A., Martinez, A., Madrigal, L., Arango-Viana, J. C., Lemere, C. A., Arango-Lasprilla, J. C., Hincapie, L., Arcos-Burgos, M., Ossa, J. E., Behrens, I. M., Norton, J., Lendon, C., Goate, A. M., Ruiz-Linares, A., Rosselli, M. & Kosik, K. S. 1997. Clinical features of early-onset Alzheimer disease in a large kindred with an E280A presenilin-1 mutation. *JAMA,* 277**,** 793-9.

Lopez, O. L., Becker, J. T., Klunk, W., Saxton, J., Hamilton, R. L., Kaufer, D. I., Sweet, R. A., Cidis Meltzer, C., Wisniewski, S., Kamboh, M. I. & Dekosky, S. T. 2000. Research evaluation and diagnosis of probable Alzheimer's disease over the last two decades: I. *Neurology,* 55**,** 1854-62.

Lovati, C., Galimberti, D., Albani, D., Bertora, P., Venturelli, E., Cislaghi, G., Guidi, I., Fenoglio, C., Cortini, F., Clerici, F., Finazzi, D., Forloni, G., Scarpini, E. & Mariani, C. 2010. APOE epsilon2 and epsilon4 influence the susceptibility for Alzheimer's disease but not other dementias. *Int J Mol Epidemiol Genet,* 1**,** 193-200.

Lycke, J. N., Karlsson, J. E., Andersen, O. & Rosengren, L. E. 1998. Neurofilament protein in cerebrospinal fluid: a potential marker of activity in multiple sclerosis. *J Neurol Neurosurg Psychiatry,* 64**,** 402-4.

Mahley, R. W. 1988. Apolipoprotein E: cholesterol transport protein with expanding role in cell biology. *Science,* 240**,** 622-30.

Mahley, R. W., Weisgraber, K. H. & Huang, Y. 2006. Apolipoprotein E4: a causative factor and therapeutic target in neuropathology, including Alzheimer's disease. *Proc Natl Acad Sci U S A,* 103**,** 5644-51.

Mandelkow, E. M. & Mandelkow, E. 1998. Tau in Alzheimer's disease. *Trends Cell Biol,* 8**,** 425-7.

Masters, C. L., Simms, G., Weinman, N. A., Multhaup, G., Mcdonald, B. L. & Beyreuther, K. 1985. Amyloid plaque core protein in Alzheimer disease and Down syndrome. *Proc Natl Acad Sci U S A,* 82**,** 4245-9.

Mauch, D. H., Nagler, K., Schumacher, S., Goritz, C., Muller, E. C., Otto, A. & Pfrieger, F. W. 2001. CNS synaptogenesis promoted by glia-derived cholesterol. *Science,* 294**,** 1354-7.

Mawuenyega, K. G., Sigurdson, W., Ovod, V., Munsell, L., Kasten, T., Morris, J. C., Yarasheski, K. E. & Bateman, R. J. 2010. Decreased clearance of CNS beta-amyloid in Alzheimer's disease. *Science,* 330**,** 1774.

Mayeux, R. & Stern, Y. 2012. Epidemiology of Alzheimer disease. *Cold Spring Harb Perspect Med,* 2.

Mckhann, G., Drachman, D., Folstein, M., Katzman, R., Price, D. & Stadlan, E. M. 1984. Clinical diagnosis of Alzheimer's disease: report of the NINCDS-ADRDA Work Group under the auspices of Department of Health and Human Services Task Force on Alzheimer's Disease. *Neurology,* 34**,** 939-44.

Mckhann, G. M., Knopman, D. S., Chertkow, H., Hyman, B. T., Jack, C. R., Jr., Kawas, C. H., Klunk, W. E., Koroshetz, W. J., Manly, J. J., Mayeux, R., Mohs, R. C., Morris, J. C., Rossor, M. N., Scheltens, P., Carrillo, M. C., Thies, B., Weintraub, S. & Phelps, C. H. 2011. The diagnosis of

dementia due to Alzheimer's disease: recommendations from the National Institute on Aging-Alzheimer's Association workgroups on diagnostic guidelines for Alzheimer's disease. *Alzheimers Dement,* 7**,** 263-9.

Mehta, P. D., Pirttila, T., Mehta, S. P., Sersen, E. A., Aisen, P. S. & Wisniewski, H. M. 2000. Plasma and cerebrospinal fluid levels of amyloid beta proteins 1-40 and 1-42 in Alzheimer disease. *Arch Neurol,* 57**,** 100-5.

Mehta, P. D., Pirttila, T., Patrick, B. A., Barshatzky, M. & Mehta, S. P. 2001. Amyloid beta protein 1-40 and 1-42 levels in matched cerebrospinal fluid and plasma from patients with Alzheimer disease. *Neurosci Lett,* 304**,** 102-6.

Mesulam, M. 2004. The cholinergic lesion of Alzheimer's disease: pivotal factor or side show? *Learn Mem,* 11**,** 43-9.

Miners, J. S., Ashby, E., Van Helmond, Z., Chalmers, K. A., Palmer, L. E., Love, S. & Kehoe, P. G. 2008. Angiotensin-converting enzyme (ACE) levels and activity in Alzheimer's disease, and relationship of perivascular ACE-1 to cerebral amyloid angiopathy. *Neuropathol Appl Neurobiol,* 34**,** 181-93.

Miners, J. S., Van Helmond, Z., Raiker, M., Love, S. & Kehoe, P. G. 2010. ACE variants and association with brain Abeta levels in Alzheimer's disease. *Am J Transl Res,* 3**,** 73-80.

Miners, S., Ashby, E., Baig, S., Harrison, R., Tayler, H., Speedy, E., Prince, J. A., Love, S. & Kehoe, P. G. 2009. Angiotensin-converting enzyme levels and activity in Alzheimer's disease: differences in brain and CSF ACE and association with ACE1 genotypes. *Am J Transl Res,* 1**,** 163-77.

Minoshima, S., Giordani, B., Berent, S., Frey, K. A., Foster, N. L. & Kuhl, D. E. 1997. Metabolic reduction in the posterior cingulate cortex in very early Alzheimer's disease. *Ann Neurol,* 42**,** 85-94.

Mori, H., Hosoda, K., Matsubara, E., Nakamoto, T., Furiya, Y., Endoh, R., Usami, M., Shoji, M., Maruyama, S. & Hirai, S. 1995. Tau in cerebrospinal fluids: establishment of the sandwich ELISA with antibody specific to the repeat sequence in tau. *Neurosci Lett,* 186**,** 181-3.

Morris, J. C., Blennow, K., Froelich, L., Nordberg, A., Soininen, H., Waldemar, G., Wahlund, L. O. & Dubois, B. 2014. Harmonized diagnostic criteria for Alzheimer's disease: recommendations. *J Intern Med,* 275**,** 204-13.

Mosconi, L. 2005. Brain glucose metabolism in the early and specific diagnosis of Alzheimer's disease. FDG-PET studies in MCI and AD. *Eur J Nucl Med Mol Imaging,* 32**,** 486-510.

Motte, J. & Williams, R. S. 1989. Age-related changes in the density and morphology of plaques and neurofibrillary tangles in Down syndrome brain. *Acta Neuropathol,* 77**,** 535-46.

Myers, R. H., Schaefer, E. J., Wilson, P. W., D'agostino, R., Ordovas, J. M., Espino, A., Au, R., White, R. F., Knoefel, J. E., Cobb, J. L., Mcnulty, K. A., Beiser, A. & Wolf, P. A. 1996. Apolipoprotein E epsilon4 association with dementia in a population-based study: The Framingham study. *Neurology,* 46**,** 673-7.

Nielsen, H. M., Londos, E., Minthon, L. & Janciauskiene, S. M. 2007. Soluble adhesion molecules and angiotensin-converting enzyme in dementia. *Neurobiol Dis,* 26**,** 27-35.

Nilselid, A. M., Davidsson, P., Nagga, K., Andreasen, N., Fredman, P. & Blennow, K. 2006. Clusterin in cerebrospinal fluid: analysis of carbohydrates and quantification of native and glycosylated forms. *Neurochem Int,* 48**,** 718-28.

Nordberg, A., Rinne, J. O., Kadir, A. & Langstrom, B. 2010. The use of PET in Alzheimer disease. *Nat Rev Neurol,* 6**,** 78-87.

Norgren, N., Rosengren, L. & Stigbrand, T. 2003. Elevated neurofilament levels in neurological diseases. *Brain Res,* 987**,** 25-31.

Nuutinen, T., Suuronen, T., Kauppinen, A. & Salminen, A. 2009. Clusterin: a forgotten player in Alzheimer's disease. *Brain Res Rev,* 61**,** 89-104.

O'caoimh, R., Healy, L., Gao, Y., Svendrovski, A., Kerins, D. M., Eustace, J., Kehoe, P. G., Guyatt, G. & Molloy, D. W. 2014. Effects of Centrally acting Angiotensin Converting Enzyme Inhibitors on Functional Decline in Patients with Alzheimer's Disease. *J Alzheimers Dis*.

Oba, R., Igarashi, A., Kamata, M., Nagata, K., Takano, S. & Nakagawa, H. 2005. The N-terminal active centre of human angiotensin-converting enzyme degrades Alzheimer amyloid beta-peptide. *Eur J Neurosci,* 21**,** 733-40.

Oda, T., Pasinetti, G. M., Osterburg, H. H., Anderson, C., Johnson, S. A. & Finch, C. E. 1994. Purification and characterization of brain clusterin. *Biochem Biophys Res Commun,* 204**,** 1131-6.

Olson, M. I. & Shaw, C. M. 1969. Presenile dementia and Alzheimer's disease in mongolism. *Brain,* 92**,** 147-56.

Otto, M., Wiltfang, J., Tumani, H., Zerr, I., Lantsch, M., Kornhuber, J., Weber, T., Kretzschmar, H. A. & Poser, S. 1997. Elevated levels of tau-protein in cerebrospinal fluid of patients with Creutzfeldt-Jakob disease. *Neurosci Lett,* 225**,** 210-2.

Pastor, P., Roe, C. M., Villegas, A., Bedoya, G., Chakraverty, S., Garcia, G., Tirado, V., Norton, J., Rios, S., Martinez, M., Kosik, K. S., Lopera, F. & Goate, A. M. 2003. Apolipoprotein Eepsilon4 modifies Alzheimer's disease onset in an E280A PS1 kindred. *Ann Neurol,* 54**,** 163-9.

Perrin, R. J., Fagan, A. M. & Holtzman, D. M. 2009. Multimodal techniques for diagnosis and prognosis of Alzheimer's disease. *Nature,* 461**,** 916-22.

Petersen, R. C. 2004. Mild cognitive impairment as a diagnostic entity. *J Intern Med,* 256**,** 183-94.

Petzold, A., Keir, G., Warren, J., Fox, N. & Rossor, M. N. 2007. A systematic review and meta-analysis of CSF neurofilament protein levels as biomarkers in dementia. *Neurodegener Dis,* 4**,** 185-94.

Pike, C. J., Walencewicz, A. J., Glabe, C. G. & Cotman, C. W. 1991. In vitro aging of beta-amyloid protein causes peptide aggregation and neurotoxicity. *Brain Res,* 563**,** 311-4.

Pimplikar, S. W., Nixon, R. A., Robakis, N. K., Shen, J. & Tsai, L. H. 2010. Amyloid-independent mechanisms in Alzheimer's disease pathogenesis. *J Neurosci,* 30**,** 14946-54.

Potter, H. & Wisniewski, T. 2012. Apolipoprotein e: essential catalyst of the Alzheimer amyloid cascade. *Int J Alzheimers Dis,* 2012**,** 489428.

Price, J. L. & Morris, J. C. 1999. Tangles and plaques in nondemented aging and "preclinical" Alzheimer's disease. *Ann Neurol,* 45**,** 358-68.

Prince, J. A., Zetterberg, H., Andreasen, N., Marcusson, J. & Blennow, K. 2004. APOE epsilon4 allele is associated with reduced cerebrospinal fluid levels of Abeta42. *Neurology,* 62**,** 2116-8.

Prince, M., Bryce, R., Albanese, E., Wimo, A., Ribeiro, W. & Ferri, C. P. 2013. The global prevalence of dementia: a systematic review and metaanalysis. *Alzheimers Dement,* 9**,** 63-75 e2.

Purandare, N., Allen, N. & Burns, A. 2000. Behavioural and psychological symptoms of dementia. *Reviews in Clinical Gerontology,* 10**,** 245-260.

Querfurth, H. W. & Laferla, F. M. 2010. Alzheimer's disease. *N Engl J Med,* 362**,** 329-44.

Ray, S., Britschgi, M., Herbert, C., Takeda-Uchimura, Y., Boxer, A., Blennow, K., Friedman, L. F., Galasko, D. R., Jutel, M., Karydas, A., Kaye, J. A., Leszek, J., Miller, B. L., Minthon, L., Quinn, J. F., Rabinovici, G. D., Robinson, W. H., Sabbagh, M. N., So, Y. T., Sparks, D. L., Tabaton, M., Tinklenberg, J., Yesavage, J. A., Tibshirani, R. & Wyss-Coray, T. 2007. Classification and prediction of clinical Alzheimer's diagnosis based on plasma signaling proteins. *Nat Med,* 13**,** 1359-62.

Reece, R. J. 2004. *Analysis of Genes and Genomes,* West Sussex, England, John Wiley & Sons Ltd.

Reiman, E. M., Chen, K., Alexander, G. E., Caselli, R. J., Bandy, D., Osborne, D., Saunders, A. M. & Hardy, J. 2004. Functional brain abnormalities in young adults at genetic risk for late-onset Alzheimer's dementia. *Proc Natl Acad Sci U S A,* 101**,** 284-9.

Reitz, C. & Mayeux, R. 2014. Alzheimer disease: Epidemiology, Diagnostic Criteria, Risk Factors and Biomarkers. *Biochem Pharmacol*.

Rensink, A. A., De Waal, R. M., Kremer, B. & Verbeek, M. M. 2003. Pathogenesis of cerebral amyloid angiopathy. *Brain Res Brain Res Rev,* 43**,** 207-23.

Riemenschneider, M., Wagenpfeil, S., Vanderstichele, H., Otto, M., Wiltfang, J., Kretzschmar, H., Vanmechelen, E., Forstl, H. & Kurz, A. 2003. Phospho-tau/total tau ratio in cerebrospinal fluid discriminates Creutzfeldt-Jakob disease from other dementias. *Mol Psychiatry,* 8**,** 343-7.

Rigat, B., Hubert, C., Alhenc-Gelas, F., Cambien, F., Corvol, P. & Soubrier, F. 1990. An insertion/deletion polymorphism in the angiotensin I-converting enzyme gene accounting for half the variance of serum enzyme levels. *J Clin Invest,* 86**,** 1343-6.

Roche 2005. LightCycler® 2.0 Instrument Operator's Manual. *Manual B: for general laboratory use.* Roche Diagnostics.

Roheim, P. S., Carey, M., Forte, T. & Vega, G. L. 1979. Apolipoproteins in human cerebrospinal fluid. *Proc Natl Acad Sci U S A,* 76**,** 4646-9.

Rosen, C. & Zetterberg, H. 2013. Cerebrospinal fluid biomarkers for pathological processes in Alzheimer's disease. *Curr Opin Psychiatry,* 26**,** 276-82.

Rosengren, L. E., Karlsson, J. E., Karlsson, J. O., Persson, L. I. & Wikkelso, C. 1996. Patients with amyotrophic lateral sclerosis and other neurodegenerative diseases have increased levels of neurofilament protein in CSF. *J Neurochem,* 67**,** 2013-8.

Rosengren, L. E., Karlsson, J. E., Sjogren, M., Blennow, K. & Wallin, A. 1999. Neurofilament protein levels in CSF are increased in dementia. *Neurology,* 52**,** 1090-3.

Rosner, B. 2011. *Fundamentals of Biostatistics,* International Edition, Brooks/Cole

Rovelet-Lecrux, A., Hannequin, D., Raux, G., Le Meur, N., Laquerriere, A., Vital, A., Dumanchin, C., Feuillette, S., Brice, A., Vercelletto, M., Dubas, F., Frebourg, T. & Campion, D. 2006. APP locus duplication causes autosomal dominant early-onset Alzheimer disease with cerebral amyloid angiopathy. *Nat Genet,* 38**,** 24-6.

Rowe, C. C., Ng, S., Ackermann, U., Gong, S. J., Pike, K., Savage, G., Cowie, T. F., Dickinson, K. L., Maruff, P., Darby, D., Smith, C., Woodward, M., Merory, J., Tochon-Danguy, H., O'keefe, G., Klunk, W. E., Mathis, C. A., Price, J. C., Masters, C. L. & Villemagne, V. L. 2007. Imaging beta-amyloid burden in aging and dementia. *Neurology,* 68**,** 1718-25.

Rozzini, L., Vicini Chilovi, B., Trabucchi, M. & Padovani, A. 2008. Antihypertensive medications influence the rate of conversion from mild cognitive impairment to Alzheimer disease. *Arch Neurol,* 65**,** 993-4; author reply 994-5.

Salloway, S., Sperling, R., Fox, N. C., Blennow, K., Klunk, W., Raskind, M., Sabbagh, M., Honig, L. S., Porsteinsson, A. P., Ferris, S., Reichert, M., Ketter, N., Nejadnik, B., Guenzler, V., Miloslavsky, M., Wang, D., Lu, Y., Lull, J., Tudor, I. C., Liu, E., Grundman, M., Yuen, E., Black, R. & Brashear, H. R. 2014. Two phase 3 trials of bapineuzumab in mild-to-moderate Alzheimer's disease. *N Engl J Med,* 370**,** 322-33.

Sando, S. B., Melquist, S., Cannon, A., Hutton, M., Sletvold, O., Saltvedt, I., White, L. R., Lydersen, S. & Aasly, J. 2008a. Risk-reducing effect of education in Alzheimer's disease. *Int J Geriatr Psychiatry,* 23**,** 1156-62.

Sando, S. B., Melquist, S., Cannon, A., Hutton, M. L., Sletvold, O., Saltvedt, I., White, L. R., Lydersen, S. & Aasly, J. O. 2008b. APOE epsilon 4 lowers age at onset and is a high risk factor for Alzheimer's disease; a case control study from central Norway. *BMC Neurol,* 8**,** 9.

Schmechel, D. E., Saunders, A. M., Strittmatter, W. J., Crain, B. J., Hulette, C. M., Joo, S. H., Pericak-Vance, M. A., Goldgaber, D. & Roses, A. D. 1993. Increased amyloid beta-peptide deposition in cerebral cortex as a consequence of apolipoprotein E genotype in late-onset Alzheimer disease. *Proc Natl Acad Sci U S A,* 90**,** 9649-53.

Schneider, P., Hampel, H. & Buerger, K. 2009. Biological marker candidates of Alzheimer's disease in blood, plasma, and serum. *CNS Neurosci Ther,* 15**,** 358-74.

Schrijvers, E. M., Koudstaal, P. J., Hofman, A. & Breteler, M. M. 2011. Plasma clusterin and the risk of Alzheimer disease. *JAMA,* 305**,** 1322-6.

Selkoe, D. J. 2002. Alzheimer's disease is a synaptic failure. *Science,* 298**,** 789-91.

Selkoe, D. J. & Schenk, D. 2003. Alzheimer's disease: molecular understanding predicts amyloid-based therapeutics. *Annu Rev Pharmacol Toxicol,* 43**,** 545-84.

Shankar, G. M., Li, S., Mehta, T. H., Garcia-Munoz, A., Shepardson, N. E., Smith, I., Brett, F. M., Farrell, M. A., Rowan, M. J., Lemere, C. A., Regan, C. M., Walsh, D. M., Sabatini, B. L. & Selkoe, D. J. 2008. Amyloid-beta protein dimers isolated directly from Alzheimer's brains impair synaptic plasticity and memory. *Nat Med,* 14**,** 837-42.

Shaw, L. M., Vanderstichele, H., Knapik-Czajka, M., Clark, C. M., Aisen, P. S., Petersen, R. C., Blennow, K., Soares, H., Simon, A., Lewczuk, P., Dean, R., Siemers, E., Potter, W., Lee, V. M. & Trojanowski, J. Q. 2009. Cerebrospinal fluid biomarker signature in Alzheimer's disease neuroimaging initiative subjects. *Ann Neurol,* 65**,** 403-13.

Sherrington, R., Rogaev, E. I., Liang, Y., Rogaeva, E. A., Levesque, G., Ikeda, M., Chi, H., Lin, C., Li, G., Holman, K., Tsuda, T., Mar, L., Foncin, J. F., Bruni, A. C., Montesi, M. P., Sorbi, S., Rainero, I., Pinessi, L., Nee, L., Chumakov, I., Pollen, D., Brookes, A., Sanseau, P., Polinsky, R. J., Wasco, W., Da Silva, H. A., Haines, J. L., Perkicak-Vance, M. A., Tanzi, R. E., Roses, A. D., Fraser, P. E., Rommens, J. M. & St George-Hyslop, P. H. 1995. Cloning of a gene bearing missense mutations in early-onset familial Alzheimer's disease. *Nature,* 375**,** 754-60.

Shoji, M., Matsubara, E., Kanai, M., Watanabe, M., Nakamura, T., Tomidokoro, Y., Shizuka, M., Wakabayashi, K., Igeta, Y., Ikeda, Y., Mizushima, K., Amari, M., Ishiguro, K., Kawarabayashi, T., Harigaya, Y., Okamoto, K. & Hirai, S. 1998. Combination assay of CSF tau, A beta 1-40 and A beta 1-42(43) as a biochemical marker of Alzheimer's disease. *J Neurol Sci,* 158**,** 134-40.

Silverman, D. H., Small, G. W., Chang, C. Y., Lu, C. S., Kung De Aburto, M. A., Chen, W., Czernin, J., Rapoport, S. I., Pietrini, P., Alexander, G. E., Schapiro, M. B., Jagust, W. J., Hoffman, J. M., Welsh-Bohmer, K. A., Alavi, A., Clark, C. M., Salmon, E., De Leon, M. J., Mielke, R., Cummings, J. L., Kowell, A. P., Gambhir, S. S., Hoh, C. K. & Phelps, M. E. 2001. Positron emission tomography in evaluation of dementia: Regional brain metabolism and long-term outcome. *JAMA,* 286**,** 2120-7.

Singh, P. P., Singh, M. & Mastana, S. S. 2006. APOE distribution in world populations with new data from India and the UK. *Ann Hum Biol,* 33**,** 279-308.

Sjogren, M., Blomberg, M., Jonsson, M., Wahlund, L. O., Edman, A., Lind, K., Rosengren, L., Blennow, K. & Wallin, A. 2001. Neurofilament protein in cerebrospinal fluid: a marker of white matter changes. *J Neurosci Res,* 66**,** 510-6.

Sjogren, M., Rosengren, L., Minthon, L., Davidsson, P., Blennow, K. & Wallin, A. 2000. Cytoskeleton proteins in CSF distinguish frontotemporal dementia from AD. *Neurology,* 54**,** 1960-4.

Skidgel, R. A. & Erdos, E. G. 1987. The broad substrate specificity of human angiotensin I converting enzyme. *Clin Exp Hypertens A,* 9**,** 243-59.

Skoog, I., Davidsson, P., Aevarsson, O., Vanderstichele, H., Vanmechelen, E. & Blennow, K. 2003. Cerebrospinal fluid beta-amyloid 42 is reduced before the onset of sporadic dementia: a population-based study in 85-year-olds. *Dement Geriatr Cogn Disord,* 15**,** 169-76.

Slooter, A. J. C., De Knijff, P., Hofman, A., Cruts, M., Breteler, M. M. B., Van Broeckhoven, C., Havekes, L. M. & Van Duijn, C. M. 1998. Serum apolipoprotein E level is not increased in Alzheimer's disease: the Rotterdam study. *Neuroscience Letters,* 248**,** 21-24.

Small, B. J., Fratiglioni, L., Viitanen, M., Winblad, B. & Backman, L. 2000. The course of cognitive impairment in preclinical Alzheimer disease: three- and 6-year follow-up of a population-based sample. *Arch Neurol,* 57**,** 839-44.

Smit, M., De Knijff, P., Rosseneu, M., Bury, J., Klasen, E., Frants, R. & Havekes, L. 1988. Apolipoprotein E polymorphism in The Netherlands and its effect on plasma lipid and apolipoprotein levels. *Hum Genet,* 80**,** 287-92.

Snowden, J. S., Stopford, C. L., Julien, C. L., Thompson, J. C., Davidson, Y., Gibbons, L., Pritchard, A., Lendon, C. L., Richardson, A. M., Varma, A., Neary, D. & Mann, D. 2007. Cognitive phenotypes in Alzheimer's disease and genetic risk. *Cortex,* 43**,** 835-45.

Soares, H. D., Potter, W. Z., Pickering, E., Kuhn, M., Immermann, F. W., Shera, D. M., Ferm, M., Dean, R. A., Simon, A. J., Swenson, F., Siuciak, J. A., Kaplow, J., Thambisetty, M., Zagouras, P., Koroshetz, W. J., Wan, H. I., Trojanowski, J. Q. & Shaw, L. M. 2012. Plasma biomarkers associated with the apolipoprotein E genotype and Alzheimer disease. *Arch Neurol,* 69**,** 1310-7.

Soto, C. 2003. Unfolding the role of protein misfolding in neurodegenerative diseases. *Nat Rev Neurosci,* 4**,** 49-60.

Sperling, R. A., Aisen, P. S., Beckett, L. A., Bennett, D. A., Craft, S., Fagan, A. M., Iwatsubo, T., Jack, C. R., Jr., Kaye, J., Montine, T. J., Park, D. C., Reiman, E. M., Rowe, C. C., Siemers, E., Stern, Y., Yaffe, K., Carrillo, M. C., Thies, B., Morrison-Bogorad, M., Wagster, M. V. & Phelps, C. H. 2011. Toward defining the preclinical stages of Alzheimer's disease: recommendations from the National Institute on Aging-Alzheimer's Association workgroups on diagnostic guidelines for Alzheimer's disease. *Alzheimers Dement,* 7**,** 280-92.

St George-Hyslop, P. H. 1999. Molecular genetics of Alzheimer disease. *Semin Neurol,* 19**,** 371-83.

Steiner, H., Winkler, E., Edbauer, D., Prokop, S., Basset, G., Yamasaki, A., Kostka, M. & Haass, C. 2002. PEN-2 is an integral component of the gamma-secretase complex required for coordinated expression of presenilin and nicastrin. *J Biol Chem,* 277**,** 39062-5.

Stern, Y. 2009. Cognitive reserve. *Neuropsychologia,* 47**,** 2015-28.

Stomrud, E., Hansson, O., Blennow, K., Minthon, L. & Londos, E. 2007. Cerebrospinal fluid biomarkers predict decline in subjective cognitive function over 3 years in healthy elderly. *Dement Geriatr Cogn Disord,* 24**,** 118-24.

Strittmatter, W. J., Saunders, A. M., Schmechel, D., Pericak-Vance, M., Enghild, J., Salvesen, G. S. & Roses, A. D. 1993. Apolipoprotein E: high-avidity binding to beta-amyloid and increased frequency of type 4 allele in late-onset familial Alzheimer disease. *Proc Natl Acad Sci U S A,* 90**,** 1977-81.

Strozyk, D., Blennow, K., White, L. R. & Launer, L. J. 2003. CSF Abeta 42 levels correlate with amyloid-neuropathology in a population-based autopsy study. *Neurology,* 60**,** 652-6.

Tapiola, T., Alafuzoff, I., Herukka, S. K., Parkkinen, L., Hartikainen, P., Soininen, H. & Pirttila, T. 2009. Cerebrospinal fluid {beta}-amyloid 42 and tau proteins as biomarkers of Alzheimer-type pathologic changes in the brain. *Arch Neurol,* 66**,** 382-9.

Terry, R. D. 1996. The pathogenesis of Alzheimer disease: an alternative to the amyloid hypothesis. *J Neuropathol Exp Neurol,* 55**,** 1023-5.

Terry, R. D., Masliah, E., Salmon, D. P., Butters, N., Deteresa, R., Hill, R., Hansen, L. A. & Katzman, R. 1991. Physical basis of cognitive alterations in Alzheimer's disease: synapse loss is the major correlate of cognitive impairment. *Ann Neurol,* 30**,** 572-80.

Thal, D. R., Rub, U., Orantes, M. & Braak, H. 2002. Phases of A beta-deposition in the human brain and its relevance for the development of AD. *Neurology,* 58**,** 1791-800.

Thies, W. & Bleiler, L. 2013. 2013 Alzheimer's disease facts and figures. *Alzheimers Dement,* 9**,** 208-45.

Tiraboschi, P., Hansen, L. A., Thal, L. J. & Corey-Bloom, J. 2004. The importance of neuritic plaques and tangles to the development and evolution of AD. *Neurology,* 62**,** 1984-9.

Tronvik, E., Stovner, L. J., Bovim, G., White, L. R., Gladwin, A. J., Owen, K. & Schrader, H. 2008. Angiotensin-converting enzyme gene insertion/deletion polymorphism in migraine patients. *BMC Neurol,* 8**,** 4.

Utermann, G., Hees, M. & Steinmetz, A. 1977. Polymorphism of apolipoprotein E and occurrence of dysbetalipoproteinaemia in man. *Nature,* 269**,** 604-7.

Van Geel, W. J., Rosengren, L. E. & Verbeek, M. M. 2005. An enzyme immunoassay to quantify neurofilament light chain in cerebrospinal fluid. *J Immunol Methods,* 296**,** 179-85.

Vanmechelen, E., Vanderstichele, H., Davidsson, P., Van Kerschaver, E., Van Der Perre, B., Sjogren, M., Andreasen, N. & Blennow, K. 2000. Quantification of tau phosphorylated at threonine 181 in human cerebrospinal fluid: a sandwich ELISA with a synthetic phosphopeptide for standardization. *Neurosci Lett,* 285**,** 49-52.

Vassar, R., Bennett, B. D., Babu-Khan, S., Kahn, S., Mendiaz, E. A., Denis, P., Teplow, D. B., Ross, S., Amarante, P., Loeloff, R., Luo, Y., Fisher, S., Fuller, J., Edenson, S., Lile, J., Jarosinski, M. A., Biere, A. L., Curran, E., Burgess, T., Louis, J. C., Collins, F., Treanor, J., Rogers, G. & Citron, M. 1999. Beta-secretase cleavage of Alzheimer's amyloid precursor protein by the transmembrane aspartic protease BACE. *Science,* 286**,** 735-41.

Walhovd, K. B., Fjell, A. M., Brewer, J., Mcevoy, L. K., Fennema-Notestine, C., Hagler, D. J., Jr., Jennings, R. G., Karow, D. & Dale, A. M. 2010. Combining MR imaging, positron-emission

tomography, and CSF biomarkers in the diagnosis and prognosis of Alzheimer disease. *AJNR Am J Neuroradiol,* 31**,** 347-54.

Walsh, D. M. & Selkoe, D. J. 2007. A beta oligomers - a decade of discovery. *J Neurochem,* 101**,** 1172-84.

Wang, C., Yu, J. T., Wang, H. F., Jiang, T., Tan, C. C., Meng, X. F., Soares, H. D. & Tan, L. 2014. Meta-analysis of peripheral blood apolipoprotein E levels in Alzheimer's disease. *PLoS One,* 9**,** e89041.

Winblad, B., Palmer, K., Kivipelto, M., Jelic, V., Fratiglioni, L., Wahlund, L. O., Nordberg, A., Backman, L., Albert, M., Almkvist, O., Arai, H., Basun, H., Blennow, K., De Leon, M., Decarli, C., Erkinjuntti, T., Giacobini, E., Graff, C., Hardy, J., Jack, C., Jorm, A., Ritchie, K., Van Duijn, C., Visser, P. & Petersen, R. C. 2004. Mild cognitive impairment--beyond controversies, towards a consensus: report of the International Working Group on Mild Cognitive Impairment. *J Intern Med,* 256**,** 240-6.

Wippold, F. J., 2nd, Cairns, N., Vo, K., Holtzman, D. M. & Morris, J. C. 2008. Neuropathology for the neuroradiologist: plaques and tangles. *AJNR Am J Neuroradiol,* 29**,** 18-22.

Wittwer, C. T., Herrmann, M. G., Moss, A. A. & Rasmussen, R. P. 1997. Continuous fluorescence monitoring of rapid cycle DNA amplification. *Biotechniques,* 22**,** 130-1, 134-8.

Wolfe, M. S., Xia, W., Ostaszewski, B. L., Diehl, T. S., Kimberly, W. T. & Selkoe, D. J. 1999. Two transmembrane aspartates in presenilin-1 required for presenilin endoproteolysis and gamma-secretase activity. *Nature,* 398**,** 513-7.

Wu, Z. C., Yu, J. T., Li, Y. & Tan, L. 2012. Clusterin in Alzheimer's disease. *Adv Clin Chem,* 56**,** 155-73.

Yan, R. & Vassar, R. 2014. Targeting the β secretase BACE1 for Alzheimer's disease therapy. *The Lancet Neurology,* 13**,** 319-329.

Zetterberg, H., Tullhog, K., Hansson, O., Minthon, L., Londos, E. & Blennow, K. 2010. Low incidence of post-lumbar puncture headache in 1,089 consecutive memory clinic patients. *Eur Neurol,* 63**,** 326-30.

Zhang, Z., Deng, L., Yu, H., Shi, Y., Bai, F., Xie, C., Yuan, Y., Jia, J. & Zhang, Z. 2012. Association of angiotensin-converting enzyme functional gene I/D polymorphism with amnestic mild cognitive impairment. *Neurosci Lett,* 514**,** 131-5.

Zou, K., Liu, J., Watanabe, A., Hiraga, S., Liu, S., Tanabe, C., Maeda, T., Terayama, Y., Takahashi, S., Michikawa, M. & Komano, H. 2013. Abeta43 is the earliest-depositing Abeta species in APP transgenic mouse brain and is converted to Abeta41 by two active domains of ACE. *Am J Pathol,* 182**,** 2322-31.

Zou, K., Yamaguchi, H., Akatsu, H., Sakamoto, T., Ko, M., Mizoguchi, K., Gong, J. S., Yu, W., Yamamoto, T., Kosaka, K., Yanagisawa, K. & Michikawa, M. 2007. Angiotensin-converting enzyme converts amyloid beta-protein 1-42 (Abeta(1-42)) to Abeta(1-40), and its inhibition enhances brain Abeta deposition. *J Neurosci,* 27**,** 8628-35.

Appendices

Appendix 1. Mini mental state examination (MMSE)

Folstein Mini-Mental State Exam		
I. **ORIENTATION** (Ask the following questions; correct = ☑)	**Record Each Answer:**	(Maximum Score = 10) Score: ____
What is today's date?	Date (eg, May 21)	1 ☐
What is today's year?	Year	1 ☐
What is the month?	Month	1 ☐
What day is today?	Day (eg, Monday)	1 ☐
Can you also tell me what season it is?	Season	1 ☐
Can you also tell me the name of this hospital/clinic?	Hospital/Clinic	1 ☐
What floor are we on?	Floor	1 ☐
What city are we in?	City	1 ☐
What county are we in?	County	1 ☐
What state are we in?	State	1 ☐
II. IMMEDIATE RECALL	(correct = ☑)	(Maximum Score = 3) Score: ____
Ask the subject if you may test his/her memory. Say "ball, "flag," "tree" clearly and slowly, about on second for each. Then ask the subject to repeat them. Check the box at right for each correct response. The first repetition determines the score. If he/she does not repeat all three correctly, keep saying them up to six tries until he/she can repeat them	Ball	1 ☐
	Flag	1 ☐
	Tree	1 ☐
		NUMBER OF TRIALS: _____
III. **ATTENTION AND CALCULATION**		
A. Counting Backwards Test	(Record each response, correct = ☑)	(Maximum Score = 5)
Ask the subject to begin with 100 and count backwards by 7. Record each response. Check one box at right for each correct response. Any response 7 or less than the previous response is a correct response. The socre is the number of correct subtractions. For example, 93, 87, 80, 72, 66 is a score of 4; 93, 86, 78 70, 62, is 2; 92, 87, 78, 70, 65 is 0.	93	1 ☐
	86	1 ☐
	79	1 ☐
	72	1 ☐
	65	1 ☐
B. Spelling Backwards Test		
Ask the subject to spell the word "WORLD" backwards. Record each response. Use the instructions to determine which are correct responses, and check one box at right fore each correct response.	D	1 ☐
	L	1 ☐
	R	1 ☐
C. Final Score	O	1 ☐
Compare the scores of the Counting Backwards and Spelling Backwards tests. Write the greater of the two socres in the box labeled FINAL SCORE at right, and use it in deriving the **TOTAL SCORE.**	W	1 ☐
		FINAL SCORE_____ (Max of 5 or Greater of the two Scores)
IV. **RECALL**	(correct = ☑)	(Maximum Score = 3) Score: ____
Ask the subject to recall the three words you previously asked him/her to remember. Check the Box at right for each correct response.	Ball	1 ☐
	Flag	1 ☐
	Tree	1 ☐
V. Language	(correct = ☑)	(Maximum Score = 9) Score: ____
Naming	Watch	1 ☐
Show the subject a wrist watch and ask him/her what it is. Repeat for a pencil.	Pencil	1 ☐
Repetition		

Ask the subject to repeat "No, ifs, ands, or buts."	Repetition	1 ☐
Three -Stage Command		
Establish the subject's dominant hand. Give the subject a sheet of blank paper and say, "Take the paper in your right/left hand, fold it in half and put it on the floor."	Takes paper in hand	1 ☐
	Folds paper in half	1 ☐
	Puts paper on floor	1 ☐
Reading		
Hold up the card that reads, "Close your eyes." So the subject can see it clearly. Ask him/her to read it and do what it says. Check the box at right only if he/she actually closes his/her eyes.	Closes eyes	1 ☐
Writing		
Give the subject a sheet of blank paper and ask him/her to write a sentence. It is to be written sponataneously. If the sentence contains a subject and a verb, and is sensible, check the box at right. Correct grammar and punctuation are not necessary.	Writes sentence	1 ☐
Copying		
Show the subject the drawing of the intersecting pentagons. Ask him/her to draw the pentagons (about one inch each side) on the paper provided. If ten angles are present and two intersect, check the box at right. Ignore tremor and rotation.	Copies pentagons	1 ☐

DERIVING THE TOTAL SCORE	
Add the number of correct responses. The maximum is 30.	TOTAL SCORE _____
23-30 = Normal / 19-23 = Borderline / <19 = Impaired	

Folstein MF, Folstein SE, and McHugh PR, 1975

Appendix 2. ELISA test procedures

Appendix 2A. Test procedure for CSF and plasma Aβ42 analysis

80324 INNOTEST® β-AMYLOID$_{(1-42)}$/ 25685 v18/ KEY-CODE: INX67497.

INNOGENETICS®
BIOTECHNOLOGY FOR HEALTHCARE

Test procedure

Please read 'Analytical precautions' before performing the test.

Note:

- Allow all specimens and test reagents to reach room temperature (18-30°C) before use.
- Have all reagents and specimens ready before starting the assay. Once the test has started, it must be performed without any interruption in order to achieve the most reliable and consistent results.
- CSF samples should be vortexed 10s before testing.

1. Take the strip-holder with the required number of strips, taking into account that for each test run, 6 standards and one blank should be included. Standards, samples and blanks must be run in duplicate. Place any unused strip in the plastic minigrip bag with the silicagel desiccant.
2. Immediately after vortexing the CSF samples for 10s, add the CSF samples and standards and blank of Sample Diluent to the polypropylene plate provided in the kit. Add sufficient sample volume to the polypropylene plate so that 2 replicates of 25 µL each can be transferred to the antibody-coated plate.
3. Prepare **conjugate working solution 1** and **standards** according to preparations for use.
4. Add **75 µL conjugate working solution 1** to each well of the antibody-coated plate.
5. Using a multi-channel pipette, transfer 25 µL from each well of the polypropylene plate to the corresponding well on the antibody-coated plate.
6. Make sure that standards and CSF samples are adequately mixed by carefully tapping the stripholder or by shaking 1 minute at 1000 rpm. **Cover** the strips with an adhesive sealer. **Incubate** for one hour at room temperature (18-30°C).
7. Prepare conjugate working solution 2 just before the end of step 6.
8. **Wash** each well 5 times (see 'Directions for washing').
9. Add **100 µL conjugate working solution 2** to each well. **Cover** the strips with a new adhesive sealer and **incubate** for 30 minutes at room temperature (18-30°C).
10. **Wash** each well 5 times (see 'Directions for washing').
11. Prepare substrate working solution just before end of step 9.
12. Add **100 µL substrate working solution** to each well. **Incubate** for 30 minutes at 18-30°C in the dark.
13. To stop the reaction, add **50 µL Stop Solution** to each well in the same sequence and at the same time intervals as the substrate solution. Tap the stripholder carefully to ensure optimal mixing.
14. **Read** (within 15 minutes after step 13) the absorbance at 450 nm (single wavelength). For dual wavelength analysis 620 nm can be used as the reference wavelength.

Appendix 2B. Test procedure for CSF and plasma Aβ40 analysis

IBL Instructions Code No. 27718

Code No. 27718

Human Amyloidβ (1-40) (FL) Assay Kit - IBL

3. Measurement procedure

All reagents shall be brought to room temperature approximately 30 minutes before use. Then mix it gently and completely before use. Confirm no change in quality of the reagents. Standard curve shall be prepared simultaneously with the measurement of test samples.

Reagents	Test Sample	Standard	Test Sample Blank	Reagent Blank
	Test sample 100µL	Diluted standard (Tube 1~7) 100µL	EIA buffer (Tube-8) 100µL	EIA buffer 100µL
Incubation for overnight at 4℃ with plate lid				
Washing 7 times				
Labeled Antibody	100µL	100µL	100µL	-
Incubation for 1 hour at 4℃ with plate lid				
Washing 9 times				
Chromogen	100µL	100µL	100µL	100µL
Incubation for 30 minutes at room temperature (shielded)				
Stop solution	100µL	100µL	100µL	100µL
Read the plate at 450nm against a Reagent Blank within 30 minutes after application of Stop solution.				

1) Determine wells for reagent blank. Put 100µL each of "4, EIA buffer" into the wells.
2) Determine wells for test sample blank, test sample and diluted standard. Then, put 100µL each of test sample blank (tube-8), test sample and dilutions of standard (tube-1~7) into the appropriate wells.
3) Incubate the precoated plate for overnight at 4℃ after covering it with plate lid.
4) Wash each well of the precoated plate vigorously with wash buffer using washing bottle. Then, fill each well with wash buffer and place the precoated plate for 15~30 seconds. Remove wash buffer completely from the precoated plate by snapping. This procedure must be repeated more than 7 times. Then, remove the remaining liquid from all wells completely by snapping the precoated plate onto paper towel.
In case of using plate washer, after 4 times washing with plate washer, washing with above washing bottle must be repeated 3 times..
5) Pipette 100µL of labeled antibody solution into the wells of test samples, diluted standard and test sample blank.
6) Incubate the precoated plate for 1 hour at 4℃ after covering it with plate lid.
7) Wash the precoated plate 9 times in the same manner above 4).
8) "6, Chromogen" should be taken the required quantity into a disposable test tube. Then, pipette 100µL from the test tube into the wells. Please avoid to return the rest of test tube into "6, Chromogen" bottle due to avoid to cause of contamination.
9) Incubate the precoated plate for 30 minutes at room temperature in the dark. The liquid will turn blue by the addition of "6, Chromogen".
10) Pipette 100µL of "7, Stop solution" into the wells. Mix the liquid by tapping the side of precoated plate. The liquid will turn yellow by the addition of "7, Stop solution".
11) Remove any dirt or drop of water on the bottom of the precoated plate and confirm there is no bubble on the surface of the liquid. Then, run the plate reader and conduct measurement at 450nm.
The measurement shall be done within 30minutes after the addition of "7, Stop solution".

Appendix 2C. Test procedure for CSF T-tau analysis

80323 INNOTEST® hTAU Ag/ 25684 v16/ KEY-CODE: INX99156.

INNOGENETICS®

Test procedure

Please read 'Analytical precautions' before performing the test.

Note:

- Allow all specimens and test reagents to reach room temperature (18-30°C) before use.
- Have all reagents and specimens ready before starting the assay. Once the test has started, it must be performed without any interruption in order to achieve the most reliable and consistent results.
- CSF samples must be vortexed 10s before testing.

1. Take the strip-holder with the required number of strips, taking into account that for each test run, 5 standards and one blank should be included. Standards, samples and blanks must be run in duplicate. Place any unused strip in the plastic minigrip bag with the silicagel desiccant.
2. Prepare **conjugate working solution 1** and **standards** according to the preparations for use.
3. Add **75 µL conjugate working solution 1** to each well of the antibody-coated plate.
4. Add **25 µL of each standard** (including the blank of 25 µL Sample Diluent) and the samples to duplicate wells of the antibody-coated plate.
5. Make sure that standards and CSF samples are adequately mixed by carefully tapping the stripholder or by shaking 1 minute at 1000 rpm. **Cover** the strips with an adhesive sealer. Incubate overnight (14-18hrs) in an incubator at 25 ± 2°C.
6. Prepare conjugate working solution 2 just before the end of step 5.
7. **Wash** each well 4 times (see 'Directions for washing').
8. Add **100 µL conjugate working solution 2** to each well. **Cover** the strips with a new adhesive sealer and incubate for 30 ± 3 minutes in an incubator at 25 ± 2°C.
9. Prepare substrate working solution at the end of step 8.
10. Wash each well 4 times (see 'Directions for washing').
11. Add **100 µL substrate working solution** to each well. Incubate for 30 ± 3 minutes at room temperature (18-30°C) in the dark.
12. To stop the reaction, add 100 µL of 2N sulfuric acid to each well (or use STOP solution of INNOTEST ß-Amyloid or INNOTEST PHOSPHO-TAU$_{(181P)}$), in the same sequence and the same time intervals as the substrate solution. Tap the stripholder carefully to ensure optimal mixing.
13. **Read** (within 15 minutes after step 12) the absorbance at 450 nm (single wavelength). For dual wavelength analysis, 620 nm can be used as the reference wavelength.

Appendix 2D. Test procedure for CSF P-tau analysis

80317 INNOTEST® PHOSPHO-TAU$_{(181P)}$ / 24898 v16/ KEY-CODE: INX27352.

INNOGENETICS®
BIOTECHNOLOGY FOR HEALTHCARE

Test procedure

Please read 'Analytical precautions' before performing the test.

Note:

- Allow all specimens and test reagents to reach room temperature (18-30°C) before use.
- Have all reagents and specimens ready before starting the assay. Once the test has started, it must be performed without any interruption in order to achieve the most reliable and consistent results.
- CSF samples must be vortexed 10s before testing.

1. Take the strip-holder with the required number of strips, taking into account that for each test run, 6 standards and one blank should be included. Standards, samples and the blank must be run in duplicate.
2. Prepare **conjugate working solution 1** and **standards** according to preparations for use.
3. Add **25 µL conjugate working solution 1** to each well of the antibody-coated plate.
4. Add **75 µL of each standard** (including the blank of 75 µL Sample Diluent) and the samples to duplicate wells of the antibody-coated plate.
5. Make sure that standards and CSF samples are adequately mixed by carefully tapping the stripholder or by shaking 1 minute at 1000 rpm. **Cover** the strips with an adhesive sealer. **Incubate** overnight (14-18hrs) in an incubator at 2-8°C.
6. Prepare conjugate working solution 2 just before the end of step 5.
7. **Wash** each well **5 times** (see 'Directions for washing').
8. Add **100 µL Conjugate working solution 2** to each well. **Cover** the strips with a new adhesive sealer and **incubate** for 60 ± 5 minutes at room temperature (18-30°C).
9. **Wash** each well **5 times** (see Directions for washing).
10. Prepare substrate working solution.
11. Add **100 µL** of **Substrate working solution** to each well and incubate for 30 ± 3 minutes at room temperature (18-30°C) in the dark.
12. Add **50 µL** of **Stop Solution** to each well, in the same sequence and at the same time intervals as the Substrate working solution. Tap the stripholder carefully to ensure optimal mixing.
13. **Read** (within 15 minutes after step 12) the absorbance at 450 nm (single wavelength). For dual wavelength analysis, 690 nm or 620 nm can be used as the reference wavelength.

Appendix 2E. Test procedure for serum ApoE analysis

Apolipoprotein E Human ELISA kit ab108813

Assay Method

1. Prepare all reagents, working standards and samples as instructed. Bring all reagents to room temperature before use. The assay is performed at room temperature (20-30°C).
2. Remove excess microplate strips from the plate frame and return them immediately to the foil pouch with desiccant inside. Reseal the pouch securely to minimize exposure to water vapor and store in a vacuum desiccator.
3. Add 50 µl of Apo E standard or sample per well. Cover wells with a sealing tape and incubate for two hours. Start the timer after the last sample addition.
4. Wash five times with 200 µl of Wash Buffer manually. Invert the plate each time and decant the contents; tap it 4-5 times on absorbent paper towel to completely remove the liquid. If using a machine wash six times with 300 µl of Wash Buffer and then invert the plate, decant the contents; tap it 4-5 times on absorbent paper towel to completely remove the liquid.
5. Add 50 µl of Biotinylated Apo E Antibody to each well and incubate for one hour.
6. Wash microplate as described above.
7. Add 50 µl of Streptavidin-Peroxidase Conjugate to each well and incubate for 30 minutes. Turn on the microplate reader and set up the program in advance.
8. Wash microplate as described above.
9. Add 50 µl of Chromogen Substrate per well and incubate for about 20 minutes or till the optimal blue color density develops. Gently tap plate to ensure thorough mixing and break the bubbles in the well with pipette tip.
10. Add 50 µl of Stop Solution to each well. The color will change from blue to yellow.
11. Read the absorbance on a microplate reader at a wavelength of 450 nm immediately. If wavelength correction is available, subtract readings at 570 nm from those at 450 nm to correct optical imperfections. Otherwise, read the plate at 450 nm only. Please note that some unstable black particles may be generated at high concentration points after stopping the reaction for about 10 minutes, which will reduce the readings.

Appendix 2F. Test procedure for CSF and serum ACE analysis

Quantikine® Human ACE Immunoassay, Catalog Number DACE00

ASSAY PROCEDURE

Bring all reagents and samples to room temperature before use. It is recommended that all samples, controls, and standards be assayed in duplicate.

Note: *High concentrations of ACE are found in saliva. Use of a face mask and gloves to protect kit reagents from contamination is recommended.*

1. Prepare all reagents, working standards, and samples as directed in the previous sections.
2. Remove excess microplate strips from the plate frame, return them to the foil pouch containing the desiccant pack, and reseal.
3. Add 100 µL of Assay Diluent RD1-34 to each well.
4. Add 50 µL of Standard, control, or sample* per well. Cover with the adhesive strip provided. Incubate for 2 hours at room temperature on a horizontal orbital microplate shaker (0.12" orbit) set at 500 ± 50 rpm. A plate layout is provided to record standards and samples assayed.
5. Aspirate each well and wash, repeating the process three times for a total of four washes. Wash by filling each well with Wash Buffer (400 µL) using a squirt bottle, manifold dispenser, or autowasher. Complete removal of liquid at each step is essential to good performance. After the last wash, remove any remaining Wash Buffer by aspirating or decanting. Invert the plate and blot it against clean paper towels.
6. Add 200 µL of ACE Conjugate to each well. Cover with a new adhesive strip. Incubate for 2 hours at room temperature on the shaker.
7. Repeat the aspiration/wash as in step 5.
8. Add 200 µL of Substrate Solution to each well. Incubate for 30 minutes at room temperature **on the benchtop. Protect from light.**
9. Add 50 µL of Stop Solution to each well. The color in the wells should change from blue to yellow. If the color in the wells is green or the color change does not appear uniform, gently tap the plate to ensure thorough mixing.
10. Determine the optical density of each well within 30 minutes, using a microplate reader set to 450 nm. If wavelength correction is available, set to 540 nm or 570 nm. If wavelength correction is not available, subtract readings at 540 nm or 570 nm from the readings at 450 nm. This subtraction will correct for optical imperfections in the plate. Readings made directly at 450 nm without correction may be higher and less accurate.

*Samples may require dilution. See Sample Preparation section.

Appendix 2G. Test procedure for CSF and plasma clusterin analysis

Human Clusterin ELISA - Cat. No.: RD194034200R

11. ASSAY PROCEDURE

1. Pipet **100 µl** of diluted Standards, Quality Controls, Dilution Buffer (=Blank) and samples, preferably in duplicates, into the appropriate wells. See *Figure 1* for example of work sheet.
2. Incubate the plate at room temperature (ca. 25°C) for **1 hour**, shaking at ca. 300 rpm on an orbital microplate shaker.
3. Wash the wells 5-times with Wash Solution (0.35 ml per well). After final wash, invert and tap the plate strongly against paper towel.
4. Add **100 µl** of Biotin Labelled Antibody solution into each well.
5. Incubate the plate at room temperature (ca. 25°C) for **1 hour**, shaking at ca. 300 rpm on an orbital microplate shaker.
6. Wash the wells 5-times with Wash Solution (0.35 ml per well). After final wash, invert and tap the plate strongly against paper towel.
7. Add **100 µl** of Streptavidin-HRP Conjugate into each well.
8. Incubate the plate at room temperature (ca. 25°C) for **30 min**, shaking at ca. 300 rpm on an orbital microplate shaker.
9. Wash the wells 5-times with Wash Solution (0.35 ml per well). After final wash, invert and tap the plate strongly against paper towel.
10. Add **100 µl** of Substrate Solution into each well. Avoid exposing the microtiter plate to direct sunlight. Covering the plate with e.g. aluminium foil is recommended.
11. Incubate the plate for **10 minutes** at room temperature. The incubation time may be extended [up to 20 minutes] if the reaction temperature is below than 20°C. Do not shake the plate during the incubation.
12. Stop the colour development by adding **100 µl** of Stop Solution.
13. Determine the absorbance of each well using a microplate reader set to 450 nm, preferably with the reference wavelength set to 630 nm (acceptable range: 550 – 650 nm). Subtract readings at 630 nm (550 - 650 nm) from the readings at 450 nm. **The absorbance should be read within 5 minutes following step 12.**

Appendix 2H. Test procedure for CSF NF-L analysis

UmanDiagnostics NF-light® (Neurofilament light) ELISA. Cat. No.: 10-7001

Assay instructions

All assay reagents should be brought to room temperature prior to use.
After each washing cycle the plate should be tapped dry against absorbent paper.

1. Dilute the CSF samples 1:1 with sample dilution buffer to a total volume of 100 µl. The standard reconstituted and diluted according to the standard dilution table are ready to use (i.e. no further dilution should be made).
2. Wash the wells to be used with washing buffer (3x300 µl). The wash solution added could be either aspirated or removed by knocking the plate against absorbing material immediately before next washing cycle.
3. Add 100 µl of each standard and sample in duplicate. Incubate 1 hour at room temperature (20-25°C) with agitation (800 rpm).
4. Wash the wells with washing buffer (3x300 µl), see point 2.
5. Add 100 µl of tracer (biotin anti-NFL) antibody to each well. Incubate 45 minutes at room temperature (20-25°C) with agitation (800 rpm).
6. Wash the wells with washing buffer (3x300 µl), see point 2.
7. Add 100 µl conjugate (streptavidin-HRP) to each well. Incubate 30 minutes at room temperature (20-25°C) with agitation (800 rpm).
8. Wash the wells with washing buffer (3x300 µl), see point 2.
9. Add 100 µl TMB to each well. Incubate 15 minutes at room temperature (20-25°C) with agitation (800 rpm).
10. Add 50 µl stop solution to each well and read the absorbance at 450 nm. **Note: The stop solution contains diluted sulfuric acid and is corresive.**

Appendix 3. ELISA plate chart

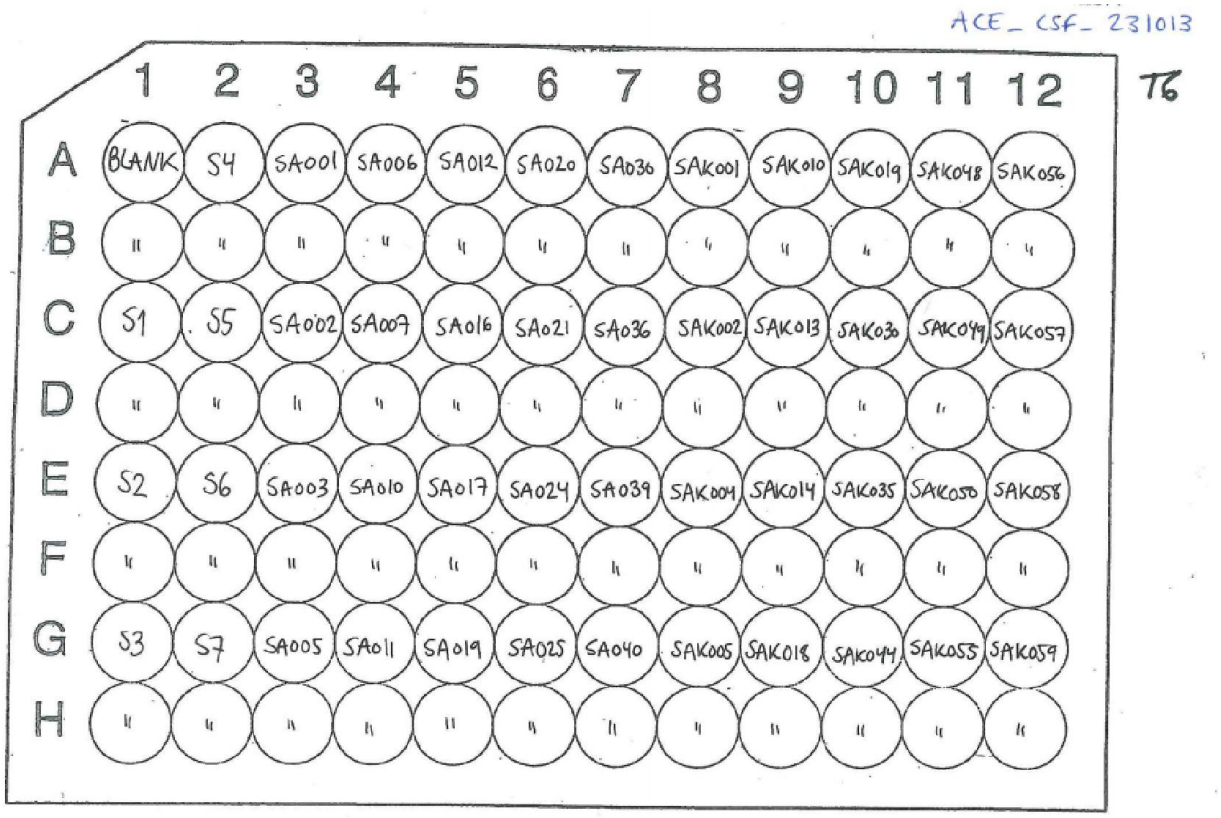

Appendix 4. Protocol for DNA isolation from whole blood

Protocol: DNA Purification from Blood or Body Fluids (Spin Protocol)

This protocol is for purification of total (genomic, mitochondrial, and viral) DNA from whole blood, plasma, serum, buffy coat, lymphocytes, and body fluids using a microcentrifuge. For total DNA purification using a vacuum manifold, see "Protocol: DNA Purification from Blood or Body Fluids (Vacuum Protocol)" on page 30.

Important points before starting

- All centrifugation steps are carried out at room temperature (15–25°C).
- Use carrier DNA if the sample contains <10,000 genome equivalents (see page 18).
- 200 µl of whole blood yields 3–12 µg of DNA. Preparation of buffy coat (see page 19) is recommended if a higher yield is required.

Things to do before starting

- Equilibrate samples to room temperature.
- Heat a water bath or heating block to 56°C for use in step 4.
- Equilibrate Buffer AE or distilled water to room temperature for elution in step 11.
- Ensure that Buffer AW1, Buffer AW2, and QIAGEN Protease have been prepared according to the instructions on page 17.
- If a precipitate has formed in Buffer AL, dissolve by incubating at 56°C.

Procedure

1. **Pipet 20 µl QIAGEN Protease (or proteinase K) into the bottom of a 1.5 ml microcentrifuge tube.**
2. **Add 200 µl sample to the microcentrifuge tube. Use up to 200 µl whole blood, plasma, serum, buffy coat, or body fluids, or up to 5 x 10^6 lymphocytes in 200 µl PBS.**

   If the sample volume is less than 200 µl, add the appropriate volume of PBS.

   QIAamp Mini spin columns copurify RNA and DNA when both are present in the sample. RNA may inhibit some downstream enzymatic reactions, but not PCR. If RNA-free genomic DNA is required, 4 µl of an RNase A stock solution (100 mg/ml) should be added to the sample before addition of Buffer AL.

   Note: It is possible to add QIAGEN Protease (or proteinase K) to samples that have already been dispensed into microcentrifuge tubes. In this case, it is important to ensure proper mixing after adding the enzyme.

3. **Add 200 µl Buffer AL to the sample. Mix by pulse-vortexing for 15 s.**

   In order to ensure efficient lysis, it is essential that the sample and Buffer AL are mixed thoroughly to yield a homogeneous solution.

   If the sample volume is larger than 200 µl, increase the amount of QIAGEN Protease (or proteinase K) and Buffer AL proportionally; for example, a 400 µl sample will require 40 µl QIAGEN Protease (or proteinase K) and 400 µl Buffer AL. If sample volumes larger than 400 µl are required, use of QIAamp DNA Blood Midi or Maxi Kits is recommended; these can process up to 2 ml or up to 10 ml of sample, respectively.

   Note: Do not add QIAGEN Protease or proteinase K directly to Buffer AL.

4. **Incubate at 56°C for 10 min.**

   DNA yield reaches a maximum after lysis for 10 min at 56°C. Longer incubation times have no effect on yield or quality of the purified DNA.

5. **Briefly centrifuge the 1.5 ml microcentrifuge tube to remove drops from the inside of the lid.**

6. **Add 200 µl ethanol (96–100%) to the sample, and mix again by pulse-vortexing for 15 s. After mixing, briefly centrifuge the 1.5 ml microcentrifuge tube to remove drops from the inside of the lid.**

   If the sample volume is greater than 200 µl, increase the amount of ethanol proportionally; for example, a 400 µl sample will require 400 µl of ethanol.

7. **Carefully apply the mixture from step 6 to the QIAamp Mini spin column (in a 2 ml collection tube) without wetting the rim. Close the cap, and centrifuge at 6000 x *g* (8000 rpm) for 1 min. Place the QIAamp Mini spin column in a clean 2 ml collection tube (provided), and discard the tube containing the filtrate.***

   Close each spin column in order to avoid aerosol formation during centrifugation.

   Centrifugation is performed at 6000 x *g* (8000 rpm) in order to reduce noise. Centrifugation at full speed will not affect the yield or purity of the DNA. If the lysate has not completely passed through the column after centrifugation, centrifuge again at higher speed until the QIAamp Mini spin column is empty.

   Note: When preparing DNA from buffy coat or lymphocytes, centrifugation at full speed is recommended to avoid clogging.

8. **Carefully open the QIAamp Mini spin column and add 500 µl Buffer AW1 without wetting the rim. Close the cap and centrifuge at 6000 x *g* (8000 rpm) for 1 min. Place the QIAamp Mini spin column in a clean 2 ml collection tube (provided), and discard the collection tube containing the filtrate.***

   It is not necessary to increase the volume of Buffer AW1 if the original sample volume is larger than 200 µl.

* Flow-through contains Buffer AL or Buffer AW1 and is therefore not compatible with bleach. See page 8 for safety information.

9. **Carefully open the QIAamp Mini spin column and add 500 µl Buffer AW2 without wetting the rim. Close the cap and centrifuge at full speed (20,000 x *g*; 14,000 rpm) for 3 min.**
10. **Recommended: Place the QIAamp Mini spin column in a new 2 ml collection tube (not provided) and discard the old collection tube with the filtrate. Centrifuge at full speed for 1 min.**

    This step helps to eliminate the chance of possible Buffer AW2 carryover.
11. **Place the QIAamp Mini spin column in a clean 1.5 ml microcentrifuge tube (not provided), and discard the collection tube containing the filtrate. Carefully open the QIAamp Mini spin column and add 200 µl Buffer AE or distilled water. Incubate at room temperature (15–25°C) for 1 min, and then centrifuge at 6000 x *g* (8000 rpm) for 1 min.**

    Incubating the QIAamp Mini spin column loaded with Buffer AE or water for 5 min at room temperature before centrifugation generally increases DNA yield.

    A second elution step with a further 200 µl Buffer AE will increase yields by up to 15%.

Volumes of more than 200 µl should not be eluted into a 1.5 ml microcentrifuge tube because the spin column will come into contact with the eluate, leading to possible aerosol formation during centrifugation.

Elution with volumes of less than 200 µl increases the final DNA concentration in the eluate significantly, but slightly reduces the overall DNA yield (see Table 5, page 26). For samples containing less than 1 µg of DNA, elution in 50 µl Buffer AE or water is recommended. Eluting with 2 x 100 µl instead of 1 x 200 µl does not increase elution efficiency.

For long-term storage of DNA, eluting in Buffer AE and storing at –20°C is recommended, since DNA stored in water is subject to acid hydrolysis.

A 200 µl sample of whole human blood (approximately 5 x 10^6 leukocytes/ml) typically yields 6 µg of DNA in 200 µl water (30 ng/µl) with an A_{260}/A_{280} ratio of 1.7–1.9.

For more information about elution and how to determine DNA yield, purity, and length, refer to pages 25–26 and Appendix A, page 51.

Appendix 5. Preparation of Master SYBR® Green I

LightCycler® FastStart DNA Master SYBR Green I Instructions Version 18, page 9:

Preparation of the Master Mix

❶	Thaw one vial of "Reaction Mix" (vial 1b, green cap) and shield it from light. ⚠ A reversible precipitate may form in the LightCycler® FastStart Reaction Mix SYBR Green I (vial 1b) during storage. If a precipitate is visible, place the Reaction Mix at 37°C and mix gently from time to time until the precipitate is completely dissolved. This treatment does not influence the performance in PCR.
❷	Briefly centrifuge one vial "Enzyme" (vial 1a, colorless cap) and the thawed vial of "Reaction Mix" (from Step 1), then place the vials back on ice.
❸	Pipette 10 µl from vial 1a (colorless cap) into vial 1b (green cap). Each vial 1a contains enough enzyme solution for three vials of "Reaction Mix" (vial 1b).
❹	Mix gently by pipetting up and down. ⚠ Do not vortex.
❺	Re-label vial 1b (green cap) with the new label (vial 1: LightCycler® FastStart DNA Master SYBR Green I) provided with the kit. ⚠ Always keep the Master Mix away from light!
❻	Store on ice or in the pre-cooled LightCycler® Centrifuge Adapters Cooling Block, until ready to use.

Appendix 6. LightCycler Melting Analysis Report

LightCycler Melting Analysis Report

User: user LightCycler ID: 4603

Filename: C:\LightCycler3\Users\user\Data\ACE samba\011013 ny run1.ABT

LC Run Version: 5.32 LCDA Version: 3.5.28

This experiment was run on Oct 01, 2013 by user.

Sample Information

Rot. Pos.	Sample Name	Rep. of ...	Sample Type*	Known Conc.	Tm1 (°C)	Area 1 (Units)	Tm2 (°C)	Area 2 (Units)	Tm3 (°C)	Area 3 (Units)	Sample Comments
1	H2O		N								
2	Grethe		U		92.20	11.81					
3	Linda		U		84.63	13.58	92.32	4.048			
4	SA001		U		92.14	10.91					
5	SA002		U		84.62	13.42	92.24	3.602			
6	SA003		U		84.48	12.42	92.22	4.288			
7	SA004		U		84.55	12.39	92.24	3.844			
8	SA005		U		92.15	11.84					
9	SA006		U		92.13	12.27					
10	SA007		U		84.62	13.55	92.10	4.874			
11	SA008		U		84.55	12.51	92.04	4.097			
12	SA010		U		84.57	13.96	92.18	3.666			
13	SA011		U		92.07	12.55					
14	SA012		U		92.08	12.13					
15	SA013		U		84.86	19.70					
16	SA015		U		84.46	12.06	91.97	4.717			
17	SA016		U		84.82	19.82					
18	SA017		U		84.81	18.74					
19	SA018		U		84.77	18.81					
20	SA019		U		91.94	12.65					
21	SA020		U		91.92	12.04					
22	SA021		U		84.77	18.60					
23	SA024		U		84.73	19.39					
24	SA025		U		91.97	11.29					
25	SA030		U		84.43	16.61	92.23	5.889			
26	SA032		U		84.90	21.47					
27	SA036		U		84.87	19.59					
28	SA039		U		92.20	13.01					
29	SA040		U		84.63	14.63	92.21	4.050			
30	SA041		U		84.97	18.39					
31	SA042		U		92.22	12.37					

* P = Positive, U = Unknown, N = Negative, S = Standard, < > = De-Selected

D/D

T/D

T/T

1

Printed on 01/10/2013 at 11:40:50

Page 2 of 2

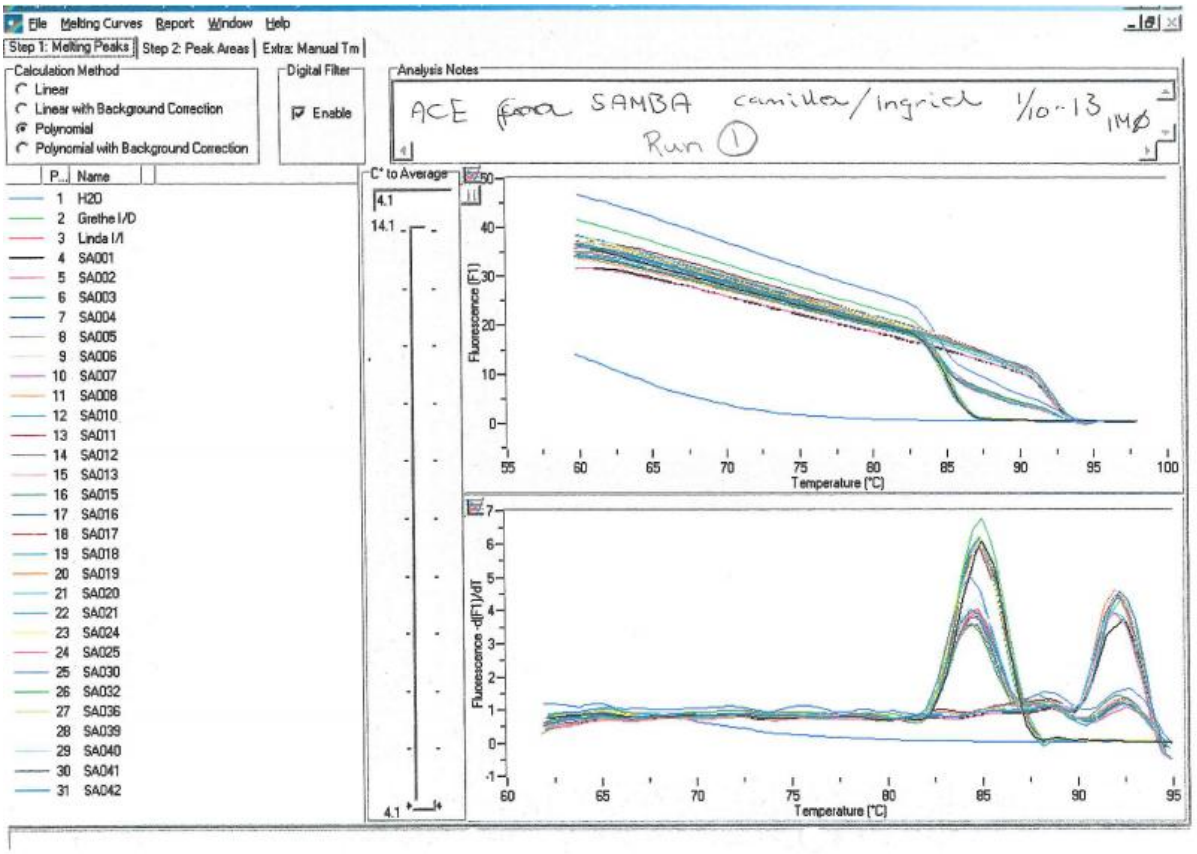
File Melting Curves Report Window Help
Step 1: Melting Peaks
Step 2: Peak Areas
Extra: Manual Tm
Calculation Method
Linear
Linear with Background Correction
Polynomial
Polynomial with Background Correction
Digital Filter
Enable
Analysis Notes
ACE from SAMBA cannulae/ingrid 1/10-13 IMØ
Run (1)
C° to Average
4.1
14.1
4.1
P... Name
1 H20
2 Grethe I/D
3 Linda I/I
4 SA001
5 SA002
6 SA003
7 SA004
8 SA005
9 SA006
10 SA007
11 SA008
12 SA010
13 SA011
14 SA012
15 SA013
16 SA015
17 SA016
18 SA017
19 SA018
20 SA019
21 SA020
22 SA021
23 SA024
24 SA025
25 SA030
26 SA032
27 SA036
28 SA039
29 SA040
30 SA041
31 SA042
Fluorescence (F1)
Temperature (°C)
Fluorescence -d(F1)/dT
Temperature (°C)